Characterization of NDR kinase signalling pathways during septum formation in *Neurospora crassa*

Dissertation

for the award of the degree

“Doctor rerum naturalium”

of the Georg-August-University Göttingen

within the doctoral program *Molecular Biology of Cells*

of the Georg-August University School of Science (GAUSS)

submitted by

Yvonne Heilig

from Bückeburg

Göttingen 2013

Thesis Committee

PD Dr. Stephan Seiler

Department of Molecular Plant Physiology, Institute for Biology II, Albert-Ludwigs University Freiburg

Prof. Dr. Andreas Wodarz

Department of Anatomy and Cell Biology, Stem Cell Biology, Georg-August-University of Göttingen

Dr. Hans Dieter Schmitt

Department of Neurobiology, Max Planck Institute for Biophysical Chemistry, Georg-August-University of Göttingen

Members of the Examination Board

Referee: **PD Dr. Stephan Seiler**
Department of Molecular Plant Physiology, Institute for Biology II
Albert-Ludwigs University Freiburg

2nd Referee: **Prof. Dr. Andreas Wodarz**
Department of Anatomy and Cell Biology, Stem Cell Biology
Georg-August-University of Göttingen

Further members of the Examination Board

Dr. Hans Dieter Schmitt

Department of Neurobiology, Max Planck Institute for Biophysical Chemistry, Georg-August-University of Göttingen

Prof. Dr. Heike Krebber

Department of Microbiology and Genetics, Molecular Genetics, Georg-August-University of Göttingen

Jun.-Prof. Dr. Kai Heimel

Department of Microbiology and Genetics, General Microbiology, Georg-August-University of Göttingen

PD Dr. Michael Hoppert

Department of Microbiology and Genetics, General Microbiology, Georg-August-University of Göttingen

Date of oral examination: .....

Meinen Eltern

&

Opa und Geli

I hereby confirm that this thesis has been written independently and with no other sources and aids than quoted.

Göttingen, 30.09.2013

Yvonne Heilig

Parts of this work have been published:

Publications:

Dettmann, A., **Heilig, Y.,** Ludwig, S., Schmitt, K., Illgen, J., Fleißner, A., Valerius, O., and Seiler, S. (2013). HAM-2 and HAM-3 are central for the assembly of the *Neurospora* STRIPAK complex at the nuclear envelope and regulate nuclear accumulation of the MAP kinase MAK-1 in a MAK-2-dependent manner. Mol Microbiol. in press. doi: 10.1111/mmi.12399.

Mähs, A.*, Ischebeck, T.*, **Heilig, Y.*,** Stenzel, I., Hempel, F., Seiler, S. and Heilmann, I. (2012). The essential phosphatidylinositolphosphate kinase MSS-4 is required for polar hyphal morphogenesis, localizing to sites of growth and cell fusion in *Neurospora crassa*. PLOS ONE, 7, e51454. (*contributed equally)

Richthammer, C., Enseleit, M., Sanchez-Leon, E., März, S., **Heilig, Y.,** Riquelme, M., and Seiler, S. (2012). RHO1 and RHO2 share partially overlapping functions in the regulation of cell wall integrity and hyphal polarity in *Neurospora crassa*. Mol. Microbiol. 85, 716-733.

Script submitted:

Yvonne Heilig, Kerstin Schmitt and Stephan Seiler.
Phospho-regulation of the *Neurospora crassa* septation initiation network

Script in preparation:

Yvonne Heilig, Anne Dettmann, Kerstin Schmitt, Rosa R. Mourino-Pérez and Stephan Seiler.
Proper actin ring formation and septum constriction requires coordination of SIN and MOR pathways through the germinal centre kinase MST1

1. SUMMARY 1

2. ZUSAMMENFASSUNG 2

3. INTRODUCTION 4

3.1 The spatial cue - mechanisms specifying the position of the division plane 4

3.2 Assembly and constriction of the contractile actomyosin ring (CAR) 6

3.3 The temporal cue - the SIN/MEN network coordinates mitosis and cytokinesis 7

3.3.1 Composition and regulation of the SIN 8

3.3.2 Functions of the SIN in cytokinesis 9

3.3.3 Crosstalk between the SIN and MOR NDR kinase pathways 10

3.4 Septation in filamentous fungi 11

3.4.1 Division site selection and CAR assembly in filamentous fungi 11

3.4.2 The SIN and MOR pathways in filamentous fungi 12

3.5 Aims of this work 13

4. MATERIALS AND METHODS 15

4.1 Media and growth conditions 15

4.2 Plasmid construction 16

4.2.1 General procedure 16

4.2.2 Plasmids of epitope-tagged fusion proteins for in vitro kinase assays and co-immunoprecipitation experiments 20

4.2.3 Plasmids for analysis of subcellular fusion protein localization 20

4.2.4 Point-mutated constructs of DBF-2, BUD-3 and BUD-4 21

4.2.5 BUD-3-Helix constructs 22

4.3 Strains 22

4.4 General molecular biological methods 26

4.4.1 Polymerase chain reaction (PCR) 26

4.4.2 DNA agarose gel electrophoresis and isolation 26

4.4.3 Modification and enzymatic digestion of DNA 27

4.4.4 Ligation 27

4.4.5 DNA Transformation 27

4.4.6 Sequence analysis 27

4.5 Biochemical and immunological techniques 28

4.5.1 N. crassa protein isolation 28

4.5.2 Separation of proteins by SDS polyacrylamide gel electrophoresis (SDS-PAGE) and Western blotting 28

4.5.3 Immunoprecipitation 29

4.5.4 Kinase assays 29

4.5.5 Displacement assays 30

4.5.6 Mass spectrometry and database analysis 30

4.5.7 Enrichment of phosphopeptides 31

4.6 Yeast two-hybrid assays 31

4.7 Microscopy 32

5. RESULTS 33

5.1 Functional analysis of the SIN kinase cascade in *Neurospora crassa* 33

5.1.1 A tripartite SIN cascade is important for septum formation and localizes constitutively to SPBs and septa 33

5.1.2 CDC-7-dependent activation of DBF-2 occurs through SID-1 36

5.1.3 Dual phosphorylation of DBF2 is required for kinase activity and septum formation 38

5.2 MST-1 controls proper CAR formation and connects the SIN and MOR pathway during septum formation 40

5.2.1 MST-1 displays features reminiscent of SIN as well as MOR components 40

5.2.2 MST-1 controls proper CAR formation 42

5.2.3 Genetic interactions connect Δ*mst-1* with SIN, but not MOR mutants 43

5.2.4 The SIN kinase CDC-7 regulates SID-1 and MST-1 in an antagonistic manner 45

5.2.5 MST-1 coordinates SIN and MOR functions during septum formation 46

5.3 The SIN antagonizes the MOR, which in turn inhibits BUD-3 localization 49

5.3.1 Genetic relationship between SIN, MOR and BUD mutants 49

5.3.2 DBF-2 inhibits COT-1 activity through formation of kinase-kinase heterodimers 50

5.3.3 COT-1, but not DBF-2 phosphorylates BUD-3/BUD-4 landmark proteins **53**

5.3.4 COT-1 phosphorylation inhibits BUD-3 localization **54**

6. DISCUSSION **57**

6.1 The *N. crassa* SIN functions as hierarchical, stepwise kinase cascade **57**

6.2 Proper actin ring formation and septum constriction requires the SIN-associated Ste20-related GC kinase MST-1 **60**

6.3 MST-1 connects the SIN and MOR pathway during septum formation **62**

6.4 Cosstalk between SIN and MOR effector kinases DBF-2 and COT-1 is mediated by heterodimerization of the NDR kinases **63**

6.5 COT-1 regulates the BUD-3 ─ BUD-4 landmark complex during septum formation **65**

6.6 Outlook **66**

7. SUPPLEMENTAL MATERIAL **69**

8. REFERENCES **72**

9. ACKNOWLEDGEMENTS **82**

10. CURRICULUM VITAE **83**

List of Abbreviations

aa	amino acid
AD	activation domain
AH	anillin-homology
APS	ammonium persulfate
AS	activation segment
A. nidulans	*Aspergillus nidulans*
ATP	adenosine triphosphate
BD	DNA-binding domain
bp	base pair
C. albicans	*Candida albicans*
CAR	actin/myosin-based contractile ring
Cdk	cyclin dependent kinase
cDNA	complementary DNA
co-IP	co-immunoprecipitation
D. melanogaster	*Drosophila melanogaster*
DNA	deoxyribonucleic acid
dNTP	deoxyribonucleotide triphosphate
DTT	dithiotreitol
E. coli	*Escherichia coli*
EDTA	ethylenediaminetetraacetic acid
FGSC	Fungal Genetic Stock Center
GAP	GTPase activating protein
GCK	germinal centre kinase
GEF	guanine nucleotide exchange factor
GFP	green fluorescent protein
GTP	guanosine triphosphate
HA	hemaagglutinin
het	heterokaryon
his	histidine
HM	hydrophobic motif
hyg	hygromycin
IP	immunoprecipitation
kD	kiloDalton
LB	Luria Broth
MEN	mitotic exit network
MOR	morphogenesis-related NDR kinase network
Mst	mammalian Ste20-type
MW	molecular weight
NCBI	National Center for Biotechnology Information
N. crassa	*Neurospora crassa*
nic	nicotinamide
NDR	nuclear Dbf2-related
NP-40	Nonidet P-4
OD	optical density
PAGE	polyacrylamide gel electrophoresis
PAK	p21-activated kinase
PBS	phosphate buffered saline
PCR	polymerase chain reaction

PH	Pleckstrin homology
MOB	MpsI one binder
RAM	regulation of Ace2p and morphogenesis
RNA	ribonucleic acid
SAT	septal actin tangle
S. cerevisiae	*Saccharomyces cerevisiae*
SD	Synthetic Defined
SDS	sodium dodecyl sulfate
Ser	serine
SIN	septation initiation network
SPB	spindle pole bodie
S. pombe	*Schizosaccharomyces pombe*
TEMED	tetramethylethylenediamine
Thr	threonine
trp	tryptophane
ts	temperature-sensitive
UV	ultraviolet
VMM	Vogel's Minimal Medium
WB	Western blot
YEPD	Yeast Extract Peptone Dextrose

1. Summary

Cytokinesis is a fundamental cellular process essential for cell proliferation of unicellular and multicellular organisms. The molecular pathways that regulate cytokinesis are highly complex and involve a large number of components that form elaborate interactive networks. The fungal septation initiation network (SIN) functions as kinase cascade that connects cell cycle progression with the initiation of cytokinesis and control septum formation. Miss-regulation of the homologous Hippo pathway in animals results in excessive proliferation and formation of tumors, underscoring the conservation and importance of these kinase networks. While septum formation is essential for proper growth and differentiation of molds, the regulation of septation and the composition of the SIN in filamentous fungi are only beginning to be unraveled.

The *in silico* analysis of the genome of the model mold *Neurospora crassa* identified homologs for most SIN network components. Analysis of these predicted SIN proteins allowed the characterization of the SIN kinase cascade consisting of CDC-7, SID-1 and DBF-2 together with their regulatory subunits CDC-14 and MOB-1, respectively. It was determined that SID-1 activates DBF-2 through hydrophobic motif phosphorylation and that SID-1-stimulated DBF-2 activity is further enhanced by CDC-7, providing the first biochemical evidence for a stepwise activation of the tripartite SIN kinase cascade in fungi. The entire SIN cascade localizes in a constitutive and cell cycle independent manner to spindle pole bodies and all SIN proteins accumulated at forming septa. Thus, in contrast to unicellular fungi the SIN localization and activity regulation is cell-cycle independent in syncytial ascomycetes. Moreover, the characterization of DBF-2 variants harbouring mutations in the two regulatory sites (Ser499 and Thr671) suggest that a dynamic phosphorylation/dephosphorylation cycle of Ser499 may be critical for *N. crassa* DBF-2 activity and function. These data have implications for NDR kinase activity regulation in general, because the sequential phosphorylation of both regulatory sites has been so far predicted for NDR kinases of higher eukaryotes.

The Ste20-related kinase MST-1 was identified as SIN-associated kinase acting in parallel to SID-1. SID-1 and MST-1 were both regulated by the upstream SIN kinase CDC-7, yet in an opposite manner, suggesting that MST-1 is required for fine-tuning the SIN. Lifeact- and formin-GFP reporter constructs revealed the formation of aberrant cortical actomyosin rings in Δ*mst-1*, which resulted in miss-positioned septa and irregular spirals. These defects phenocopy those of mutants defective in a NDR kinase pathway required for cell polarization called MOR, and it was determined that MST-1 also interacted with the central MOR kinases POD-6 and COT-1. MST-1 functions as promiscuous enzyme by activating the SIN and MOR effector kinases DBF-2 and COT-1. Moreover, crosstalk of the SIN and MOR pathways is also achieved by heterodimer formation between DBF-2 and COT-1. The multiple levels of cross-communication between the SIN and MOR identified in this study and other model systems such as *S. pombe* or *D. melanogaster*, suggest the possibility that the antagonistic interactions between homologous NDR kinase networks may be a general mechanism to coordinate these pathways in higher organisms.

The annotation of multiple fungal genomes revealed the presence of several genes homologous to the bud site selection genes of budding yeast. Epistasis and biochemical analysis revealed that the MOR functions as negative regulator upstream of the BUD complex and COT-1, but not DBF-2 phosphorylates BUD-3/BUD-4 landmark proteins. Thus, regulation of BUD-3 (and possibly also BUD-4) by COT-1 may be one mechanism of the MOR pathway to inhibit septum formation in *N. crassa*.

2. Zusammenfassung

Die Zellteilung/Zytokinese ist ein grundlegender zellulärer Prozess und essentiell für das Wachstum von einzelligen und mehrzelligen Organismen. Reguliert wird dieser Prozess durch komplexe molekulare Mechanismen sowie einer Vielzahl von interaktiven Netzwerken. In Pilzen koordiniert eine Kinase-Kaskade, das Septierungs-Initiierungs Netzwerk (SIN) das Fortschreiten des Zellzyklus mit dem Beginn der Zellteilung und kontrolliert die Septenbildung. Fehlregulation des homologen Hippo Netzwerks in Tieren führt zu Gewebewucherungen und Tumorbildung, was die konservierte Bedeutung dieser Regulationsnetzwerke in verschiedenen Organismen unterstreicht. Obwohl die Septenbildung essentiell für das Wachstum und die Differenzierung von Schimmelpilzen ist, bleibt die Frage wie die Septierung reguliert wird und aus welchen Komponenten sich das SIN Netzwerk in filamentösen Pilzen zusammensetzt bisher noch unbeantwortet.

Mit Hilfe von *in silico* Analysen konnten homologe Proteine für fast alle SIN Netzwerk Komponenten im Modellorganismus *Neurospora crassa* identifiziert werden. Die Analyse dieser vorhergesagten SIN Komponenten ermöglichte die Charakterisierung der SIN-Kinase-Kaskade, bestehend aus CDC-7, SID-1 und DBF-2 sowie den entsprechenden, regulatorischen Untereinheiten CDC-14 und MOB-1. Es konnte gezeigt werden, dass DBF-2 durch SID-1 am hydrophoben Motiv phosphoryliert und aktiviert wird und dass eine SID-1 abhängige Stimulation von DBF-2 durch Zugabe von CDC-7 weiter gesteigert wird. Diese Daten liefern den ersten biochemischen Nachweis für die schrittweise Aktivierung einer dreistufigen SIN-Kinase-Kaskade in Pilzen. Es wurde weiterhin gezeigt, dass die gesamte SIN Kaskade konstitutiv und Zellzyklus unabhängig an den Spindelpolkörpern akkumuliert und dass alle SIN Proteine an kontrahierenden Septen lokalisieren. Demzufolge ist im Gegensatz zu den einzelligen Pilzen die Lokalisation und Aktivität der SIN Komponenten in Synzytium-bildenden Ascomyzeten Zellzyklus unabhängig. Darüber hinaus deutet die Charakterisierung von DBF-2 Mutanten, in denen die beiden regulatorischen Aminosäuren (Ser499 and Thr671) mutiert sind, darauf hin, dass ein dynamischer Phosphorylierungs-/Dephosphorylierungszyklus des Ser499 entscheidend für die Aktivität und Funktion von DBF-2 in *N. crassa* ist. Diese Daten haben Einfluss auf das allgemeine Verständnis der Aktivierung von NDR Kinasen, denn bisher wurde für NDR Kinasen höherer Eukaryonten eine folgegebundene Phosphorylierung beider regulatorischer Reste angenommen.

Der Ste20-verwandten Kinase MST-1 konnte eine Funktion als SIN-assoziierte Kinase, die parallel zu SID-1 agiert, zugeordnet werden. SID-1 und MST-1 werden auf entgegengesetzte Weise von der oberhalb agierenden SIN Kinase CDC-7 reguliert, was nahelegt, dass MST-1 für die Feinabstimmung des SIN erforderlich ist. Lifeact- und Formin-GFP Reporter Konstrukte zeigten, dass in der Δ*mst-1* Mutante abnormale, kortikale Actomyosin-Ringe gebildet werden, was eine Fehlpositionierung der Septen und die Bildung von unregelmäßigen Spiralen zur Folge hat. Diese Defekte entsprechen partiell jenen der MOR Mutanten. Diese Mutanten weisen ein defektes NDR Kinase Netzwerk auf, welches für das polare Wachstum verantwortlich ist (MOR). Es stellte sich heraus, dass MST-1 mit den zentralen MOR Kinasen POD-6 und COT-1 interagiert und sowohl die SIN Effektor Kinase DBF-2 als auch die MOR Effektor Kinase COT-1 aktiviert. Somit fungiert MST-1 als dual-spezifisches Enzym. Eine weitere Vernetzung beider Signalwege ist durch die Bildung von Heterodimeren gegeben.

Die in dieser Studie identifizierten verschiedenen Ebenen der Vernetzung des SIN und MOR, sowie entsprechende Daten aus anderen Modellorganismen wie *S. pombe* und *D. melanogaster*, lassen vermuten, dass antagonistische Interaktionen zwischen homologen NDR Kinase Netzwerken ein genereller Mechanismus zur Koordination beider Signalwege darstellt und auch in höheren Organismen konserviert ist.

Durch die Annotierung mehrerer Pilzgenome wurden zahlreiche Gene mit einer Homologie zu den *S. cerevisiae* BUD Genen auch in filamentösen Pilzen identifiziert. Epistatische und biochemische Analysen ergaben, dass das MOR Netzwerk als negativer Regulator der Septenbildung oberhalb des BUD komplex fungiert und dass COT-1 im Gegensatz zu DBF-2, die beiden Septierungsmarkerproteine BUD-3/BUD-4 phosphoryliert. Folglich könnte die Regulation von BUD-3 (und eventuell auch BUD-4) durch COT-1 ein Mechanismus des MOR Netzwerks sein, um die Septenbildung in *N. crassa* zu inhibieren.

3. Introduction

Cytokinesis is a fundamental cellular process essential for cell proliferation of unicellular and multicellular organisms. It is the final stage of the cell cycle, during which a cell is physically divided into two daughter cells that contain a full set of chromosomes and other cellular organelles. Research on eukaryotic cytokinesis using advantageous model systems like *Drosophila melanogaster, Caenorhabditis elegans* and yeasts are continuously enlarging our understanding of most aspects of the process. Cytokinesis is a crucial step in cell proliferation, and remarkably, it is also an important mechanism for developmental regulation in the generation of diverse cell types in eukaryotic organisms. In all eukaryotic species except plants, successful cytokinesis relies on the assembly and activation of an actomyosin-based contractile ring and membrane deposition/fusion in a spatially and temporally precise manner. The molecular pathways regulating cytokinesis are highly complex and involve a large number of components forming elaborate interactive networks. The complexity of this system, however, may have also provided a rich platform for evolutionary variation to achieve specific morphogenetic and developmental outcomes. As an irreversible event, defective cytokinesis can alter cell geometry or size, prevent the accurate transmission of the genetic material, causing polyploidy, which can affect the survival of unicellular species or favor cancer and tumor progression in animal species. Thus, spatial and temporal regulation of cytokinesis is important for cell fate establishment in several developmental contexts across kingdoms.

3.1 The spatial cue - mechanisms specifying the position of the division plane

Spatial regulatory pathways define the position of the division plane depending on the position of the nucleus at mitotic entry, the cell divisional history or the mitotic apparatus. Moreover, in many eukaryotic organisms, cytokinesis is strictly coordinated with mitotic progression in order to successfully fulfill chromosome segregation. The regulatory pathways that control the spatial aspects of division plane positioning are poorly conserved among different organisms (Laporte *et al.*, 2010, Pollard & Wu, 2010, Balasubramanian *et al.*, 2012). For instance, in animal cells, the division site is determined by the orientation of the mitotic spindle, while in the budding yeast *Saccharomyces cerevisiae*, the division site positioning mechanism is based on the cell divisional history. In contrast, the selection of the division site in the fission yeast *Schizosaccharomyces pombe* depends on the position of the nucleus and inhibitory signals generated from the cell ends.

In *S. cerevisiae* the division site of the previous cell cycle (bud scar) is used as a cue to determine the position for initiating growth and cytokinesis. Distinct landmark proteins mark the axial (Bud3p, Bud4p, Axl1p and Axl2p/Bud10p) and bipolar (Bud8p, Bud9p, Rax1p and Rax2p) division sites (Casamayor & Snyder, 2003, Balasubramanian *et al.*, 2004, Oliferenko *et al.*, 2009). The axial landmark Bud4p contains the conserved anillin-homology (AH) domain, which is located adjacent to the putative pleckstrin homology (PH) domain as in other anillin-related proteins such as Mid1 and Mid2 in *S. pombe* (Berlin *et al.*, 2003, Tasto *et al.*, 2003). The AH domain of Bud4p is important for its association with Bud3p and other components of the axial landmark (Kang *et al.*, 2013). Thus, based on the cell divisional history, the bud-site-selection machinery predefines the position of the future division site and serves to recruit other components to the CAR. In contrast, CAR assembly in fission yeast relies on the position of anillin-containing nodes as precursors of the CAR (Wu *et al.*, 2006, Vavylonis *et al.*, 2008). Nodes distribution is restricted to the medial cortex by negative signals from the cell ends and a positive local influence provided by the nuclear position (Laporte *et al.*, 2011, Martin, 2009, Moseley *et al.*, 2009, Almonacid *et al.*, 2009). Both, positive and negative regulatory mechanisms promote the specific association of the anillin-like protein Mid1 to the medial cortex, where it predefines the position of the division site and serves to recruit other components for CAR assembly, thereby establishing the division site (Bahler *et al.*, 1998, Paoletti & Chang, 2000, Moseley et al., 2009, Almonacid et al., 2009).

In animal cells, the orientation of the mitotic spindle dictates the position of the division site. In smaller cells, such as somatic cells, the midzone of the mitotic spindle signals to the cortex to promote cytokinetic furrow assembly (Cao & Wang, 1996, Bonaccorsi *et al.*, 1998, Giansanti *et al.*, 2001). By contrast, in larger cells, such as in embryos, the cleavage furrow is positioned by astral microtubules, which originate from the spindle poles, and are thought to transport signals that promote cytokinetic furrow formation (Rappaport, 1961, Rappaport, 1985, Barr & Gruneberg, 2007). Moreover, microtubule asters have been shown to inhibit myosin recruitment at cell poles, promoting contractility at the cell equator (Werner *et al.*, 2007). Moreover, recent studies suggest that anillin might act early in cytokinesis as scaffolding protein to recruit other components of the CAR to the division site (Oegema *et al.*, 2000, Piekny & Glotzer, 2008, D'Avino, 2009, Zhang & Maddox, 2010). Thus, while using conserved components, different strategies of controlling division plane positioning have emerged to ensure the successful segregation of the genetic material in the two cellular compartments generated during cytokinesis.

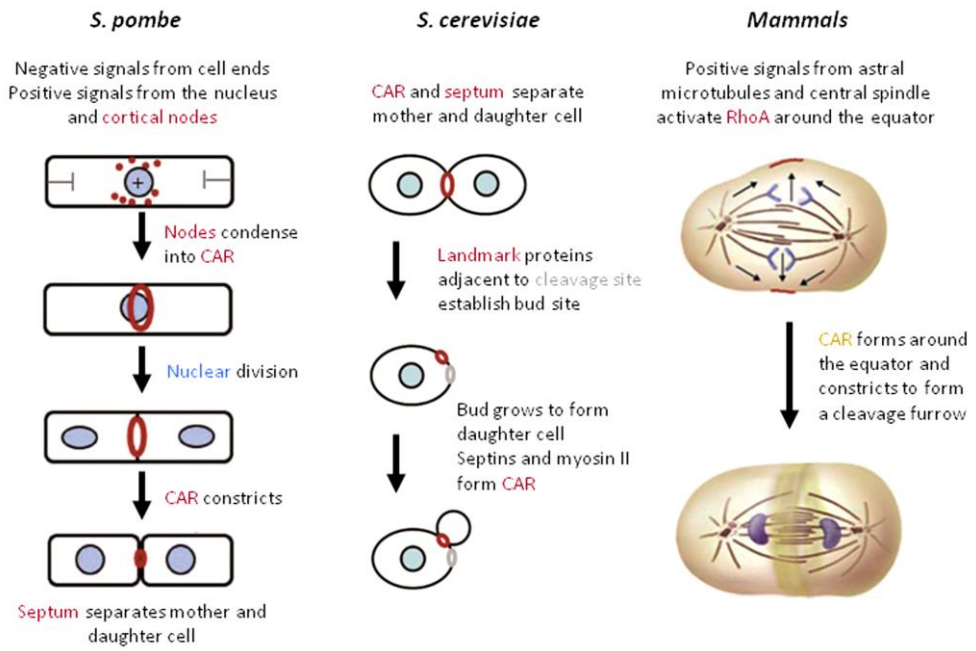

Figure 1: Division site selection and contractile ring assembly in *S. pombe*, *S. cerevisiae* and mammals (modified from Pollard, 2010).

3.2 Assembly and constriction of the contractile actomyosin ring (CAR)

Animal and fungal cells use an actin/myosin-based contractile ring (CAR) placed at a chosen division site to accomplish cytokinesis (Figure 1). Although the majority of proteins that contribute to CAR assembly are evolutionary conserved from yeast to animals, their specific use during the establishment of the CAR is distinct (Park & Bi, 2007, Pollard & Wu, 2010). Research on fungal model organisms has led to the functional characterization of many proteins involved in CAR assembly. Both yeasts establish a CAR during mitosis and its assembly is well understood in the fission yeast *S. pombe* and occurs in the medial cortex by the ordered recruitment of the anillin-like protein Mid1 and other ring components (Laporte et al., 2011, Wu *et al.*, 2003, Wu et al., 2006, Vavylonis et al., 2008, Pollard & Wu, 2010). Mid1 accumulates prior to spindle pole body separation at the future division site, forming a broad band of nodes that defines the site for recruitment of ring components. Subsequently, most ring components arrive at the division site within minutes of each other. Type II myosin Myo2 is anchored at the medial cortex through its interaction with Mid1, which is followed by cortical accumulation of the two myosin light chains Cdc4 and Rlc1. Next, the IQGAP protein Rng2 and the F-BAR protein Cdc15 join the broad band of nodes. Cdc15 interacts through its F-BAR domain with the formin Cdc12 and type I myosin Myo1, thereby coordinating medial F-actin nucleation (Carnahan & Gould, 2003, Roberts-Galbraith *et al.*, 2009, Laporte et al., 2011, Padmanabhan *et al.*, 2011).

The basic composition of the *S. cerevisiae* actomyosin ring is very similar but the order of assembly of the ring components is different and CAR components accumulate over long time periods (Luo *et al.*,

2004, Shannon & Li, 2000, Wloka & Bi, 2012, Balasubramanian et al., 2004, Bi *et al.*, 1998, Lippincott & Li, 1998). In budding yeast the CAR assembles at the bud neck (the constriction site between mother and daughter cells) and depends on a family of small GTPases called the septins (Gladfelter *et al.*, 2001, McMurray & Thorner, 2009). In contrast, fission yeast septins localize to the division plane only after the CAR has formed. They serve as positional markers to target secretory vesicles for the dissolution of the primary septum (Longtine *et al.*, 1996, Berlin et al., 2003, Tasto et al., 2003, An *et al.*, 2004, Martin-Cuadrado *et al.*, 2005). The second anillin homologue Mid2 in fission yeast, organizes the septin ring during late mitosis and thereby promotes cell separation as the final step of cytokinesis (Berlin et al., 2003, Tasto et al., 2003, An et al., 2004).

Less is known about CAR assembly in animal cells, but the overall impression is that the strategy is similar to fission yeast. Myosin-II concentrates in cortical node-like patches, followed by formin assembling actin filaments around the equator (Zhou & Wang, 2008, Noguchi & Mabuchi, 2001). The Rho-family GTPase RhoA plays a central role in the CAR assembly in animal cells. The RhoGEF Ect2 activates RhoA which in turn activates mDia formins and ROCK and Citron kinases, promoting F-actin polymerization and myosin II contractility at the equatorial cortex, leading to CAR assembly and constriction (Somers & Saint, 2003, Nishimura & Yonemura, 2006). Furthermore, the RacGAP stabilizes the contractile ring by binding to anillin, which also interacts with other components of the CAR, myosin-II, F-actin and septins, thereby acting as scaffold for RhoA signalling and CAR assembly (Gregory *et al.*, 2008, Field & Alberts, 1995, Straight *et al.*, 2005, Oegema et al., 2000). This dual function of anillin is very reminiscent of *S. pombe* Mid1, which takes part in division-plane signalling and scaffolding CAR components during assembly.

3.3 The temporal cue - the SIN/MEN network coordinates mitosis and cytokinesis

While the position of the anillin-related proteins (Mid1 nodes and cortical Bud4 landmark complexes) provides the spatial cues for cytokinesis in fission and budding yeast, respectively, the temporal coordination of mitosis and cytokinesis is mediated by a signalling cascade known as the septation initiation network (SIN) (Gould & Simanis, 1997, Simanis, 2003, Wolfe & Gould, 2005). This network is analogous to the mitotic exit network (MEN) of budding yeast with two differences; first, the MEN lacks a homolog of the fission yeast Ste20-related kinase Sid1, thus the effector kinase Dbf2p is directly phosphorylated by Cdc15p (Mah *et al.*, 2001). Second, budding yeast MEN mutants arrest late in the mitotic cell cycle, while the fission yeast SIN is not essential for mitotic exit, and SIN mutants generate one of two phenotypes: multinucleate cells or multiseptated cells that fail in cell cleavage. The former phenotype is caused by SIN inactivation; the latter phenotype results from SIN hyperactivity (Minet *et al.*, 1979, Fankhauser & Simanis, 1994, Ohkura *et al.*, 1995, Schmidt *et al.*,

1997). Both scenarios uncouple cell division from nuclear division; thus, the SIN coordinates cytokinesis with other cell cycle phases. Also mammals utilize a highly conserved signalling module (Hippo) analogous to the central components of the yeast SIN/MEN, but the regulatory mechanisms and the involvement of the Hippo core cassette in mitotic exit, cytokinesis and morphogenesis are not yet fully understood.

3.3.1 Composition and regulation of the SIN

The SIN consists of a cascade of three kinases that associate with spindle pole bodies (SPB; the yeast counterpart of the centrosome), via the scaffolding proteins Sid4 and Cdc11 (Krapp & Simanis, 2008). The central sensor of the SIN is the GTPase Spg1, which is activated by the kinase Plo1 that phosphorylates and thereby likely inhibits the bipartite GTPase activating protein (GAP) Cdc16–Byr4 at the end of mitosis (Tanaka *et al.*, 2001, Krapp & Simanis, 2008). Spg1 activation triggers the localization of the Ste20-related kinase Cdc7 (homologue of budding yeast Cdc15p), resulting in the assembly and activation of the downstream kinases Sid1 and Sid2 and their respective regulatory subunits Cdc14 (no relation to its *S. cerevisiae* namesake) and Mob1 at the SPB. Active Sid2 (the homologue of budding yeast Dbf2p) phosphorylates and activates the phosphatase Clp1, thereby promoting mitotic exit and cytokinesis by counteracting the function of Cdk1 (cyclin dependent kinase 1) (Reynolds & Ohkura, 2003, Chen *et al.*, 2008).

So far, no biochemical evidence for direct targets of the Ste20-related kinases Cdc7 and Sid1 are provided, although by analogy to the *S. cerevisiae* homologs, the NDR (nuclear Dbf2-related) kinase Sid2 is a potential candidate. NDR kinases represent a subcategory of the AGC group of protein kinases, and possess the typical features of this kinase family; the activation segment (AS) and the C-terminal hydrophobic motif phosphorylation site (HM), both essential for catalytic activity (Millward *et al.*, 1999). NDR kinases are regulated by autophosphorylation within the AS, resulting in basal kinase activity (Bichsel *et al.*, 2004, Tamaskovic *et al.*, 2003). For full catalytic activity, a second phosphorylation event within the HM is required, which is targeted by an upstream kinase. In budding yeast, Cdc15p's direct phosphorylation of Dbf2p's C-terminal HM site is a key part of MEN activation (Hergovich & Hemmings, 2009, Emoto, 2011).

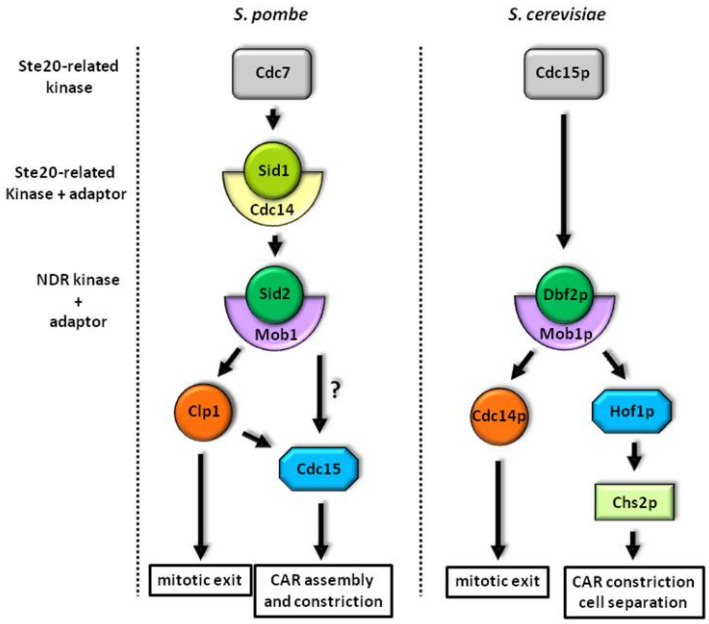

Figure 2: Highly conserved signalling components of the septation initiation network (SIN) in *S. pombe* and the homologous mitotic exit network (MEN) in *S. cerevisiae*. For details see text.

3.3.2 Functions of the SIN in cytokinesis

In addition to the importance of the SIN for providing the temporal cue for CAR constriction, the SIN is also essential for CAR assembly. In the absence of Mid1, fission yeast cells can assemble a functional CAR, though inefficiently and at random locations (Sohrmann *et al.*, 1996, Chang & Nurse, 1996). In this case, CAR assembly is strictly dependent on the activity of the SIN, suggesting that both pathways cooperate in parallel to regulate CAR assembly (Balasubramanian *et al.*, 1998, Wu et al., 2003). *mid1* mutants assemble ectopic rings in anaphase when the SIN becomes active, implying that the major function of Mid1 is to direct CAR assembly to the correct location (Chang & Nurse, 1996, Sohrmann et al., 1996). In contrast SIN-defective mutants form a CAR in early mitosis, which dissolves again in anaphase, suggesting that SIN signalling is required for CAR maintenance/assembly in late mitosis (Balasubramanian et al., 1998). Disrupting both *mid1* and the SIN blocks CAR assembly completely, indicating that each pathway makes important contributions to CAR assembly (Hachet & Simanis, 2008, Huang *et al.*, 2008).

The only SIN component that localizes to the SPBs and the CAR is the terminal SIN kinase Sid2. One reported Sid2 target at the CAR is the Cdc14-like phosphatase Clp1 (Chen et al., 2008). In addition to the essential function of Clp1 in regulating cell cycle progression by inhibition of mitotic CDK activity , Clp1-dependent dephosphorylation of the *S. pombe* PCH-family protein Cdc15 is essential for CAR assembly (Clifford *et al.*, 2008, Roberts-Galbraith *et al.*, 2010, Trautmann *et al.*, 2001). The budding yeast MEN is also required for CAR constriction, yet not its assembly (Vallen *et al.*, 2000, Lippincott *et*

al., 2001). Several studies suggested that the MEN promotes cytokinesis by influencing multiple pathways involved in CAR constriction and septum formation. For instance, the MEN is involved in targeting the Chitin synthase Chs2p to the bud neck (Meitinger *et al.*, 2010) and also directly regulates the late cytokinetic components Hof1p/Cyk2p and Inn1p (both are PCH proteins and homologs of *S. pombe* Cdc15; Figure 2; (Sanchez-Diaz *et al.*, 2008, Nishihama *et al.*, 2009, Meitinger et al., 2010, Meitinger *et al.*, 2011).

3.3.3 Crosstalk between the SIN and MOR NDR kinase pathways

Another fundamental mechanism by which the SIN promotes cytokinesis is the inhibition of a competing polarity pathway called the MOR (morphogenesis-related NDR kinase network), which is required for initiation of polarized growth following completion of cytokinesis (Gupta & McCollum, 2011, Ray *et al.*, 2010). Mutants in any of the MOR components fail to grow in a polarized manner resulting in a round morphology of the cells. The MOR signalling pathway represents the second NDR kinase network with an analogous organization similar to the SIN. The MOR includes the NDR kinase Orb6 with its binding partner Mob2 and its upstream activator the Ste20-related kinase Nak1 (Figure 3; (Verde *et al.*, 1998, Hou *et al.*, 2003, Kanai *et al.*, 2005, Kume *et al.*, 2007, Leonhard & Nurse, 2005, Huang *et al.*, 2003). The scaffolding protein Mor2 is thought to promote the activation of Orb6 by Nak1 (Hirata *et al.*, 2002). Also, Pmo25 has been identified as a binding partner of Nak1 and is essential for the activities of both kinases in the pathway (Kanai et al., 2005). In a recent study Lrp1 (budding yeast Sog2 homolog) was also identified as a MOR component and suggested to form a complex with Nak1 and to act upstream of Orb6 (Kume *et al.*, 2013).

Mutual antagonism between the two NDR kinase pathways, the SIN and MOR, is required to coordinate cell growth and division. To promote polarized growth, actin is confined to the cell ends where it is required for cell wall deposition. As cells enter mitosis, actin relocalizes to site of cell division to form the CAR (Marks *et al.*, 1986). Since, both processes involve restructuring of the actin cytoskeleton, coordination is presumably important to keep competing actin polarity programs from interfering with each other. This view is supported by a recent study, which indicated that phosphorylation of Nak1 by Sid2 (SIN-associated NDR kinase) promotes SIN activation and inhibits MOR-mediated polarized growth by blocking interaction of Nak1 with the scaffold protein Mor2 (Gupta *et al.*, 2013). In addition, it has been reported that *S. cerevisiae* MEN and RAM networks (Regulation of Ace2p and morphogenesis; homologous to *S. pombe* MOR) function together to regulate the Ace2 transcription factor during cell separation (McCollum & Gould, 2001, Maerz & Seiler, 2010, Weiss *et al.*, 2002).

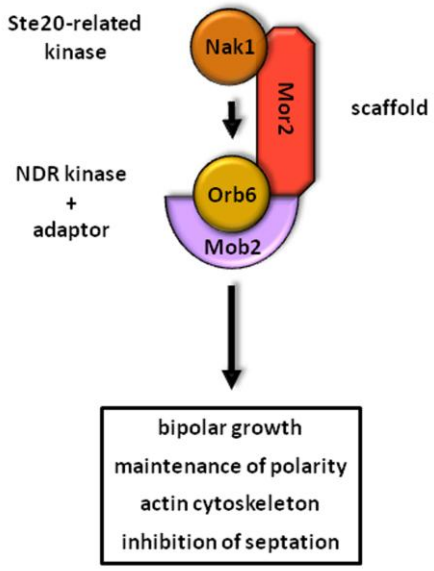

Figure 3: Highly conserved signalling components of the morphogenesis-related NDR kinase network (MOR) in *S. pombe*. For details see text.

3.4 Septation in filamentous fungi

Filamentous fungi represent the vast majority of the fungal kingdom. However, despite the importance of septum formation for growth and differentiation of molds, our understanding of septum formation and its regulation in molds is highly fragmentary. In contrast to unicellular yeast, mitosis is not evidently linked with cytokinesis/septation in filamentous fungi, resulting in the formation of multinuclear hyphal compartments (Harris, 2001, Gladfelter, 2006). In conformity with both yeasts, the CAR presumably guides deposition of the septal wall material, but unlike in yeasts, the septum is subsequently not degraded and cells remain attached. Furthermore, in most filamentous fungi, a small pore is retained to enable intercellular communication and transport of cytoplasm and organelles between adjacent hyphal compartments (Gull, 1978, Madhani & Fink, 1998, Pringle & Taylor, 2002). The controlled partitioning of hyphal units through septal cross-walls in a multicellular context is the basis for the morphological complexity achieved by filamentous fungi. Moreover, septation in molds is required for certain developmental processes, such as conidiation (asexual spore production) and protoperithecial (female sexual structure) development (Gull, 1978).

3.4.1 Division site selection and CAR assembly in filamentous fungi

At the beginning of this thesis work, not much was known about how filamentous fungi select the division site and control assembly of the CAR. The annotation of multiple fungal genomes revealed the presence of several genes homologous to the *S. cerevisiae BUD* genes. The functional analysis of these *BUD* genes in various filamentous fungi like *Ashbya gossypii* (AgBud3), *Candida albicans* (Int1)

and *Aspergillus nidulans* (Bud3 and Bud4) indicate a general function of anillin-related proteins during septum formation (Gale *et al.*, 2001, Walther & Wendland, 2003, Kaufmann & Philippsen, 2009, Si *et al.*, 2010). However, considerable differences exist in the specific use of BUD proteins during the establishment of the future septation site and CAR assembly in organisms from different ascomycete clades.

The *N. crassa* proteins BUD-3 and BUD-4 are essential for septum formation. BUD-4 appears prior to the formation of a detectable septum by forming motile cortical dots in internal regions of the hypha that subsequently coalesce into a cortical ring. In *bud-3* and *bud-4* mutants no CAR is formed, and consequently hypha lack septa (Justa-Schuch *et al.*, 2010). Septum formation in *N. crassa* and *A. nidulans* is at least partially controlled by the small Rho-type GTPases Rho4 which is activated by its specific guanine nucleotide exchange factor (GEF) Bud3 (Rasmussen & Glass, 2005, Rasmussen & Glass, 2007, Justa-Schuch et al., 2010, Si et al., 2010). In *A. nidulans and N. crassa*, AnBud3/BUD-3 and AnRho4/BUD-4 were recently defined as essential components of a GTPase module that direct CAR assembly during septation (Si et al., 2010, Justa-Schuch et al., 2010). Coinciding, the localization of BUD-3 prior to septum formation depends on the presence of BUD-4 and both proteins recruit RHO-4 to the division site. Deletion of either BUD-3 or RHO-4 result in aseptated strains indicating the indispensable function of both proteins during septation (Justa-Schuch et al., 2010, Seiler & Justa-Schuch, 2010).

3.4.2 The SIN and MOR pathways in filamentous fungi

Intriguingly, recent studies confirmed that most components of the fission yeast SIN are also present in the filamentous fungi *A. nidulans* and *N. crassa* (Figure 4). Deletion of any positive network component results in aseptate strains, indicating that SIN function is essential for septum formation (Bruno *et al.*, 2001, Harris, 2001, Harris *et al.*, 1994, Kim *et al.*, 2009, Dvash *et al.*, 2010, Maerz *et al.*, 2009). *A. nidulans* SidB and its co-activator MobA (orthologues of *S. pombe* Sid2 and Mob1) localize to the SPB and the forming septum and function upstream of CAR assembly in response to unknown mitotic signals (Bruno et al., 2001, Kim *et al.*, 2006). Furthermore, AnBud3 is not recruited to incipient septation sites in conditional *SepH1* (homolog to *S. pombe* Cdc7) mutants at restrictive temperature, suggesting a SIN function upstream of the AnBud3–AnRho4 module (Si et al., 2010). However, despite the essential role of the SIN in CAR assembly and septum formation, no function in mitosis is described for the SIN in *A. nidulans* (Bruno et al., 2001, Kim et al., 2006, Kim et al., 2009).

In addition to these positive regulators of septum formation, several negative regulators were identified in filamentous fungi. Most notably are *N. crassa* POD-6, COT-1 and MOB-2A/B (orthologues of *S. pombe* Nak1, Orb6 and Mob2), the central elements of the *N. crassa* MOR network, which controls maintenance of cell polarity (Yarden *et al.*, 1992, Seiler *et al.*, 2006, Maerz et al., 2009).

Deletion of any negative MOR component results not only in loss of polarity, but also in hyperseptation, indicating that the MOR is involved in septum formation and antagonizes SIN function (Seiler & Plamann, 2003). In addition to the pathway-specific accumulation of MOR proteins at the site of polarization, all MOR components localize to forming septa, further supporting MOR function during septation (Vogt & Seiler, 2008, Richthammer *et al.*, 2012, Maerz *et al.*, 2012, Dettmann *et al.*, 2012).

3.5 Aims of this work

Proper cell division is essential for growth and development of uni- and multicellular organisms. In unicellular yeasts, spatial regulatory pathways define the position of the division plane, while the temporal coordination of mitosis and cytokinesis is mediated by the SIN. A mechanistic picture how SIN proteins transmit signals through the cascade to trigger CAR assembly and constriction is only beginning to be understood. Moreover, our understanding of septum formation and its regulation in filamentous fungi is highly fragmentary. However, the functional connection between the competing SIN and MOR pathways and the mechanisms that define septum placement are poorly understood. Thus, the aim of this study was to establish a relationship between both NDR kinase pathways and the essential landmark proteins BUD-3 and BUD-4. This aim further implied the characterization of the SIN network and the analysis of key regulatory phosphorylation sites of the NDR kinase DBF-2.

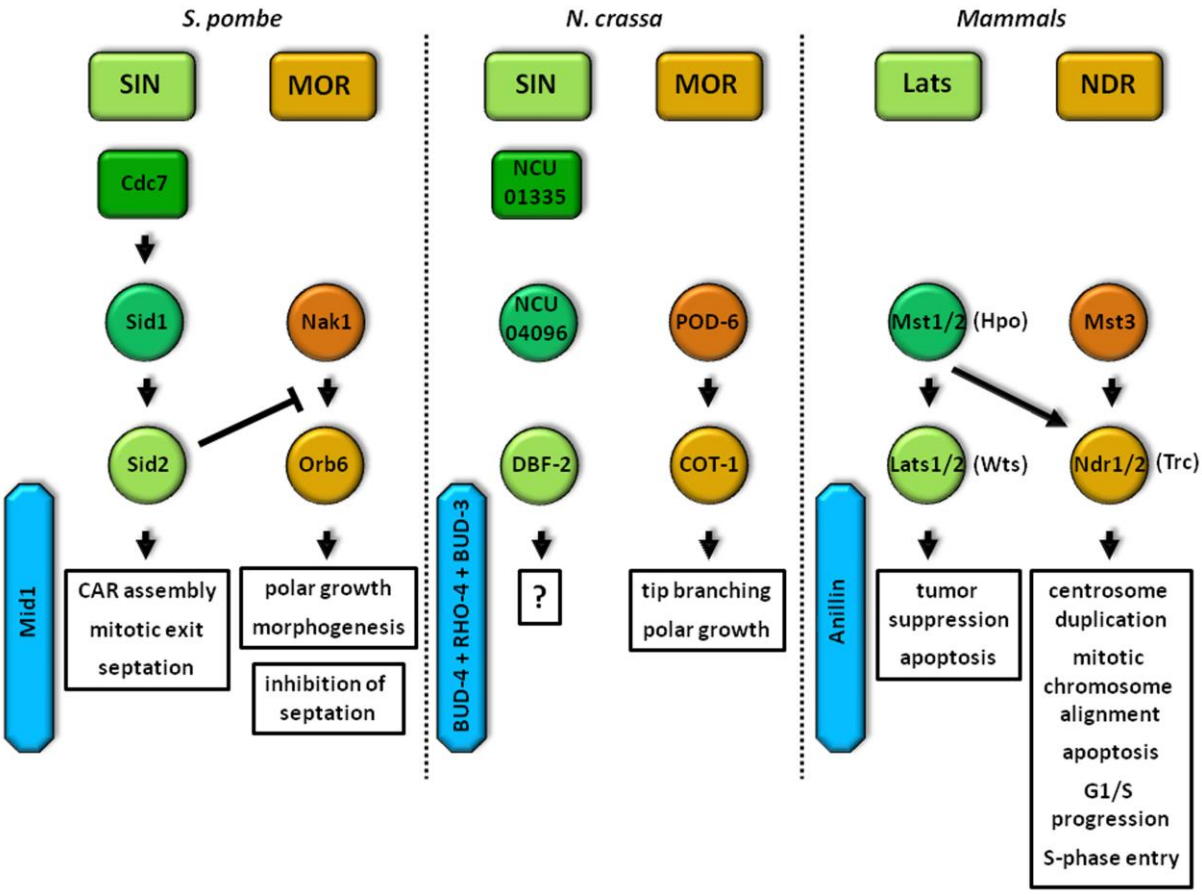

Figure 4: Comparison of highly conserved NDR signalling pathways in *S. pombe*, *N. crassa* and mammals. *D. melanogaster* orthologous Hippo core components are shown in brackets. See text for details.

4. Materials and Methods

4.1 Media and growth conditions

Standard chemicals and culture media components used in this study were obtained from AppliChem GmbH, Carl Roth GmbH & Co. KG, Invitrogen GmbH and Sigma-Aldrich Chemie GmbH (all Germany).

General handling of growth and genetic manipulation of *Neurospora crassa* was accomplished as described in (Davis, 1970) or in protocols provided by the Fungal Genetics Stock Center at http://www.fgsc.net.

Escherichia coli DH5α cells were grown on solid (with 1.5% agar) or in liquid LB medium (1% NaCl, 0.5% yeast extract, 1% tryptone) modified from (Bertani, 1951). For selection media 100 µg/ml ampicillin or 50 µg/ml kanamycin were added (all from Sigma-Aldrich, Taufkirchen, Germany). Cultures were incubated at 37°C.

Saccharomyces cerevisiae was grown at 30°C under non-selective conditions in Yeast Extract Peptone Dextrose (YEPD) medium (2% peptone, 1% yeast extract, 2% glucose, for solid medium 2% agar was added) or in Synthetic Defined (SD) minimal medium lacking several amino acids for selection of plasmid expression or interaction in the yeast two-hybrid assay (0.17% yeast nitrogen base (w/o amino acids, w/o ammonium sulphate), 0.5% ammonium sulphate, 10mg L-adenine sulphate, 10mg L-argenine, 10mg L-histidine, 15mg L-isoleucine, 50mg L-leucine, 15mg L-lysine, 10mg L-methionine, 25mg L-phenylalanine, 100mg L-threonine, 10mg L-tryptophane, 15mg L-tyrosine, 10mg uracil and 75mg L-valine, 2% glucose, 2% agar)(see also section 4.6).

Neurospora crassa strains were cultured on solid (with 2% (w/v) agar) or in liquid Vogel 's Minimal Medium (VMM) (Vogel, 1956, Vogel, 1964) with 2% (w/v) sucrose. Crosses were made on solid medium containing 2% corn meal agar (Sigma, St. Louis, USA) and 0.1% glucose (w/v) to induce protoperithecia formation in the female parent before inoculation with the male parent. For auxotrophic strains, culture media were supplemented with 150 µg/ml histidine, and for selection of resistant strains, 200 µg/ml hygromycin B (InvivoGen, USA), 15 µg/ml nourseothricin (Werner BioAgents, Jena, D) and 200 µg/ml glufosinate-ammonium (Sigma-Aldrich, Taufkirchen, Germany) were used. Cultures were grown at 37°C, whereas temperature sensitive strains were usually propagated at 20-25°C unless stated otherwise.

4.2 Plasmid construction

4.2.1 General procedure

DNA sequences of predicted genes were obtained from the Broad Neurospora crassa Database www.broadinstitute.org. Cloning procedures were designed and documented using the DNASTAR® SeqBuilder (Version 8.0.3(1); DNASTAR, Inc., USA). DNA fragments amplified by polymerase chain reaction (PCR) were first subcloned into vector pJet1.2 blunt of the CloneJET™ PCR Cloning Kit (Fermentas GmbH, Germany). Accuracy of resulting plasmids was ensured by restriction digests and complete sequencing of inserts. After ligation of inserts into the respective end vector, plasmids again were checked by restriction digests and inserts were reconfirmed by sequencing.

Primers and plasmids used in this study are listed in Table 1 and Table 2, respectively.

Table 1: Primers used in this study. Restriction enzyme recognition sites are bold and underlined, mismatched nucleotides for insertion of mutations are depicted in lower, italic letters.

Primer name	Sequence 5‘- 3‘
Point mutation constructs:	
YH-DBF2-T2E-forw	GAG CTT GTT TGT CGG ATT C*ga g*TT CCG TCA TCG CAA GCC GG
YH-DBF2-T2E-rev	CCG GCT TGC GAT GAC GGA A*ct c*GA ATC CGA CAA ACA AGC TC
YH-DBF2-T2A-forw	GAG CTT GTT TGT CGG ATT C*gc c*TT CCG TCA TCG CAA GCC GG
YH-DBF2-T2A-rev	CCG GCT TGC GAT GAC GGA Agg cGA ATC CGA CAA ACA AGC TC
YH-DBF2-S2E-forw	GAT ACC AAC TAC GCC AAG *gag* ATT GTT GGA TCT CCA GAC TAC
YH-DBF2-S2E-rev	GTA GTC TGG AGA TCC AAC AAT *ctc* CTT GGC GTA GTT GGT ATC
YH-DBF2-S2A-forw	GGA TAC CAA CTA CGC CAA G*gc g*AT TGT TGG ATC TCC AGA CTA C
YH-DBF2-S2A-rev	GTA GTC TGG AGA TCC AAC AAT *cgc* CTT GGC GTA GTT GGT ATC C
YH-DBF2-D2A-forw	CTG GGT TAC ATT CAT CGC *gca* CTC AAG CCG GAG AAC TTC C
YH-DBF2-D2A-rev	GGA AGT TCT CCG GCT TGA G*tg c*GC GAT GAA TGT AAC CCA G
YH-CDC7-D2A-forw	ATG GCA CCG TCA AGT TAG CA*g cc*T TTG GCG TGT CAA CCA GCA C
YH-CDC7-D2A-rev	GTG CTG GTT GAC ACG CCA AA*g gc*T GCT AAC TTG ACG GTG CCA T
YH-BUD3-S2A-f	GGC CAT AAG CGC TCA CAA *gcc* GCG TCC CCC GTC AAG TTG
YH-BUD3-S2A-rev	CAA CTT GAC GGG GGA CGC *ggc* TTG TGA GCG CTT ATG GCC
YH-BUD3-S2E-f	GGC CAT AAG CGC TCA CAA *gag* GCG TCC CCC GTC AAG TTG

Primer name	**Sequence 5‘- 3‘**
YH-BUD3-S2E-rev	CAA CTT GAC GGG GGA CGC *ctc* TTG TGA GCG CTT ATG GCC
YH-BUD4-S2A-1-f	GGT GCA TCC CCT *ccg* CCT TGC CAA GGG CAA CAC TAT GCC
YH-BUD4-S2A-1-rev	GGC ATA GTG TTG CCC TT*g gc*A AGG CGG AGG GGA TGC ACC
YH-BUD4-S2A-2-f	GTG GCC ATG GGA GGA GCC AA*g cc*A GCA CCA GCA TCC CCG TC
YH-BUD4-S2A-2-rev	GAC GGG GAT GCT GGT GCT *ggc* TTG GCT CCT CCC ATG GCC AC
YH-BUD4-S2A-3-f	CGC CAC CGT AGC CGT ATC *gcg* AAA GAC ATG GAG CCA GAA C
YH-BUD4-S2A-3-rev	GTT CTG GCT CCA TGT CTT T*cg c*GA TAC GGC TAC GGT GGC G
YH-BUD4-S2A-4-f	GTA CAC TCG AGA ACG AAG *gcc* AGT CTT GTA TTA ATT AAC
YH-BUD4-S2A-4-rev	GTT AAT TAA TAC AAG ACT *ggc* CTT CGT TCT CGA GTG TAC
3xHA-tag constructs:	
YH-4096-SpeI-ATG	**act agt** ATG GCC GAC GAA GGA GTC G
YH-4096-PacI-Stopp	**tta att aaC TA**A GAT CCC GCA ACG GGT CCC
3xmyc-tag constructs:	
YH-DBF2-AscI-ATG	**ggc gcg ccg** ATG TCT AGC TAC
YH-DBF2-PacI-Stopp	GG**t taa tta a**CT ACA GCA TCG TAC C
GFP-fusion constructs:	
YH-DBF2-AscI-ATG	**ggc gcg ccg** ATG TCT AGC TAC
YH-DBF2-PacI-Stopp	GG**t taa tta a**CT ACA GCA TCG TAC C
YH-4096-SpeI-ATG	**act agt** ATG GCC GAC GAA GGA GTC G
YH-4096-PacI-Stopp	**tta att aa**A GAT CCC GCA ACG GGT CCC
YH-Pod6-ATG-SpeI	**act agt** ATG GCG ACC CTA TCG
YH-Pod6-Stop-PacI	**tta att aa**G ACA CTC GTG TCC AC
YH-6636-SpeI-ATG	**act agt** ATG GAG TCC CTA CTA TC
YH-6636-PacI-Stopp	**tta att aa**G CTC AAC ACA CCC CC
YH-1335-XbaI-ATG	**tct aga** ATG GCG CCG AAC C
YH-1335-PacI-Stopp	**tta att aa**C GAC CAC CTC ATG TCC G
YH-BUD3-Helix-ATG	**act agt** CCC ACT TGG ACT TTG C

Primer name	Sequence 5‘- 3‘
YH-BUD3-Helix-Stopp	**tta att aa**g cCT TTA CGA GCC TG
Endogenous-GFP-fusion constructs:	
DJ_DBF2_ATG_PacI_f	**tta att aa**A TGT CTA GCT ACT TGA CAA AC
DJ_DBF2_Stopp_PacI_r	**tta att aa**C AGC ATC GTA CCA AAA TTG TTG
DJ_3UTR_DBF2_KpnI_f	**ggt acc** AGC CAG CAC CGG CAA CAA C
DJ_3UTR_DBF2_KpnI_r	**ggt acc** GCT GGT GTG GTG TAA GAG C

Table 2: Plasmids used in this study. Construction intermediates (DNA fragments inserted into the pJet1.2 blunt for subcloning) are not listed.

Plasmid	Short description	Source
pJet1.2 blunt	Cloning vector for subcloning of PCR fragments	Fermentas GmbH, Germany
pGBKT7	Yeast two-hybrid vector for expression of N-terminal GAL4 DNA binding domain fusion proteins under control of truncated P_{ADH1}; carrying *TRP1*	Clontech, USA
pGBKT7-53	pGBKT7; murine $p53_{aa72-390}$ cDNA	Clontech, USA
pGBKT7-Lam	pGBKT7; human laminin C cDNA	Clontech, USA
pGBKT7-9071	pGBKT7; NCU09071 (*dbf-2*) cDNA	kind gift of S. Maerz
pGBKT7-7296	pGBKT7; NCU07296 (*cot-1*) cDNA	(Maerz et al., 2009)
pGBKT7-7296-short	pGBKT7; NCU07296-short cDNA	(Maerz et al., 2009)
pGBKT7-7296-long	pGBKT7; NCU07296-long cDNA	(Maerz et al., 2009)
pGBKT7-0772	pGBKT7; NCU00772 cDNA	Kind gift of A. Dettmann
pGADT7	Yeast two-hybrid vector for expression of N-terminal GAL4 activation domain fusion proteins under control of full-length P_{ADH1}; carrying *LEU2*	Clontech, USA
pGADT7-T	pGADT7; SV40 large T-$antigen_{aa86-708}$ cDNA	Clontech, USA
pGADT7-9071	pGADT7; NCU09071 (*dbf-2*) cDNA	kind gift of S. Maerz
pGADT7-11235	pGADT7; NCU11235 (*pod-6*) cDNA	(Maerz et al., 2009)
pGADT7-7296	pGADT7; NCU07296 (*cot-1*) cDNA	(Maerz et al., 2009)
pGADT7-7296-short	pGADT7; NCU07296-short cDNA	(Maerz et al., 2009)
pGADT7-7296-long	pGADT7; NCU07296-long cDNA	(Maerz et al., 2009)
pGADT7-0772	pGADT7; NCU00772 cDNA	Kind gift of A. Dettmann
pFLAGN1	Fungal expression vector for N-terminal 3xFLAG fusion proteins under control of P_{ccg-1}; target to *his-3* locus	(Kawabata & and Inoue, 2007)
pFLAGN1-1605	pFLAGN1; NCU01605 (*mob-1*)	kind gift of S. Maerz

Plasmid	Short description	Source
pHAN1	Fungal expression vector for N-terminal HA fusion proteins under control of P_{ccg-1}; target to *his-3* locus	(Kawabata & and Inoue, 2007)
pHAN1-0772	pHAN1; NCU00772 (*mst-1*)	kind gift of A. Dettmann
pHAN1-4096	pHAN1; NCU04096 (*sid-1*)	this study
pCCG::N-3xMyc	Fungal expression vector for N-terminal 3xmyc fusion proteins under control of P_{ccg-1}; target to *his-3* locus	(Honda & Selker, 2009)
pCCG::N-3xMyc-9071	pCCG::N-3xMyc, NCU09071 (*dbf-2*)	this study
pCCG::N-3xMyc-9071 S499A	pCCG::N-3xMyc, NCU09071 ^{S499A}	this study
pCCG::N-3xMyc-9071 S499E	pCCG::N-3xMyc, NCU09071 ^{S499E}	this study
pCCG::N-3xMyc-9071 T671A	pCCG::N-3xMyc, NCU09071 ^{T671A}	this study
pCCG::N-3xMyc-9071 T671E	pCCG::N-3xMyc, NCU09071 ^{T671E}	this study
pCCG::N-3xMyc-9071 S499A T671A	pCCG::N-3xMyc, NCU09071 $^{S499A\ T671A}$	this study
pCCG::N-3xMyc-9071 S499A T671E	pCCG::N-3xMyc, NCU09071 $^{S499A\ T671E}$	this study
pCCG::N-3xMyc-9071 S499E T671A	pCCG::N-3xMyc, NCU09071 $^{S499E\ T671A}$	this study
pCCG::N-3xMyc-9071 S499E T671E	pCCG::N-3xMyc, NCU09071 $^{S499E\ T671E}$	this study
pCCG::N-3xMyc-9071 D422A	pCCG::N-3xMyc, NCU09071 ^{D422A}	this study
pCCG::N-GFP	Fungal expression vector for N-terminal GFP fusion proteins under control of P_{ccg-1}; target to *his-3* locus	(Honda & Selker, 2009)
pCCG::N-GFP-9071	pCCG::N-GFP, NCU09071 (*dbf-2*)	this study
pCCG::N-GFP-9071 ^{T671E}	pCCG::N-GFP, NCU09071 ^{T671E}	this study
pCCG::N-GFP-9071 D422A	pCCG::N-GFP, NCU09071 ^{D422A}	this study
pMF272ATGtoATC	Fungal expression vector for C-terminal GFP fusion proteins under control of P_{ccg-1}; target to *his-3* locus; start codon ATG was mutated to ATC	(Freitag *et al.*, 2004), modified by A. Dettmann
pMF272ATGtoATC-4096	pMF272ATGtoATC; NCU04096 *(sid-1)*	this study
pMF272ATGtoATC-0772	pMF272ATGtoATC; NCU00772 *(mst-1)*	kind gift of A. Dettmann
pMF272ATGtoATC-11235	pMF272ATGtoATC; NCU11235 *(pod-6)*	this study
pMF272ATGtoATC-6636	pMF272ATGtoATC; NCU06636 *(cdc-14)*	this study
pMF272ATGtoATC-1335	pMF272ATGtoATC; NCU01335 *(cdc-7)*	this study
pMF272ATGtoATC-1335 ^{D195A}	pMF272ATGtoATC; NCU01335 ^{D195A}	this study

Plasmid	Short description	Source
pMF272ATGtoATC-6579	pMF272ATGtoATC; NCU06579 *(bud-3)*	Kind gift of D. Justa Schuch
pMF272ATGtoATC-6579 ^{S798A}	pMF272ATGtoATC; NCU06579 ^{S798A}	this study
pMF272ATGtoATC-6579 ^{S798E}	pMF272ATGtoATC; NCU06579 ^{S798E}	this study
pMF272ATGtoATC-6579-helix	pMF272ATGtoATC; NCU06579-helix (*bud-3-helix*)	this study
pMF272ATGtoATC-6579-helix ^{S798A}	pMF272ATGtoATC; NCU06579-helix ^{S798A} (*bud-3-helix* ^{S798A})	this study
pMF272ATGtoATC-6579-helix ^{S798E}	pMF272ATGtoATC; NCU06579-helix ^{S798E} (*bud-3-helix* ^{S798E})	this study
pMF272ATGtoATC-0152	pMF272ATGtoATC; NCU00152 *(bud-4)*	this study
pMF272ATGtoATC-0152 $^{S13A;S167A;S796A;S1411A}$	pMF272ATGtoATC; NCU00152 $^{S13A;S167A;S796A;S1411A}$	this study
pGFP::hph::loxP	Fungal expression vector for C-terminal GFP fusion proteins under control of the endogenous promotor	(Honda & Selker, 2009)
pGFP::hph::loxP-9071	pGFP::hph::loxP; NCU09071 (*dbf-2*)	this study

4.2.2 Plasmids of epitope-tagged fusion proteins for in vitro kinase assays and co-immunoprecipitation experiments

For construction of a plasmid encoding N-terminally 3xmyc-tagged DBF2 protein, the corresponding coding region was amplified from genomic DNA using primers YH-DBF2-AscI-ATG/YH-DBF2-PacI-Stopp and ligated with pCCG::N-3xMyc (Honda and Selker, 2009). The generated plasmid was linearized by digestion with *Nde*I for transformation by electroporation.

A N-terminally HA-tagged version of SID1 was expressed from pHAN1-4096. The plasmid was created by amplifying *sid-1* from genomic DNA using primers YH-4096-SpeI-ATG/YH-4096-PacI-Stopp and inserted into pHAN1 (Kawabata & and Inoue, 2007) via *Spe*I/*Pac*I sites. For electroporation, plasmid was digested with *Ssp*I.

4.2.3 Plasmids for analysis of subcellular fusion protein localization

For generation of a plasmid allowing expression of N-terminally green fluorescent protein (GFP)-tagged DBF-2 protein, the construct originally amplified for insertion into pCCG::N-3xMyc (see section 4.2.3) was used and ligated with pCCG::N-GFP (Honda & Selker, 2009) via *Asc*I/*Pac*I sites. The resulting plasmid pCCG::N-GFP-9071 was routinely prepared for use in electroporation of *N. crassa* by linearization with *Nde*I.

Vectors for expression of C-terminally GFP-tagged fusion proteins of SID-1 (NCU04096), CDC-7 (NCU01335), POD-6 (NCU11235) and CDC-14 (NCU06636), were created by amplifying the genomic sequence using primers YH-4096-SpeI-ATG/YH-4096-PacI-Stopp, YH-1335-XbaI-ATG/YH-1335-PacI-Stopp, YH-Pod6-ATG-SpeI/YH-Pod6-Stopp-PacI and YH-6636-SpeI-ATG/YH-6636-PacI-Stopp. The PCR products were cleaved with corresponding restriction enzymes and ligated into the adapted plasmid pMF272ATGtoATC. Resulting plasmids were linearized using suitable restriction enzymes for use in electroporation of *N. crassa*.

To generate a C-terminal GFP-tagged *dbf-2* construct under the endogenous promoter, the ORF was amplified by PCR using wild type DNA and the primer pairs DJ_DBF2_ATG_PacI_f and DJ_DBF2_Stopp_PacI_r. After subcloning into the pJet1.2 blunt vector, sequencing and digestion with the respective restriction enzyme *Pac*I, the PCR fragment was introduced into the pGFP::hph::loxP vector. 1kb fragment of the 3'UTR was also amplified by PCR using the primer pairs DJ_3UTR_DBF2_KpnI_f and DJ_3UTR_DBF2_KpnI_r to ensure homologous recombination at the endogenous locus in the fungus.

4.2.4 Point-mutated constructs of DBF-2, BUD-3 and BUD-4

To establish point-mutated versions of DBF-2 (NCU09071), BUD-3 (NC06579) and BUD-4 (NCU00152) site-directed mutagenesis PCRs using primer pairs YH-DBF2-S2A-forw and YH-DBF2-S2A-rev; YH-DBF2-S2E-forw and YH-DBF2-S2E-rev; YH-DBF2-T2A-forw and YH-DBF2-T2A-rev; YH-DBF2-T2E-forw and YH-DBF2-T2E-rev; YH-BUD3-S2A-f and YH-BUD3-S2A-rev; YH-BUD3-S2E-f and YH-BUD3-S2E-rev, YH-BUD4-S2A-1-f and YH-BUD4-S2A-1-rev; YH-BUD4-S2A-2-f and YH-BUD4-S2A-2-rev; YH-BUD4-S2A-3-f and YH-BUD4-S2A-3-rev; YH-BUD4-S2A-4-f and YH-BUD4-S2A-4-rev were performed according to manufacturer's manuals. The plasmids pCCG::N-3xMyc-9071, pMF272ATGtoATC-6579 and pMF272ATGtoATC-0152 were used as templates. The resulting plasmids pCCG::N-3xMyc-9071^{S499A}, pCCG::N-3xMyc-9071^{S499E}, pCCG::N-3xMyc-9071^{T671A}, pCCG::N-3xMyc-9071^{T671E}, pCCG::N-3xMyc-9071$^{S499A;T671A}$, pCCG::N-3xMyc-9071$^{S499A;T671E}$, pCCG::N-3xMyc-9071$^{S499E;T671A}$, pCCG::N-3xMyc-9071$^{S499E;T671E}$, pMF272ATGtoATC-6579^{S798A} and pMF272ATGtoATC-0152$^{S13A;S167A;S796A;S1411A}$ were linearized with respective restriction enzymes and electroporated into *N. crassa*.

To generate kinase-dead constructs of DBF-2 and CDC-7 site-directed mutagenesis PCRs using plasmids pCCG::N-3xMyc-9071 and pMF272ATGtoATC-1335 as templates and primer pairs YH-DBF2-D2A-forw/YH-DBF2-D2A-rev and YH-CDC7-D2A-forw/YH-CDC7-D2A-rev were performed. The resulting plasmids were electroporated into *N. crassa*. Loss of kinase activity was verified by an *in vitro* kinase assay (see section 4.5.4).

4.2.5 BUD-3-Helix constructs

Truncated versions of BUD-3 i.e. the BUD-3-Helix (aa 739-816) constructs were amplified using plasmids pMF272ATGtoATC-6579, pMF272ATGtoATC-6579^{S798A} and pMF272ATGtoATC-6579^{S798E} as templates, primer pair YH-BUD3-Helix-ATG and YH-BUD3-Helix-Stopp and inserted into the vector pMF272ATGtoATC. Resulting plasmids pMF272ATGtoATC-6579-helix, pMF272ATGtoATC-6579-helix^{S798A} and pMF272ATGtoATC-6579-helix^{S798E} were digested with *Nde*I and electroporated in *N. crassa.*

4.3 Strains

N. crassa strains used in this work are listed in Table 3. Strains provided by the Fungal Genetics Stock Center (FGSC) at the University of Missouri, USA are indicated. Single deletion strains used in this study were generated within the framework of the Neurospora genome project hosted at Dartmouth Medical School, Great Britain, following the procedure described in (Dunlap *et al.*, 2007). Detailed descriptions are available at http://dartmouth.edu/~neurosporagenome/protocols.html. The full-length open reading frames were replaced by a hygromycin resistance cassette and targeted integration was verified by Southern hybridization. Δ*dbf-2,* Δ*sid-1*, Δ*cdc-7,* Δ*bud-3 and* Δ*bud-4* were deposited at the Fungal Genetics Stock Center as heterokaryotic strains carrying two types of nuclei: one harbouring the deletion (marked by the hygromycin resistance) and a second wild type nucleus which suppresses the deletion defect. Homokaryotic deletion strains were obtained by back-crossing heterokaryotic deletion strains with wild type and selecting for progeny carrying the deletion nucleus i.e. the hygromycin resistance cassette.

N. crassa strains expressing epitope tagged fusion proteins (e.g. GFP, HA, myc) were generated by transformation of the auxotrophic *his-3* strain applying plasmids targeted to the his-3 locus (Table 2). These constructs contain the expression cassette flanked by the regions for homologous recombination to the *his-3* locus and restoration of a functional *his-3* allele (Margolin *et al.*, 1997, Aramayo & and Metzenberg, 1996). Transformants were selected for histidine prototrophy i.e. on minimal medium. Expression of all fusion proteins was verified by Western blotting (see 4.5.2) using respective epitope tag antibodies. Functionality of expressed fusion proteins was tested by crossing resulting strains with the respective hygromycin-resistant deletion mutant. Suppression of phenotypic defects and hygromycin resistance were used as evidence for functionality.

N. crassa strains expressing HA-, GFP- and myc-tagged fusion proteins for co-immunoprecipitation studies were generated by transforming auxotrophic strains *trp-3; his-3 or nic-3; his-3*. Histidine-prototrophic transformants were selected and expression of fusion proteins was verified. Growth of resulting strains is still dependent on medium supplemented with tryptophane or nicotinamide. For

co-immunoprecipitation studies, combinations of these strains were fused to generate prototrophic heterokaryotic strains expressing both fusion proteins. Therefor, conidia of the respective strains, one *nic-1*, second *trp-1* were fused on VMM (Kawabata & and Inoue, 2007).

The strain *mus52::bar his-3* was used to transform GFP-tagged fusion proteins at the endogenous locus by homologous recombination. Transformants were selected by their ability to grow on hygromycin and the expression level was checked by Western blotting. To remove the *mus52* mutation the resulting strains were crossed with *wild type* or *his-3* strain, verification by Southern analysis was performed.

Table 3: *N. crassa* strains used in this study. Genetic features are marked as (EC) for ectopical integration. Heterokaryotic fusion strains used in co-immunoprecipitation analysis are not listed.

Strains	Genotype	Source
wild type 74	*OR231 Mat A*	FGSC #987
wild type ORS	*SL6 Mat a*	FGSC #4200
his-3 A	*his-3 Mat A*	FGSC #6103
his-3 a	*his-3 Mat a*	FGSC #718
trp-1;his-3	*trp-1- his-3-*	(Maerz et al., 2009)
nic-3;his-3	*nic-3- his-3-*	(Maerz et al., 2009)
Δdbf-2	*hph::dbf-2Δ his-3-*	(Maerz et al., 2009)
Δmob-1	*hph::mob-1Δ + mob-1^{+} bar::mus-51Δ*	(Maerz et al., 2009)
Δcdc-7	*hph::cdc-7Δ + cdc-7^{+} bar::mus-51Δ*	FGSC #16741
Δsid-1	*hph::sid-1Δ + sid-1^{+} bar::mus-51Δ*	FGSC #11317
Δcdc-14	*hph::cdc-14Δ*	FGSC #12648
Δbud-3	*hph::bud-3Δ + bud-3^{+} bar::mus-51Δ*	(Justa-Schuch et al., 2010)
Δbud-4	*hph::bud-4Δ + bud-4^{+} bar::mus-51Δ*	(Justa-Schuch et al., 2010)
Δmst-1	*hph::mst-1Δ*	FGSC #11478
Δmst-1 his-3	*hph::mst-1Δ his-3-*	A. Dettmann
Δpod-6	*Δpod-6::natR*	(Seiler et al., 2006)
Δcot-1	*Δcot-1::hph^{R} + cot-1^{+} Δmus51::bar^{R} a*	FGSC #14525
cot-1(ts)	*cot-1(H351R)*	(Seiler & Plamann, 2003)
gfp-dbf-2	*Pccg-1-sgfp-dbf-2::his-3 hph::dbf-2Δ*	This study

Strains	Genotype	Source
gfp-dbf-2(D422A)	*Pccg-1-sgfp-dbf-2(D422A)::his-3*	This study
gfp-dbf-2(T671E)	*Pccg-1-sgfp-dbf-2(T671E)::his-3 hph::dbf-2Δ*	This study
sid-1-gfp	*Pccg-1-sid-1-sgfp::his-3 hph::sid-1Δ*	This study
cdc-14-gfp	*Pccg-1-cdc-14-sgfp::his-3 hph::cdc-14Δ*	This study
cdc-7-gfp	*Pccg-1-cdc-7-sgfp::his-3 hph::cdc-7Δ*	This study
cdc-7-gfp-(D195A)	*Pccg-1-cdc-7-sgfp-(D195A)::his-3*	This study
cot-1-gfp	*Pccg-1-cot-1-sgfp::his-3 hph::cot-1Δ*	(Maerz et al., 2012)
pod-6-gfp	*Pccg-1-pod-6-sgfp::his-3 natR::pod-6Δ*	This study
bud-3-gfp	*Pccg-1-bud-3-sgfp::his-3 hph::bud-3Δ*	(Justa-Schuch et al., 2010)
bud-4-gfp	*Pccg-1-bud-4-sgfp::his-3 hph::bud-4Δ*	(Justa-Schuch et al., 2010)
bud-3-gfp(S798A)	*Pccg-1-bud-3(S798A)-sgfp::his-3*	This study
bud-4-gfp(4xS2A)	*Pccg-1-bud-4(S2A-4)-sgfp::his-3*	This study
bud-3-helix-gfp	*Pccg-1-bud-3-helix-sgfp::his-3*	This study
bud-3(S798A)-helix-gfp	*Pccg-1-bud-3(S798A)-helix-sgfp::his-3*	This study
bud-3(S798E)-helix-gfp	*Pccg-1-bud-3(S798E)-helix-sgfp::his-3*	This study
lifeact-gfp	*Pccg-1-lifeact-egfp::his-3*	(Delgado-Alvarez *et al.*, 2010)
h1-rfp	*Pccg-1-rfp-h1::his-3 mat A*	M. Freitag, USA
h1-rfp	*Pccg-1-rfp-h1::his-3 mat a*	A. Dettmann
myc-dbf-2	*Pccg-1-myc-dbf2-2::his-3 hph::dbf-2Δ*	This study
myc-dbf-2(D422A)	*Pccg-1-myc-dbf2-2(D422A)::his-3 hph::dbf-2Δ*	This study
myc-dbf-2(S499A)	*Pccg-1-myc-dbf2-2(S499A)::his-3 hph::dbf-2Δ*	This study
myc-dbf-2(S499E)	*Pccg-1-myc-dbf2-2(S499E)::his-3 hph::dbf-2Δ*	This study
myc-dbf-2(T671A)	*Pccg-1-myc-dbf2-2(T671A)::his-3 hph::dbf-2Δ*	This study
myc-dbf-2(T671E)	*Pccg-1-myc-dbf2-2(T671E)::his-3 hph::dbf-2Δ*	This study
myc-dbf-2(S499A/T671A)	*Pccg-1-myc-dbf2-2(S499A/T671A)::his-3 hph::dbf-2Δ*	This study
myc-dbf-2(S499A/T671E)	*Pccg-1-myc-dbf2-2(S499A/T671E)::his-3 hph::dbf-2Δ*	This study
myc-dbf-2(S499E/T671A)	*Pccg-1-myc-dbf2-2(S499E/T671A)::his-3 hph::dbf-2Δ*	This study

Strains	Genotype	Source
myc-dbf-2(S499E/T671E)	*Pccg-1-myc-dbf2-2(S499E/T671E)::his-3 hph::dbf-2Δ*	This study
myc-cot-1	*Pcot-1-myc-cot-1*	(Ziv *et al.*, 2009)
myc-cot-1(T589E)	*Pcot-1-myc-cot-1(T589E)*	(Ziv et al., 2009)
myc-cot-1 his-3	*Pcot-1-myc-cot-1 his-3-*	(Ziv et al., 2009)
myc-cot-1; bud-3-gfp	*Pcot-1-myc-cot-1; Pccg-1-bud-3-gfp::his-3*	This study
myc-cot-1; bud-4-gfp	*Pcot-1-myc-cot-1; Pccg-1-bud-4-gfp::his-3*	This study
myc-cot-1; HA-mst-1	*Pcot-1-myc-cot-1; Pccg-1-HA-mst-1::his-3*	A. Dettmann
myc-cot-1; dbf-2-gfp	*Pcot-1-myc-cot-1; Pccg-1-dbf-2-gfp::his-3*	This study
myc-cot-1; HA-mob-2a	*Pcot-1-myc-cot-1; Pccg-1-HA-mob-2a::his-3*	This study
HA-sid-1	*Pccg-1-HA-sid-1::his-3 hph::sid-1Δ*	This study
HA-mst-1	*Pccg-1-HA-mst-1::his-3 hph::mst-Δ*	A. Dettmann
HA-pod-6	*Ppod-6-HA-pod-6*; *his-3-*	(Maerz et al., 2012)
myc-dbf-2 trp-1	*Pccg-1-myc-dbf-2::his-3 trp-1-*	This study
myc-dbf-2(D422A) trp-1	*Pccg-1-myc-dbf-2(D422A)::his-3 trp-1-*	This study
myc-dbf-2(S499A) trp-1	*Pccg-1-myc-dbf-2(S499A)::his-3 trp-1-*	This study
myc-dbf-2(S499E) trp-1	*Pccg-1-myc-dbf-2(S499E)::his-3 trp-1-*	This study
myc-dbf-2(T671A) trp-1	*Pccg-1-myc-dbf-2(T671A)::his-3 trp-1-*	This study
myc-dbf-2(T671E) trp-1	*Pccg-1-myc-dbf-2(T671E)::his-3 trp-1-*	This study
FLAG-mob-1 nic-1	*Pccg-1-FLAG-mob-1::his-3 nic-1-*	(Maerz et al., 2009)
HA-sid-1;trp-1	*Pccg-1-HA-sid-1::his-3 trp-1-*	This study
sid-1-gfp;nic-1	*Pccg-1-sid-1-sgfp::his-3 nic-1-*	This study
cdc-7-gfp;nic-1	*Pccg-1-cdc-7-sgfp::his-3 nic-1-*	This study
HA-mst-1;trp-1	*Pccg-1-HA-mst-1::his-3 trp-1-*	A. Dettmann
myc-cot-1; HA-pod-6	*Pcot-1-myc-cot-1; Pccg-1-HA-pod-6::his-3*	(Maerz et al., 2012)

For amplification of DNA the *Escherichia coli* strain DH5α [F–, Φ80dΔ(*lacZ*)M15-1, Δ(*lacZYA-argF*)U169, *recA1*, *endA1*, *hsdR17* (rK–, mK+), *supE44*, λ–, *thi1*, *gyrA96*, *relA1*] (Woodcock, 1989) was used.

For yeast two-hybrid analyses the *Saccharomyces strain* AH109 [*MATa, trp1-901, leu2-3, 112, ura3-52, his3-200, gal4Δ, gal80Δ, LYS2::GAL1$_{UAS}$-GAL1$_{TATA}$-HIS3, GAL2$_{UAS}$-GAL2$_{TATA}$-ADE2, URA3::MEL1$_{UAS}$-MEL1$_{TATA}$-lacZ*] (James *et al.*, 1996); Clontech , USA) was used.

4.4 General molecular biological methods

Standard molecular methods were performed as described in (Sambrook & and Russell, 2001, Ausubel *et al.*, 2002) with minor modifications.

4.4.1 Polymerase chain reaction (PCR)

Phusion® High Fidelity polymerase (Finnzymes AG, Espoo, FIN) was used for amplification of DNA by polymerase chain reaction in accordance with standard protocols (Ausubel et al., 2002) or to manufacturer's manual. For analytical PCRs *Taq* DNA polymerase was used. Oligonucleotides used as PCR primers were synthesized by Eurofins MWG Operon (Ebersberg, Germany). Plasmid or genomic DNA served as templates for the reactions. In case of colony PCRs (Zon *et al.*, 1989) which were performed to identify positive *E. coli* transformants, *E. coli* cells of a single colony were directly used as templates.

A standard PCR reaction consisted of an initial template denaturation step (2 min , 94°C) followed by 30 cycles each consisting of 30 s denaturation at 94°C, primer annealing (30 s, 50-60°C depending on primer used), product elongation at 72°C (1 min/1kb template length), and a final elongation step of 3 min at 72°C.

Site-directed mutagenesis was performed with *Phusion*® High Fidelity polymerase (Finnzymes AG, Espoo, FIN) according to the QuickChangeR Site-Directed Mutagenesis Kit protocol (Stratagen, La Jolla, USA). Amplified PCR products were directly digested with *Dpn*I to separate mutated non-methylated output plasmid DNA from non-mutated methylated input plasmid DNA. The digested DNA was subsequently transformed into *E. coli*.

4.4.2 DNA agarose gel electrophoresis and isolation

DNA was separated by horizontal agarose gel electrophoresis using the Mini Sub-Cell System (Bio-Rad Laboratories GmbH, Germany). Gene Ruler™ 1 kb DNA ladder (Fermentas GmbH, Germany) served as DNA molecular weight marker, DNA was stained with ethidiumbromide and visualized by using the Molecular Imager Gel Doc XR System (Bio-Rad Laboratories GmbH, Germany).

DNA gel extraction was performed using the peqGOLD Gel Extraction Kit (PeqLab GmbH, Erlangen, Germany) and *E. coli* plasmid DNA was purified using peqGOLD Plasmid Miniprep Kit II (PeqLab GmbH, Erlangen, Germany) according to manufacturer's manuals.

4.4.3 Modification and enzymatic digestion of DNA

Restriction enzymes and buffers for endonucleolytic digestion of DNA were obtained from Fermentas GmbH (Germany) and New England Biolabs GmbH (USA) and used in accordance to product manuals.

4.4.4 Ligation

DNA ligation reactions were performed in 20 µl reaction volumes using T4 DNA ligase (Fermentas GmbH, Germany) in a 2 fold concentrated quick ligation buffer (50mM HEPES pH7.6, 10mM $MgCl_2$, 2mM DTT, 2mM ATP and 7% (v/v) PEG4000) for 20 min at room temperature (RT).

4.4.5 DNA Transformation

Preparation and transformation of chemically competent *E. coli* cells were performed as described in (Inoue *et al.*, 1990).

Transformation of *N. crassa* was done by electroporation of plasmid DNA into conidia as mentioned in (Margolin et al., 1997) with minor modifications. *N. crassa* conidia were harvested after 9-11 days and electroporation was performed in cuvettes obtained from PEQLAB Biotechnologie GmbH (Germany) using a Bio-Rad Gene Pulser® II (Bio-Rad Laboratories GmbH, Germany) with well-established settings (voltage 1.5 kV; capacitance: 50 µF; resistance: 200 Ω). Conidia were resuspended in 1M sorbitol and plated on minimal medium. For selection of transformants with dominant markers, conidia were resuspended in VMM, incubated for 3 hours at room temperature and plated on selective medium.

4.4.6 Sequence analysis

DNA was sequenced by the Göttingen Genomics Laboratory at the Institute of Microbiology and Genetics, University of Göttingen (G2L, Göttingen, Germany) and GATC Biotech AG (Germany). Sequences were analysed using 4Peaks (version 1.7.2; Mekentosj B.V., The Netherland), Lasergene (DNASTAR, Inc., Madison, USA) and GATCViewer™ (GATC Biotech AG, Germany) software. Alignments of sequences were performed with BLAST searches at NCBI (http://www.ncbi.nlm.nih.gov/).

4.5 Biochemical and immunological techniques

4.5.1 N. crassa protein isolation

N. crassa strains were grown in liquid minimal medium, harvested by filtration using a Büchner funnel and ground in liquid nitrogen. The pulverized mycelium was homogenized in protein extraction buffer (50mM Tris pH 7.5, 100mM KCl, 10mM $MgCl_2$, 0.1% NP40; freshly added 2mM benzamidine, 2mM DTT, 1mM Pefabloc SC). After centrifugation (14000 g) at 4°C for 10 min the clear supernatant was mixed with 3x Laemmli sample buffer (10% glycerol, 5% β-mercaptoethanol, 15% SDS, 12,5% upper-buffer (0,5M Tris-HCl pH 6.8), 0,75% bromophenol blue, 3M urea; modified from (Laemmli, 1970) and boiled at 98°C for 10 min.

4.5.2 Separation of proteins by SDS polyacrylamide gel electrophoresis (SDS-PAGE) and Western blotting

Protein samples were separated by a vertical discontinuous polyacrylamide gel electrophoresis (PAGE) (Davis, 1964, Ornstein, 1964) in the presence of sodium dodecyl sulfate (SDS) (Laemmli, 1970) using the Mini-Protean® 3 Cell System (Bio-Rad Laboratories GmbH, Germany). Electrophoretic separation was performed by a constant current of 15mA per gel submerged in running buffer (2.5mM Tris base, 19.2mM glycine and 0.1% SDS). For molecular weight determination of proteins PageRuler™ Prestained Protein Ladder (Fermentas GmbH, Germany) was used. Proteins were visualized by staining with Coomassie Brilliant Blue (0.1% Coomassie Brilliant Blue, 40% methanol, 10% acetic acid; (Merril, 1990) or alternatively by Western blotting.

For Western blot analysis, proteins were transferred electrophoretically from polyacrylamide gels to Protran® nitrocellulose membranes (Whatman GmbH, Germany) using Mini Trans-Blot® Cells (Bio-Rad Laboratories GmbH, Germany). After electroblotting for 1 hour at 100 V in cooled transfer buffer (2.5mM Tris, 19.2mM glycine, 20% methanol), the nitrocellulose membrane was stained with Ponceau S (0.1% Ponceau S in 5% acetic acid; (Salinovich & Montelaro, 1986). The immunological detection was based on the method described by (Towbin *et al.*, 1979). For initial blocking and incubation with antibodies 5% Sucofin milk powder (TSI GmbH & Co. KG, Germany) in PBS solution (10mM sodium phosphate, 150mM NaCl, pH 7.4) was used. Unbound antibodies were washed off with PBS. Mouse monoclonal Anti-c-myc antibody 9E10 (Santa Cruz Biotechnology, Heidelberg, Germany), Anti-GFP (B-2) (Santa Cruz Biotechnology, Heidelberg, Germany), Anti-HA (clone HA-7) or Anti-FLAG® M2 (both Sigma-Aldrich, Taufkirchen, Germany) were used as primary antibodies and were detected by peroxidase-coupled goat anti-mouse IgG (Dianova Gesellschaft für biochemische, immunologische und mikrobiologische Diagnostik GmbH, Germany). Detection was performed using

Immobilon™ Chemiluminescent Western HRP Substrate (Millipore, USA) in combination with Amersham™ Hyperfilm™ ECL (GE Healthcare Europe GmbH, Germany).

4.5.3 Immunoprecipitation

For immunoprecipitation *N. crassa* strains were grown in liquid minimal medium and mycelium was harvested by filtration and ground in liquid nitrogen. All buffers used contained following additives: 25mM β-glycerophosphate, 10 ng/µl leupeptine, 10 ng/µl aprotinine, 2 ng/µl Pepstatin A, 2mM DTT, 1mM PEFAbloc SC, 2mM benzamidine, 5mM NaF and 1mM Na_3VO_4. The pulverized mycelium was homogenized in lysis buffer (50mM Tris pH 7.5, 100mM KCl, 10mM $MgCl_2$, 0.1% NP40) and centrifuged two times at 4°C (15 min at 4500g and 30 min at 14000g). The cleared lysate was incubated on a rotation device for one hour with 4 µl/ml lysate monoclonal mouse Anti-c-myc (Santa Cruz Biotechnology, Inc., USA), 2 µl/ml GFP trap beads (Chromotek, Germany) or 2 µl/ml monoclonal mouse Anti-HA antibody (Sigma-Aldrich Corporation, USA) and with 5 mg/ml Protein-A-Sepharose™ CL-4B beads (GE Healthcare Life Sciences, USA) for an additional hour at 4°C. Subsequently, the suspension was centrifuged (2 min at 4000g) to remove supernatant and washed twice with lysis buffer. Immunoprecipitated proteins were recovered by boiling sepharose beads for 10 min at 98°C in 3x Laemmli buffer.

4.5.4 Kinase assays

For peptide-based *in vitro* activity determinations using the peptide KKRNRRLSVA as an artificial substrate, myc-tagged DBF-2 and COT-1 were purified as described in 4.5.3. Total protein levels of cell extracts were determined by Bradford analysis with bovine serum albumin standard solutions as a reference, using Roti®-Quant (Carl Roth) and a Tecan Infinite® M200 microplate reader (Tecan) and adjusted with IP buffer. The resulting antigen-antibody-bead complexes were washed once with lysis buffer, twice with lysis buffer containing 0,5M NaCl followed by two times with kinase reaction buffer (20mM Tris pH 7.5, 10mM $MgCl_2$, 1mM DTT, 1mM benzamidine, 1mM Na_3VO_4, 5mM NaF). The kinase reaction was started by resuspending the beads in 50 µl kinase reaction buffer containing 2mM synthetic substrate peptide, 0.5mM ATP and 1 µCi [^{32}P]-ATP. After incubation for 1 h at 37°C, samples were centrifuged for 2 min at 4000g and the supernatant was spotted onto P81 phospho-cellulose paper circles (Whatman, UK). Dried circles were washed two times with 1% phosphoric acid before incorporation of phosphate into the substrate peptide was measured by liquid scintillation counting. The remaining protein-sepharose pellet was boiled for 10 min at 98°C in 3x Laemmli buffer and used to determine equal protein concentration by SDS-PAGE and Western blot (see section 4.5.2).

For *in vitro* kinase assays with two or more kinases (using DBF-2 or COT-1 kinase activity as readout), all proteins were purified seperately and mixed during the washing procedure, just before kinase reaction.

To determine ^{32}P incorporation into BUD-3/BUD-4 by DBF-2 and COT-1, kinase assays were performed as described above with minor modifications. The kinase reaction was started by resuspending the beads of analyzed kinase and substrate in 50 µl of kinase reaction buffer containing 0.5mM ATP and 1 µCi [^{32}P]-ATP. After incubation for 1 h at 37°C, samples were centrifuged for 2 min at 4000g and the supernatant was discarded. The protein-sepharose pellet was boiled for 10 min at 98°C in 3x Laemmli buffer and used to determine ^{32}P incorporation and equal protein concentration by SDS-PAGE/autoradiography and Western blot, respectively (see section 4.5.2).

For analysis of phosphopeptides, purified proteins were washed once with lysis buffer, twice with lysis buffer containing 0,5M NaCl followed by two times with kinase reaction buffer (20mM Tris pH 7.5, 10mM $MgCl_2$, 1mM DTT, 1mM benzamidine, 1mM Na_3VO_4, 5mM NaF). A "cold" kinase reaction was started by resuspending the beads in 50 µl of kinase reaction buffer containing 0.5mM ATP. After incubation for 1 h at 37°C, samples were centrifuged for 2 min at 4000g and the supernatant was discarded. The protein-sepharose pellet was boiled for 10 min at 98°C in 3x Laemmli buffer and used for SDS-PAGE followed staining with Coomassie Brilliant Blue (0.1% Coomassie Brilliant Blue, 40% methanol, 10% acetic acid; (Merril, 1990). For further procedure see section 4.5.5 and 4.5.6.

4.5.5 Displacement assays

For displacement assays, immunoprecipitation of CDC-7-GFP from cell extracts co-expressing CDC-7-GFP and HA-SID-1 was separated and the resulting two samples were washed once with lysis buffer to remove non-co-purified HA-SID-1 (50mM Tris pH 7.5, 100mM KCl, 10mM $MgCl_2$, 0.1% NP40). Separately purified MST-1-GFP was added to one of the two samples while the other one was treated with lysis buffer. Both samples were incubated for 30 min at RT and subsequently, the suspensions were centrifuged (2 min at 4000g) to remove supernatant and washed once with lysis buffer to remove displaced/unbound HA-SID-1. Immunoprecipitated proteins were recovered by boiling sepharose beads for 10 min at 98°C in 3x Laemmli buffer. A similar approach was performed to test for displacement of HA-MST-1 by SID-1-GFP, using precipitated CDC-7-GFP from cell extracts co-expressing CDC-7-GFP and HA-MST-1. Further displacement assay followed the same procedure.

4.5.6 Mass spectrometry and database analysis

For protein identification by mass spectrometry, peptides of in-gel trypsinated proteins were extracted from Commassie-stained gel slices. Peptides of 5 µl sample solution were trapped and

washed with 0.05% trifluoroacetic acid on an Acclaim® PepMap 100 column (75 µm x 2 cm, C18, 3 µm, 100 Å, P/N164535 Thermo Scientific) at a flow rate of 4 µl/min for 12 min. Analytical peptide separation by reverse phase chromatography was performed on an Acclaim® PepMap RSLC column (75 µm x 15 cm, C18, 3 µm, 100 Å, P/N164534 Thermo Scientific) running a gradient from 96 % solvent A (0.1 % formic acid) and 4 % solvent B (acetonitrile, 0.1% formic acid) to 50% solvent B within 25 min at a flow rate of 250 nl/min (solvents and chemicals: Fisher Chemicals). Peptides eluting from the chromatographic column were on-line ionized by nano-electrospray using the Nanospray Flex Ion Source (Thermo Scientific) and transferred into the mass spectrometer. Full scans within m/z of 300-1850 were recorded by the Orbitrap-FT analyzer at a resolution of 60.000 at m/z 400. Each sample was analyzed using two different fragmentation techniques applying a data-dependent top 5 experiment: collision-induced decay with multistage activation and readout in the LTQ Velos Pro linear ion trap, and higher energy collision dissociation and subsequent readout in the Orbitrap-FT analyzer. LC/MS method programming and data acquisition was performed with the software XCalibur 2.2 (Thermo Fisher). Orbitrap raw files were analyzed with the Proteome Discoverer 1.3 software (Thermo Scientific) using the Mascot and Sequest search engines against the *N. crasssa* protein database with the following criteria: peptide mass tolerance 10 ppm, MS/MS ion mass tolerance 0.8 Da, and up to two missed cleavages allowed.

4.5.7 Enrichment of phosphopeptides

Based on the method developed by Mazanek et al. (2007), phosphopeptides were enriched using TiO_2 columns (TopTip TiO_2 10-200 µl Glygen Corporation, Columbia, USA). Trypsin-digested peptide samples were dissolved in loading solvent (420mM 1-octanesulfonic acid (OSA), 50 mg/ml dihydroxybenzoic acid (DHB), 0.1% heptafluorobutyric acid (HFBA), 20% acetic acid) and applied onto a TiO_2 column equilibrated by wash solution I (80% acetonitrile) and loading solvent. After the peptide sample had entered the column, the column was washed with loading solvent and two times wash solution II (80% acetonitrile, 0.1% trifluoric acid). For elution two times elution buffer (50mM ammonium dihydrogen phosphate adjusted to pH 10.5 with ammonium hydroxide) was applied onto the column. The eluates were acidified by addition of formic acid. Dried eluates were dissolved in sample buffer (95% H_2O, 5% acetonitrile, 0.1% formic acid) for mass spectrometric analysis.

4.6 Yeast two-hybrid assays

For yeast two-hybrid analysis (Fields & Song, 1989), the Matchmaker™ Two-Hybrid System 3 (Clontech, USA) was used according to manufacturer's manuals. Plasmids encoding proteins fused to the GAL4 activation domain (cDNA constructs inserted into pGADT7) or the DNA-binding domain (cDNA constructs inserted into pGBKT7), respectively, were co-transformed into *S. cerevisiae* AH109 cells as described in protocols of (Schiestl & Gietz, 1989). Co-transformants were selected by their

restored ability to grow on SD medium lacking leucine and tryptophane. Interaction of fusion proteins was shown by activation of the reporter genes *HIS3* and *ADE2*. For a yeast drop test, single colonies were collected, suspended in water and serial dilutions were plated on SD medium. To exclude autoactivation of the fusion proteins each plasmid was tested with the empty vector of the counterpart.

4.7 Microscopy

Low magnification documentation of fungal hyphae or colonies was performed using an SZX16 stereomicroscope, equipped with a Colorview III camera and Cell^{D} imaging software (Olympus SoftImaging Solutions GmbH, Germany). Images were further processed using Photoshop CS2 (Adobe). An inverted Axiovert Observer Z1 microscope (Carl Zeiss AG, Germany) equipped with a CSU-X1 A1 confocal scanner unit and a QuantEM 512SC camera (Photometrics, USA) was used for spinning disk confocal microscopy (Araujo-Palomares *et al.*, 2011). Slidebook 5.0 software (version 5.0; Intelligent Imaging Innovations GmbH, Germany) was used for image/movie acquisition, deconvolution and image analysis. The "inverted agar block" method (Hickey *et al.*, 2002) was used for live cell imaging. Cell wall and plasma membrane were stained with Calcofluor White (2 µg/ml^{-1}) and FM4-64 (1 µg/ml^{-1}), respectively. Time-lapse imaging was performed at capture intervals of 20-120 s for periods up to 18 min using the oil immersion objective 100x/1.3.

5. Results

5.1 Functional analysis of the SIN kinase cascade in *Neurospora crassa*

5.1.1 A tripartite SIN cascade is important for septum formation and localizes constitutively to SPBs and septa

The fission yeast septation initiation network (SIN) has been identified as a tripartite kinase cascade that connects cell cycle progression with the initiation of cytokinesis (Krapp & Simanis, 2008). This network is analogous to the mitotic exit network (MEN) of budding yeast with two differences; first, the MEN lacks a homolog of the fission yeast Ste20-related kinase Sid1, thus the effector kinase Dbf2p is directly phosphorylated by Cdc15p (Mah et al., 2001). Second, budding yeast MEN mutants arrest late in the mitotic cell cycle, while the fission yeast SIN is not essential for mitotic exit (Minet et al., 1979, Fankhauser & Simanis, 1994, Ohkura et al., 1995, Schmidt et al., 1997). BLAST searches of the *N. crassa* genome using *S. pombe* and *S. cerevisiae* SIN proteins identified homologs for all SIN network components except one scaffold protein, which is slightly conserved among different species (Table 4).

Table 4. (Predicted) SIN components in yeasts and filamentous fungi

Protein feature	*S. pombe*	*S. cerevisiae*	*N. crassa* *	*A. nidulans* *
Polo kinase	Plo1	Cdc5p	NCU09258	PLKA
GTPase	Spg1	Tem1p	NCU08878	AN7206
two component GAP	Cdc16	Bub2p	NCU03237	BUBA
	Byr4	Bfa1p	NCU11967	BYRA
STE kinase	Cdc7	Cdc15	NCU01335	SEPH
GC kinase	Sid1	/	NCU04096	AN8033
GC kinase adaptor	Cdc14	/	NCU06636	AN0655
NDR kinase	Sid2	Dbf2p	DBF-2	SIDB
NDR kinase adaptor	Mob1	Mob1p	MOB-1	MOBA
Leucin-rich scaffold	Cdc11	Nud1p	NCU03545	SEPK
Coiled coil scaffold	Sid4	?	?	SNAD

* Generic NCUxxxxx and ANxxxx nomenclature indicates uncharacterized proteins

As part of the Neurospora Genome project, mutants defective in predicted components of the tripartite kinase cascade were available as heterokaryotic strains. Those strains, Δ*NCU01335,* Δ*NCU04096,* Δ*NCU06636*, Δ*dbf-2* and Δ*mob-1* carry two types of nuclei: one harbouring the deletion (marked by a hygromycin resistance) and a second wild type nucleus, which suppresses the deletion defect. Analysis of deletion phenotypes was performed using homokaryotic strains which were obtained by back-crossing heterokaryotic deletion strains with wild type. Crosses of Δ*NCU01335* and Δ*NCU04096* with wild type resulted in the expected segregation of the hygromycin cassette (Colot *et al.*, 2006), and the hygromycin-resistent progeny produced thin and aseptate hyphae, which frequently lysed (Figure 5 A, B). This led to the conclusion that NCU01335 and NCU04096 function as part of the SIN, and the proteins were designated CDC-7 and SID-1, respectively, corresponding to their *S. pombe* homologs.

As previously described for Δ*dbf-2* and Δ*mob-1* (Maerz et al., 2009), within 1-2 days the vegetative growth defects of Δ*cdc-7* resulted in the frequent appearance of suppressor mutations that regained the ability to form septa and subsequently the ability to conidiate. Back-crosses of septum-forming Δ*cdc-7* colonies (and of Δ*sid-1* or Δ*cdc-14* colonies; see below) with *wild type* resulted in two types of hygromycin-resistent progeny: aseptate germlings that produced septa only at later stages of colony development and germlings with septation rates that were similar to those of wild type germlings. The comparison of the frequency of suppressor occurrence between the different strains, revealed that Δ*sid-1* behaved differently than Δ*cdc-7*, Δ*dbf-2* and Δ*mob-1*. In this mutant septa appeared much faster, resulting in the fast generation of abundant aerial mycelium and abundant sporulation (Figure 5 A, B). Therefore, a deletion strain of the predicted regulatory subunit NCU06636/CDC-14, which is essential for Sid1 function in fission yeast (Krapp & Simanis, 2008) was analyzed. Δ*cdc-14* germlings were initially aseptate, but produced septa with frequencies comparable to Δ*sid-1* and faster than the other SIN deletion strains (Figure 5 A, B). In support of the different vegetative defects caused by Δ*sid-1* and Δ*cdc-14* versus Δ*cdc-7*, Δ*dbf-2* and Δ*mob-1*, the morphology of sexual progeny generated in wt x Δ*sid-1* crosses was normal, while wt x Δ*cdc-14* crosses did not result in mature perithecia (Figure 5 C). These sexual defects were different compared to the generation of large, banana-shaped ascospores produced in wt x Δ crosses with Δ*cdc-7* and as previously shown for Δ*dbf-2* and Δ*mob-1* (Maerz et al., 2009).

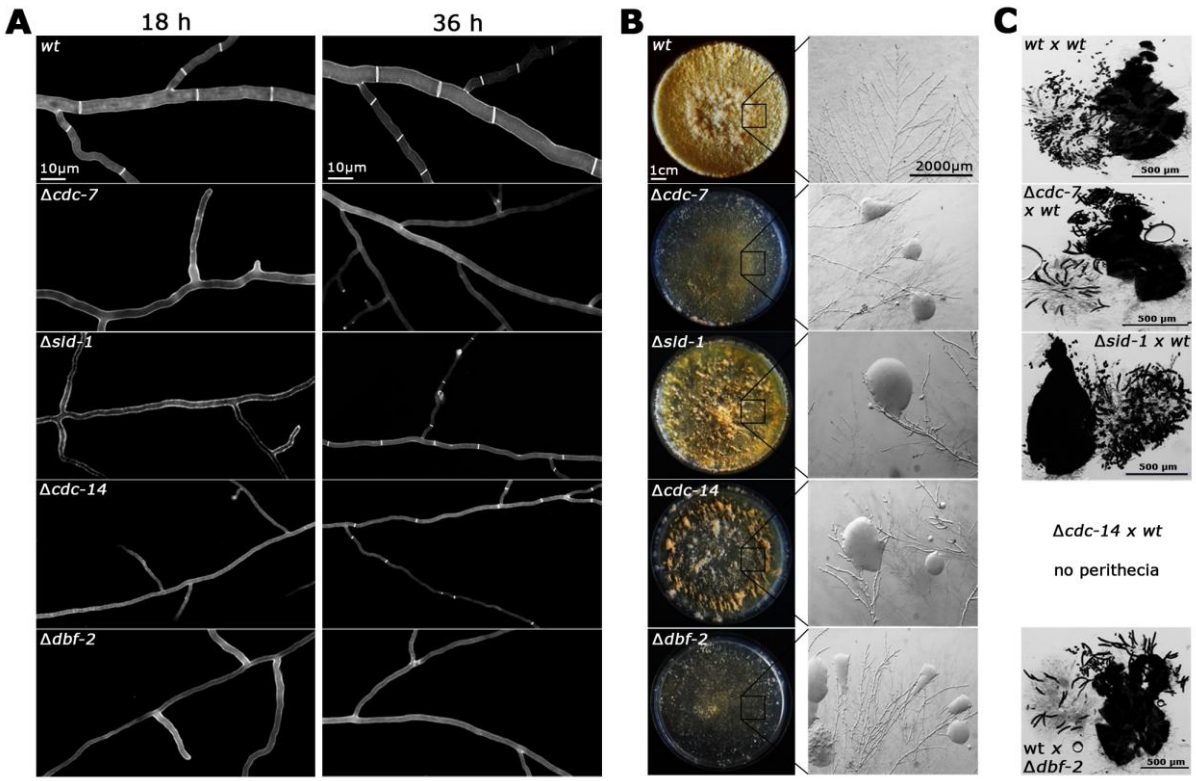

Figure 5: *N. crassa* SIN components are required for septum formation but display distinct mutant characteristics (A) Deletion strains defective in the indicated SIN components generated thin and aseptate hypha in young colonies (18 h time point). In older colonies, the septation defects were suppressed in Δ*sid-1* and Δ*cdc-14* strains (36 h time point). Cell wall and septa were labeled with Calcofluor White. (B) SIN mutants showed cytoplasmic leakage (magnified inserts), but, due to the fast ability to septate, Δ*sid-1 and* Δ*cdc-14* generated abundant aerial mycelium and asexual spores (conidia; plate morphology). (C) SIN mutants displayed distinct abnormalities during sexual development. wt x Δ crosses with Δ*cdc-7(het)* and Δ*dbf-2(het)* resulted in the frequent formation of large, banana-shaped ascospores. In contrast, wt x Δ*sid-1(het)* progeny morphology was normal, while crosses of wt x Δ*cdc-14(het)* produced no mature perithecia.

To investigate the cellular distribution of the SIN proteins, *N. crassa* strains expressing GFP-fusion proteins of CDC-7, SID-1, CDC-14 and DBF-2 were generated. All constructs were expressed under the control of the *ccg-1* promoter and targeted to the *his-3* locus in the respective deletion strain to confirm functionality of the fusion proteins. To exclude potential effects of ectopic overexpression, also the endogenous locus of *dbf-2* was modified to allow expression of DBF-2-GFP under the control of its endogenous regulatory elements. Although the *ccg-1* driven GFP-DBF-2 protein expression level was ca. 3-fold higher and resulted in enhanced cytoplasmic fluorescence (Figure S1), no differences in the localization pattern of GFP-DBF-2 in the two strains was observed (data not shown).

All three *N. crassa* SIN kinases and CDC-14 displayed identical localization patterns in that they all are associated with septa (Figure 6 A). DBF-2, SID-1 and CDC-14 accumulated first as cortical ring at the cell cortex prior to the initiation of septum constriction and remained associated with the septal pore after completion of the septation process. CDC-7-GFP was only visible at the septal pore of the

mature septum, but the failure to observe CDC-7 at early stages of septum formation is consistent with the low expression level of *ccg-1* driven CDC-7-GFP (Figure S1). Moreover, all SIN components associated with spindle pole bodies (SPBs) in a constitutive manner and independently of the cell cycle state (Figure 6 B).

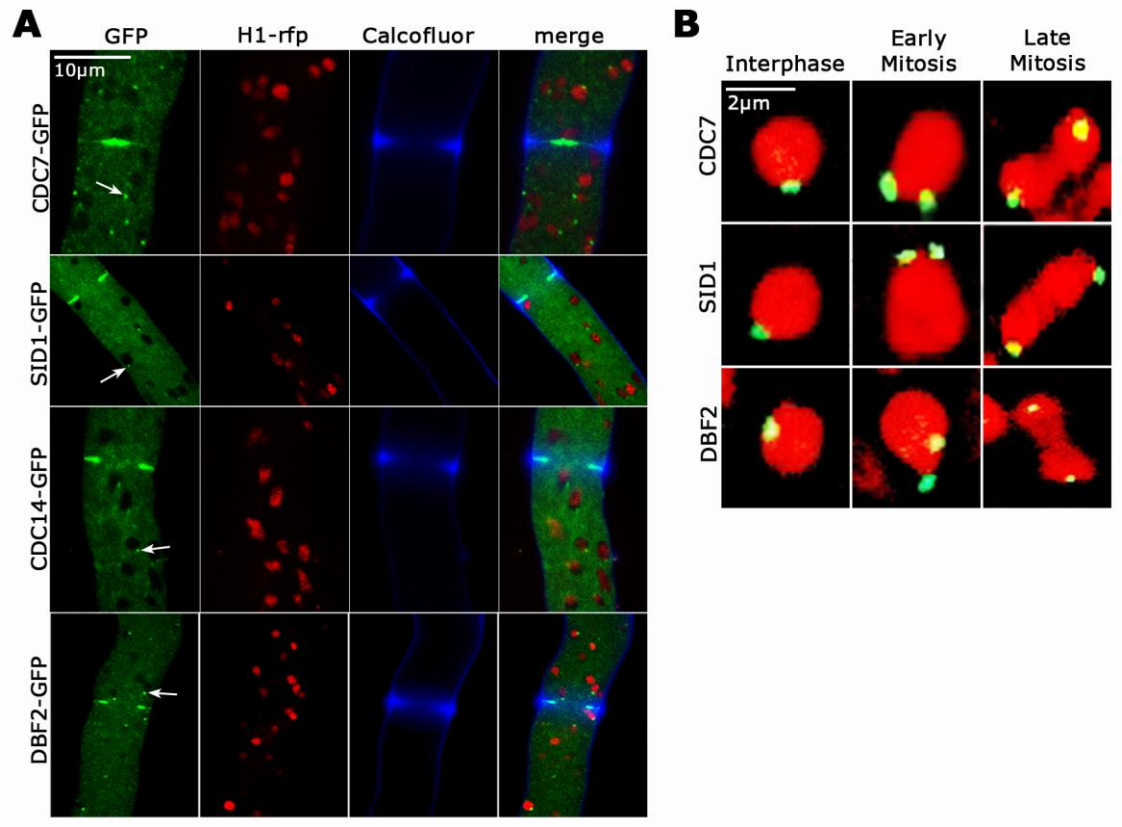

Figure 6: *N. crassa* SIN components localize to SPBs and septa (A) Functional GFP fusion proteins of CDC-7, SID-1, CDC-14 and DBF-2 localized to spindle pole bodies (arrows) and as constricting rings at forming septa. Nuclei were labeled with histone H1-RFP, the cell wall was stained with Calcofluor White. (B) The localization of the three SIN kinases CDC-7, SID-1 and DBF-2 to SPBs is constitutive and cell cycle independent. The three SIN kinases associated with SPBs of interphase nuclei as well as during early and late mitotic stages (as indicated by nuclear morphology). Nuclei were labeled with histone H1-RFP.

5.1.2 CDC-7-dependent activation of DBF-2 occurs through SID-1

The *S. cerevisiae* MEN cascade lacks a homolog of the fission yeast kinase Sid1, and the activation of Dbf2p involves direct phosphorylation by the Cdc7 homolog Cdc15p (Mah et al., 2001). In contrast, the *S. pombe* SIN likely follows a stepwise activation pattern of Cdc7, Sid1 and Sid2, but biochemical evidence for this gradual phospho-regulation is still missing (Hou *et al.*, 2004, Johnson *et al.*, 2012).

In order to determine the functional relationship between the three *N. crassa* SIN kinases, reciprocal co-immunoprecipitation (co-IP) experiments were performed to test if CDC-7 interacted with SID-1 and/or DBF-2. Strains expressing functionally tagged proteins of either CDC-7-GFP and HA-SID-1 or

CDC-7-GFP and myc-DBF-2 were constructed. Precipitation of CDC-7-GFP allowed detection of HA-SID-1 and vice versa, which verified the stable interaction of these two kinases (Figure 7 A). In contrast, in co-IP experiments performed under identical conditions no interaction between CDC-7 and DBF-2 and between CDC-7 and SID-1 could be observed (data not shown), suggesting that these proteins may interact in a more dynamic manner.

In addition, to preserve a mechanism for activation of the SIN effector kinase DBF-2 several *in vitro* kinase activity assays were performed. Wild type DBF-2 precipitated from *N. crassa* extracts displayed activity towards a synthetic peptide (KKRNRRLSVA) encompassing the consensus NDR kinase target motif, which was previously used for *in vitro* activity assays with the related NDR kinase COT-1 (Ziv et al., 2009). Incubation of precipitated SID-1 with separately purified DBF-2 enhanced the activity of DBF-2 (Figure 7 B). If the *N. crassa* SIN functions as a predicted tripartite and stepwise kinase cascade, CDC-7 should further increase the SID-1-dependent stimulation of DBF-2 activity. To test this assumption all three kinases were purified individually and combined in an *in vitro* kinase assay, which showed that addition of CDC-7 to a SID-1 ― DBF-2 mixture resulted in a continuing increase of stimulated DBF-2 kinase activity (Figure 7 B). This continuing increase was not observed by addition of a catalytically inactive version of CDC-7. Moreover, individually precipitated CDC-7 was unable to stimulate purified DBF-2, and control approaches using SID-1 and CDC-7 precipitates proved the specificity of this assay for the NDR kinase and established that SID-1 is required to transmit CDC-7-dependent signals towards DBF-2.

Activation of NDR kinases requires phosphorylation of a specific C-terminal hydrophobic motif (Stegert *et al.*, 2005, Jansen *et al.*, 2006, Maerz et al., 2012). To determine whether SID-1-dependent stimulation of DBF-2 occurs at the predicted hydrophobic motif of DBF-2, a DBF-2(T761A) variant, which contains a threonine to alanine substitution of the predicted hydrophobic motif phosphorylation site, was used. These assays showed that the specific stimulation of DBF-2 by SID-1 is only possible with purified wild type DBF-2, but not with DBF-2(T761A) (Figure 7 C). In addition, phosphorylation experiments coupled with mass-spectrometric analysis further supported Thr671 phosphorylation of DBF-2 by SID-1: phosphopeptides of the hydrophobic motif of DBF-2 precipitated under high-stringency conditions were only identified when DBF-2 was co-incubated with separately purified SID-1 in *in vitro* kinase reactions (Figure S2). Collectively, the data show that SID-1 transmits CDC-7-dependent signals towards the effector kinase DBF-2 through phosphorylation of DBF-2 at Thr671.

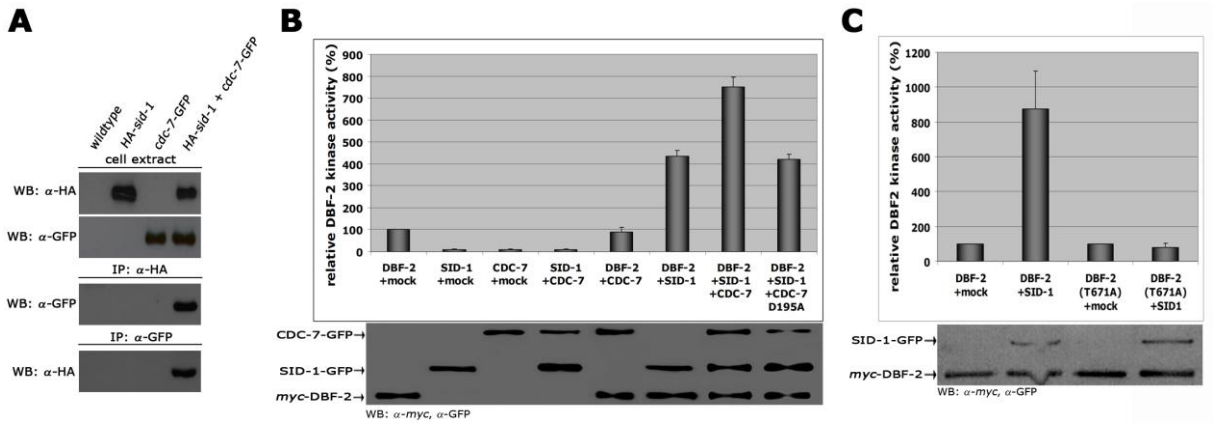

Figure 7: CDC-7-dependent activation of DBF-2 occurs through SID-1 (A) Reciprocal co-immunoprecipitation experiments of CDC-7-GFP and HA-SID-1 from cell extracts co-expressing both functionally tagged proteins indicated a stable interaction of the two kinases. (B) *In vitro* DBF-2 activity assays revealed that addition of individually purified SID-1 stimulated DBF-2 activity. SID-1-dependent stimulation of DBF-2 was further enhanced by addition of CDC-7 to the reaction, while addition of the kinase dead variant CDC-7(D195A) did not. As control, CDC-7 did not stimulate DBF-2 and approaches using SID-1 and CDC-7 precipitates proved the specificity of this assay for the NDR kinase. (C) SID-1 was able to stimulate DBF-2, but not DBF-2(T671A). Western blot analysis of the precipitated proteins was used to determine comparable kinase levels (n = 5).

5.1.3 Dual phosphorylation of DBF2 is required for kinase activity and septum formation

NDR kinase activity is regulated through interaction with adaptor proteins of the MOB family, auto-phosphorylation in the activation segment, and phosphorylation of the C-terminal hydrophobic motif by an upstream-acting germinal centre (GC) family kinase (Hergovich *et al.*, 2006, Maerz & Seiler, 2010). In order to further dissect the phospho-regulation of DBF-2, strains expressing DBF-2 variants harboring point mutations in the predicted auto-phosphorylation and hydrophobic motif sites Ser499 and Thr671, respectively, were characterized. Both, the Ser499 to alanine (non-phosphorylated, inactive mimic) and to glutamate (phosphorylated, active mimic) substitutions were nonfunctional, and these kinase variants were unable to complement the septation defects of Δ*dbf-2* (Figure 8 A). Mutations of the Thr671 to alanine/glutamate revealed that DBF-2(T671E), but not DBF-2(T671A) was functional and complemented the deletion strain.

In vitro kinase assays using DBF-2 variants harboring either of the two Ser499 substitutions displayed activities reduced to ca. 1/3 of the wild type DBF-2 control (33±6% and 30±12% for DBF-2(S499A) and DBF-2(S499E), respectively; n = 5; Figure 8 B). In contrast, the kinase activity of DBF-2(T671A) was slightly increased (200±7%; n = 5), while DBF-2(T671E) displayed >30-fold increased activity (3300±240%; n = 5). Although modification of homologous residues affected the interaction of the *S. pombe* NDR kinase Sid2 with Mob1 (Hou et al., 2004), MOB-1 binding was not affected by these modifications in *N. crassa*, and equal MOB-1 levels co-precipitated with each DBF-2 variant (Figure 8 B). To confirm Ser499 as auto-phosphorylation site, *in vitro* phosphorylation experiments coupled with mass-spectrometric analysis of DBF-2 kinase variants precipitated under high-stringency

conditions were performed. Tryptic peptides generated from wild type DBF-2 and hyperactive DBF-2(T671E) showed strong phosphorylation of S499, while a catalytically inactive DBF-2(D422A) variant did not, indicating that Ser499 is the primary site of DBF-2 auto-phosphorylation (Figure S2). Moreover, phosphorylation of multiple S/T residues in the N-terminal, non-catalytic region of the DBF-2(T671E) variant was identified.

Based on the fact that both Ser499 modifications exhibited reduced DBF-2 activity *in vitro* and were nonfunctional *in vivo* may suggest that dynamic modification of the activation segment (i.e. the regulated phosphorylation/dephosphorylation) could modulate DBF-2 function. To further explore this possibility strains carrying various combinations of both S499 and T671 to alanine/glutamate substitutions were generated (Figure 8 B). None of these double modifications resulted in functional protein, and complementation of the Δ*dbf-2* defects failed with all constructs (data not shown). Kinase assays revealed that the two Thr671 to alanine variants DBF-2(S499A;T671A) and DBF-2(S499E;T671A) displayed reduced activities, which were similar to the individual Ser499 mutations (34±4% and 31±13% of wild type DBF-2, respectively; n = 5). Furthermore, substitution of the hydrophobic motif threonine with glutamate in a S499A and S499E background increased kinase activity 3.6- and 5.3-fold compared to the respective Ser499-modified protein (n = 5). Thus, phosphorylation of Thr671 can partly overcome the lack of activation segment modification, but the stable modification of Ser499 prevented full activation of DBF2.

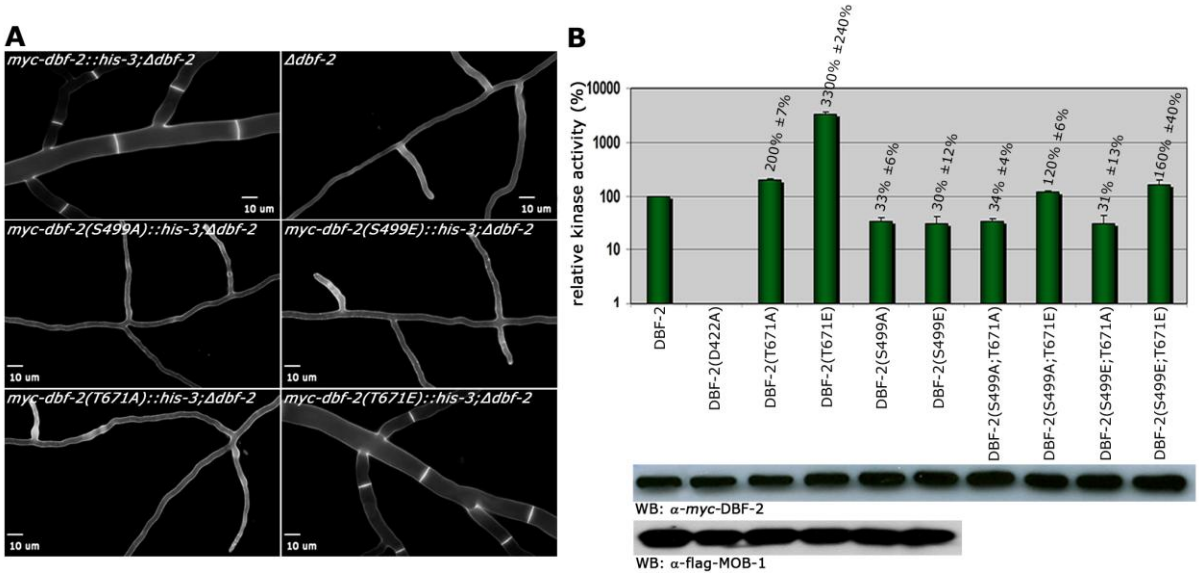

Figure 8: Dual phosphorylation of DBF-2 is required for kinase activity and septum formation. (A) Functional characterization of two conserved phosphorylation sites of DBF-2. The phosphomimetic DBF-2(T671E) variant complemented Δ*dbf-2*, while substitution of Ser499 to alanine and glutamate and Thr671 to alanine did not. Cell wall and septa were labeled with Calcofluor White. (B) Kinase activity and MOB-1 interaction pattern of the indicated DBF-2 variants. Hydrophobic motif phosphorylation of Thr671 was required for maximal kinase activity, while modification of Ser499 within the activation segment reduced DBF-2 activity to ca. 30% of the wild type DBF-2 control. Phospho-site double mutant analysis indicated that substitution of Thr671 to glutamate in a S499A and S499E background could only partly restore kinase activity. Precipitated DBF-2 variants were assayed *in vitro* using the synthetic NDR kinase peptide (KKRNRRLSVA) as substrate (n =

5). Western blot analysis indicated equal precipitation of the co-activator protein MOB-1 with DBF-2 activation segment and hydrophobic motif variants.

5.2 MST-1 controls proper CAR formation and connects the SIN and MOR pathway during septum formation

5.2.1 MST-1 displays features reminiscent of SIN as well as MOR components

The germinal center kinases (GCK) constitute a large, highly conserved family of proteins that has been implicated in a wide variety of cellular processes including cell growth, proliferation and polarity (Boyce & Andrianopoulos, 2011, Dan *et al.*, 2001). A phylogenetic analysis of the three *N. crassa* germinal centre (GC) kinases proposed a classification into functionally distinct subgroups (Figure 9 A). *N. crassa* POD-6 and the related budding and fission yeast kinases Kic1p and Nak1 clustered together, in line with their conserved function as upstream components of the MOR pathway (Huang et al., 2003, Nelson *et al.*, 2003, Seiler et al., 2006). The second phylogenetic subgroup is composed of *S. pombe* Sid1, *N. crassa* SID-1 and *A. nidulans* SEPM, supporting a conserved function during septation (Guertin *et al.*, 2000, Kim et al., 2009). Proteins of the third subgroup are most closely related to animal group III GC kinases and the fission yeast member Ppk11 was recently characterized as auxiliary factor of the MOR pathway that supports cell separation (Goshima *et al.*, 2010). However, the *N. crassa* protein NCU00772/MST-1 had been implicated as part of the SIN in a preliminary analysis (Dvash et al., 2010).

In order to determine the potential role of *N. crassa* MST-1 as a component of the SIN/MOR pathways, the localization pattern and deletion mutant characteristics of *mst-1* were compared to those of SIN and MOR components. As previously shown *N. crassa sin* mutants are aseptate (Maerz et al., 2009), while *mor*-defective cells produce multiple, closely spaced septa (Seiler et al., 2006, Maerz et al., 2009). Analysis of *Δmst-1* revealed the formation of multiple, closely spaced septa and the presence of abnormal cross walls in the form of cortical spirals in older hyphal segments (Figure 9 B). Next, the localization of a functional MST-1-GFP fusion construct showed the constitutive association with spindle pole bodies (SPBs) independently of the cell cycle state and also with constricting septa, a localization pattern characteristic for fungal SIN components (Guertin et al., 2000, Kim et al., 2006, Kim et al., 2009). In contrast, a GFP fusion construct of the MOR GC kinase POD-6 localized at the hyphal tip in a dot-like structure in the distal region of the Spitzenkörper, as membrane-associated apical crescent and at forming septa (Figure 9). This localization pattern is consistent with the reported localization of the morphogenesis pathway complex COT-1 ─MOB-2A (Maerz et al., 2012, Dettmann et al., 2012). Due to the weak expression level of POD-6-GFP, the detection as cortical ring during the initial stages of septum constriction was impossible.

Nevertheless, POD-6-GFP strongly labeled septa at later stages of septum constriction and accumulated around the mature septal pore. Neither POD-6 nor COT-1 associated with SPBs (Figure 9 C and Figure S3).

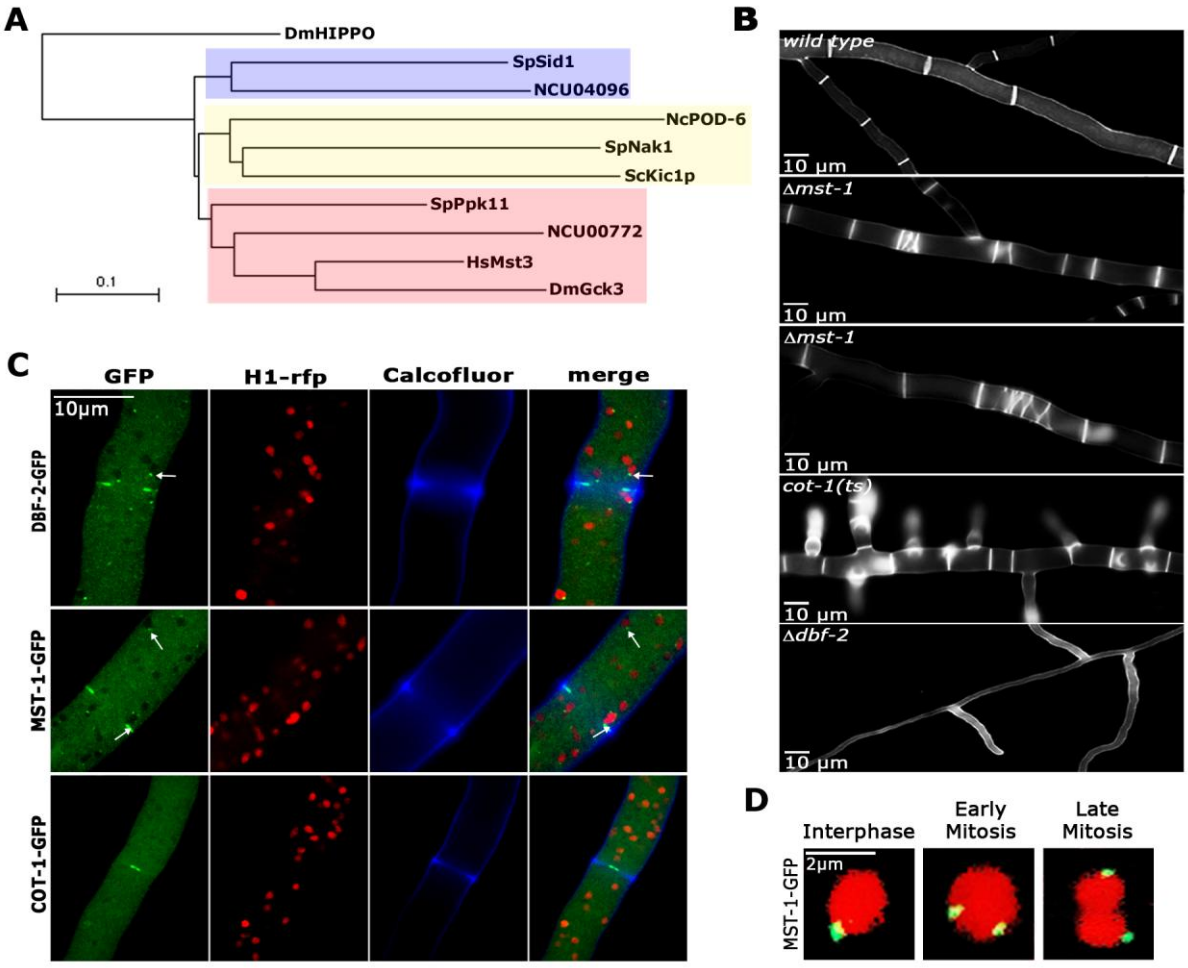

Figure 9: The germinal centre kinase MST-1 reveals characteristics of SIN as well as MOR components (A) Phylogenetic comparison of fungal GC kinases. The tree was generated by the neighbour-joining method based on a ClustalW alignment of the indicated *S. cerevisiae*, *S. pombe* and *N. crassa* proteins. HsMst3 and DmGck3 were used as examples for animal group III GC kinases, DmHippo was used as GC kinase II outgroup (multiple alignment parameters: open gap penalty 10.0, extend gap penalty 0.0, delay divergent 40%, gap distance 8, similarity matrix blosum). (B) Phenotypic characteristics of *Δmst-1, cot-1(ts) and Δdbf-2* during septum formation. Note the presence of closely spaced septa (second panel) and abnormal spirals (third panel) of *Δmst-1*. Also *cot-1*-defective cells produce multiple, closely spaced septa, whereas *Δdbf-2* cells are aseptate. Cell wall and septa were labeled with Calcofluor White. (C) Functional GFP fusion proteins of DBF-2, MST-1 and COT-1 localized as constricting rings at forming septa, while DBF-2 and MST-1 also localized to spindle pole bodies (arrows). Nuclei were labeled with histone H1-RFP, the cell wall was stained with Calcofluor White and plasma membrane and Spitzenkörper with FM4-64. (D) MST-1-GFP associated with SPBs of interphase nuclei as well as during early and late mitotic stages (as indicated by nuclear morphology). Nuclei were labeled with histone H1-RFP.

5.2.2 MST-1 controls proper CAR formation

It was recently shown that components of the *S. cerevisiae* mitotic exit network (MEN) play a direct role in promoting cytokinesis by acting upon components of the contractile actomyosin ring (CAR) and cell separation machineries (Meitinger *et al.*, 2012). For instance, localization of Dbf2p to the future site of septum formation is required for the assembly and constriction of the CAR (Meitinger et al., 2012, Weiss, 2012). Due to the formation of abnormal cross walls in the form of cortical spirals in the *Δmst-1* mutant the dynamics of septum constriction in wild type and *Δmst-1* by monitoring the behavior of the formin BNI1 (Justa-Schuch et al., 2010) were analyzed. A functional BNI-1-GFP fusion construct formed cortical rings with equal signal intensity in wild type cells, and septum constriction was concentric, resulting in centrally positioned septal pores (Figure 10 A). In contrast, BNI-1 frequently (i.e. in 38 of 47 septation events analyzed) formed asymmetric rings and open circles that led to acentric constriction and asymmetric septal pores in *Δmst-1*. Furthermore, BNI-1 also associated with extensive cortical Calcofluor white-labeled spirals (Figure 10 B). Moreover, a lifeact-GFP construct, which was recently developed for *N. crassa* (Delgado-Alvarez et al., 2010) was utilized to directly monitor actin dynamics during CAR assembly and constriction. Lifeact-GFP labeled a mesh of F-actin cables and patches named the septal actin tangle (SAT) around the future septation site in wild type cells, which subsequently coalesced to form the CAR (Figure 10 C). However, in a *Δmst-1* mutant the F-actin meshwork was miss-organized and the actin cables were irregularly distributed. The SAT to CAR transition lasted 2:48(±0:36) min in wild type (n = 15), but 8:42(±2:00) min (n = 12) in *Δmst-1*. The failure of correct CAR assembly resulted in acentric constriction and asymmetric position of septal pores or the formation of open actin spirals, which were unable to constrict (Figure 10 D).

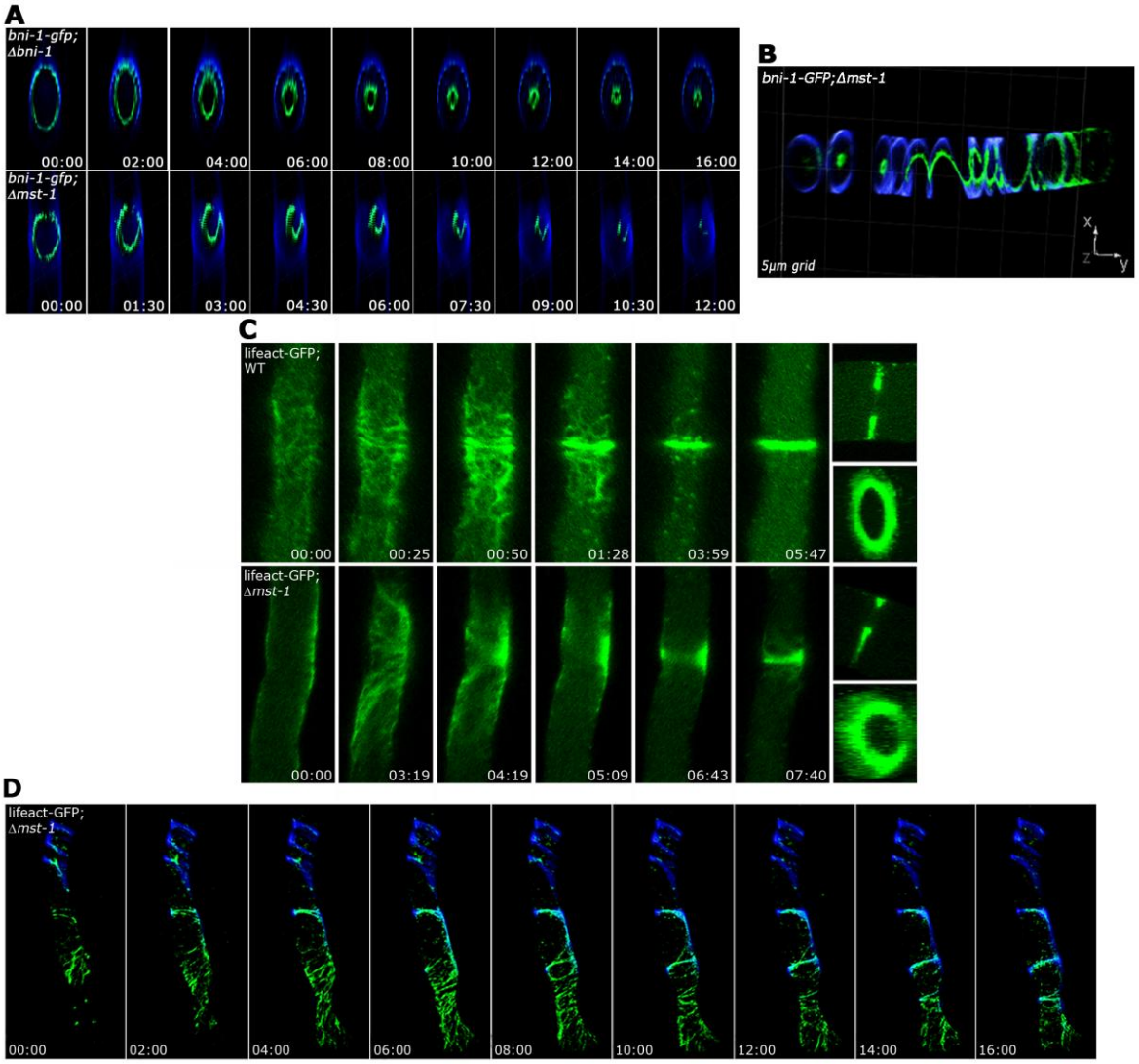

Figure 10: MST-1 is required for proper contractile actin ring formation. (A) 4D reconstruction of z-stacks in time lapse series revealed cortical, concentrically constricting BNI-1-GFP rings in wild type cells, which resulted in centrally positioned septal pores. In contrast, BNI-1 formed asymmetric and frequently open BNI-1-GFP rings in *Δmst-1* that led to acentric CAR constriction and asymmetric septal pores. (C) 3D reconstruction of z-stacks illustrates BNI-1-GFP association with extensive cortical Calcofluor white-labeled spirals in *Δmst-1*. (D) Comparison of actin dynamics during CAR assembly and constriction in wild type and *Δmst-1*. Lifeact-GFP labeled a dynamic meshwork of actin cables and patches around the future septation site in wild type cells, which subsequently coalesced to form the CAR. The actin meshwork was miss-organized and irregularly distributed in *Δmst-1* (E) 4D reconstruction of z-stacks in time lapse series visualized open actin spirals labeled by lifeact-GFP, which were unable to constrict. Cell wall, septa and cortical spirals were labeled by Calcofluor White.

5.2.3 Genetic interactions connect *Δmst-1* with SIN, but not MOR mutants

Besides the described septation defects observed in *Δmst-1*, this mutant displayed only minor vegetative abnormalities. Hyphal growth rates, colony behavior and conidiation pattern were similar to wild type (data not shown). However, sexual development of *Δmst-1* was affected in that mutant x wild type crosses resulted in ca. 50% of round (yet fully viable) ascospores, in contrast to the typical

pea-shaped progeny generated in wild type x wild type crosses (Figure 11 A). Moreover, Δ x Δ crosses resulted in the formation of empty perithecia lacking asci, and the formation of ascospores was abolished.

In order to test for genetic interactions between Δ*mst-1* and the SIN/MOR mutants, several double mutants were generated (Figure 11 B). Crosses of the MOR mutants *Δcot-1* or *Δpod-6* with *Δmst-1* resulted in the expected segregation of round and normally shaped ascospores, although the total number of generated ascospores was reduced. In contrast, double mutants of *Δmst-1* and the SIN mutants *Δdbf-2* or *Δsid-1* showed a synthetic effect represented by empty perithecia and no ascospore formation (Figure 11 B).

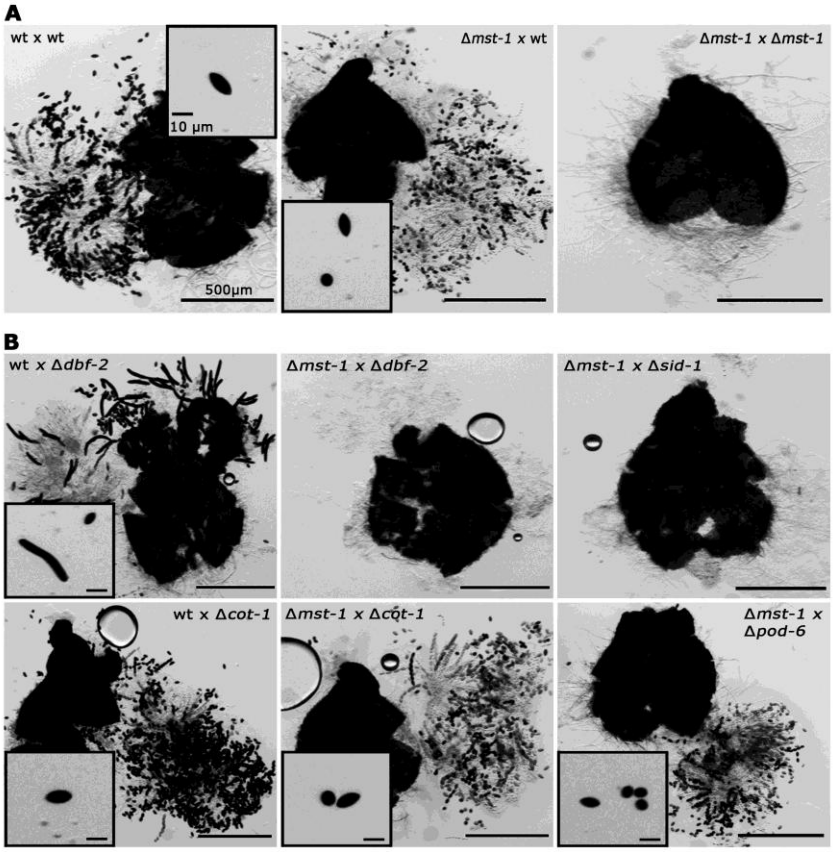

Figure 11: *Δmst-1* displays synthetic interactions with SIN, but not MOR pathway mutants. (A) *Δmst-1* x wild type crosses produced a large number of round ascospores, in contrast to the typical pea-shaped ascospores generated in wild type crosses. *Δmst-1 x Δmst-1* crosses were blocked after perithecium formation, resulting in fruiting bodies that lacked most asci and all ascopores. (B) Synthetic defects were observed in crosses of *Δmst-1* with SIN but not MOR mutants. *Δmst-1 x Δdbf-2* and *Δmst-1 x Δsid-1* crosses generated empty perithecia. In contrast, *Δmst-1 x Δcot-1* and *Δmst-1 x Δpod-6* crosses resulted in the expected segregation of round and normally shaped ascospores.

5.2.4 The SIN kinase CDC-7 regulates SID-1 and MST-1 in an antagonistic manner

The distinct localization of MST-1 at SPBs and the genetic interaction of *Δmst-1* with SIN mutants identified MST-1 as a regulatory SIN component. Thus, GFP-trap affinity purification experiments coupled with mass spectrometry were performed to determine the composition of the *N. crassa* SIN and MST-1 interacting proteins (Figure 12 A). Precipitates of CDC-7-, SID-1- and DBF-2-GFP fusion proteins recovered the central components of the SIN, including the three kinases, the predicted GTPase SPG-1/NCU08878 and the GC and NDR kinase adaptors CDC-14 and MOB-1, respectively. The Ste20-like GC kinases SID-1 and MST-1 only co-purified together, when CDC-7 was used as bait, while only one of the two GC kinases was detected in the other purifications. Furthermore, the interaction of CDC-7 with MST-1 was confirmed *in vivo* by reciprocal co-immunoprecipitation experiments (Figure 12 B). In order to prove distinct CDC-7 ―MST-1/SID-1 complexes, GC-kinase displacement assays were performed. For this purpose a *N. crassa* strain, co-expressing functionally tagged proteins of CDC-7-GFP and HA-MST-1 was used. Precipitation of CDC-7-GFP allowed detection of co-purified HA-MST-1, whereas addition of seperately purified SID-1-GFP to a CDC-7-GFP precipitation resulted in a reduced abundance of co-purified HA-MST-1 (Figure 12 C). Due to the fact that precipitation of CDC-7-GFP also allowed detection of co-purified HA-SID-1 (Figure 7), the same approach was performed using a *N. crassa* strain expressing functionally tagged proteins of CDC-7-GFP and HA-SID-1. Addition of individually precipitated MST-1-GFP to a CDC-7-GFP purification resulted in a reduced abundance of co-purified HA-SID-1 (Figure 12 D). Thus, the CDC-7 occurance is distributed to individual complexes, either CDC-7 ―MST-1 or CDC-7 ―SID-1. As already described in section 5.1.2 purified SID-1 stimulated DBF-2 *in vitro* through phosphorylation of the hydrophobic motif of DBF-2 and the SID-1-dependent activation of DBF-2 is further enhanced by addition of separately purified CDC-7. Analogous, *in vitro* kinase assays, using precipitated MST-1 instead of SID-1 indicated that also MST-1 is able to stimulate DBF-2 activity (Figure 12 E). However, addition of purified CDC-7 to a MST-1-DBF-2 mixture resulted in a decrease of MST-1-dependent stimulation of DBF-2 activity. A similar decrease of MST-1-mediated DBF-2 activity could be observed by addition of a catalytically inactive version of CDC-7 (Figure 12 E).

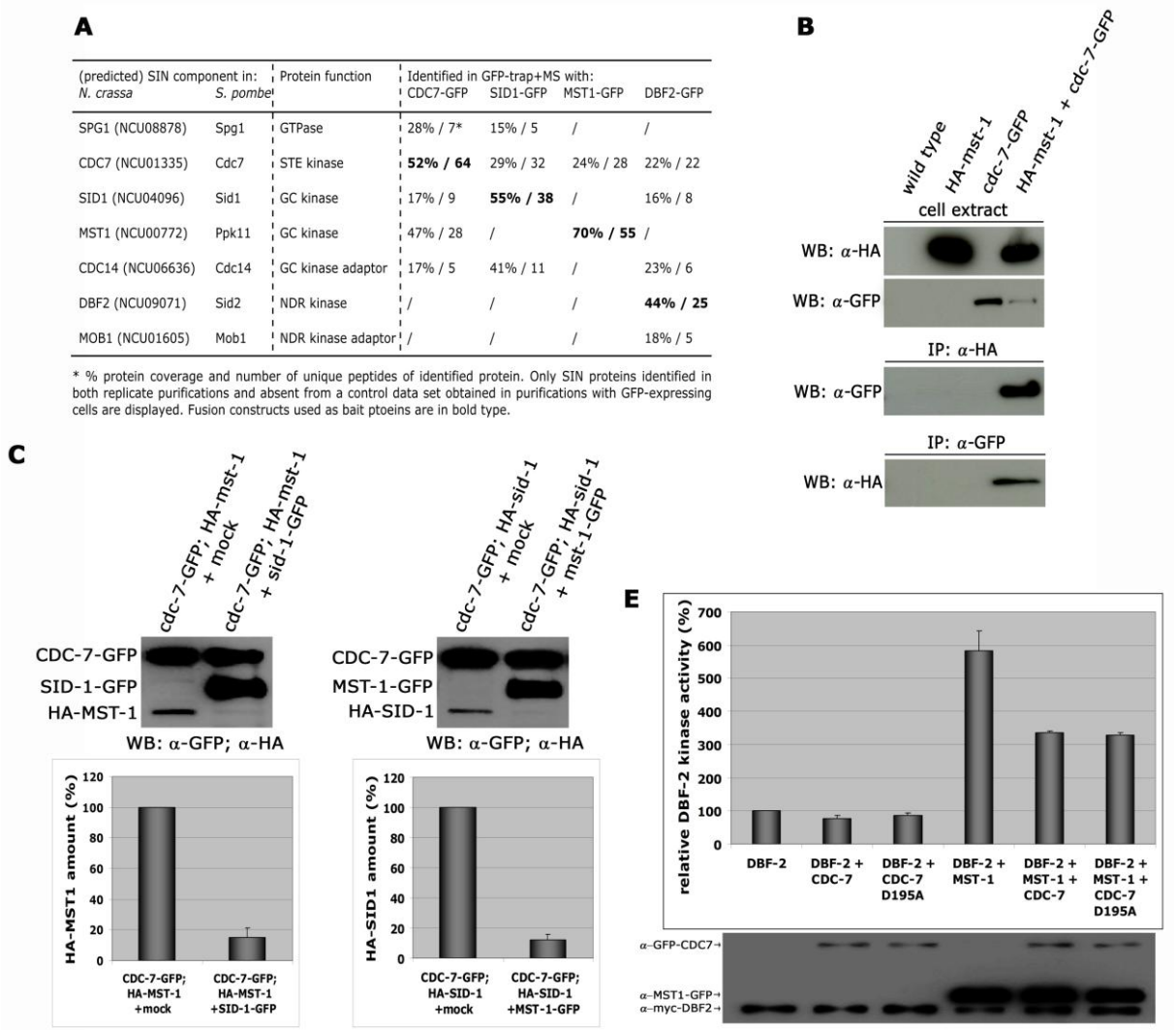

(predicted) SIN component in: *N. crassa*	*S. pombe*	Protein function	Identified in GFP-trap+MS with: CDC7-GFP	SID1-GFP	MST1-GFP	DBF2-GFP
SPG1 (NCU08878)	Spg1	GTPase	28% / 7*	15% / 5	/	/
CDC7 (NCU01335)	Cdc7	STE kinase	**52% / 64**	29% / 32	24% / 28	22% / 22
SID1 (NCU04096)	Sid1	GC kinase	17% / 9	**55% / 38**	/	16% / 8
MST1 (NCU00772)	Ppk11	GC kinase	47% / 28	/	**70% / 55**	/
CDC14 (NCU06636)	Cdc14	GC kinase adaptor	17% / 5	41% / 11	/	23% / 6
DBF2 (NCU09071)	Sid2	NDR kinase	/	/	/	**44% / 25**
MOB1 (NCU01605)	Mob1	NDR kinase adaptor	/	/	/	18% / 5

* % protein coverage and number of unique peptides of identified protein. Only SIN proteins identified in both replicate purifications and absent from a control data set obtained in purifications with GFP-expressing cells are displayed. Fusion constructs used as bait ptoeins are in bold type.

Figure 12: The SIN kinase CDC-7 regulates SID-1 and MST-1 in an opposite manner. (A) AP-MS data from two independent biological replicates were used for identification of predicted SIN components. (B) Co-immunoprecipitation experiments of CDC-7-GFP with HA-SID-1 or HA-MST-1 in extracts of forced heterokaryons expressing the labeled proteins. (C) GC-kinase displacement assay showed that precipitation of CDC-7-GFP allowed detection of HA-MST-1, whereas addition of seperately purified SID-1-GFP to a CDC-7-GFP precipitation resulted in a reduced abundance of co-purified HA-MST-1 to 15,1±6,3% (n= 3) (D) GC-kinase displacement assay showed that precipitation of CDC-7-GFP allowed detection of HA-SID-1, whereas addition of seperately purified MST-1-GFP to a CDC-7-GFP precipitation resulted in a reduced abundance of co-purified HA-SID-1 to 12,1±3,5% (n= 3) (E) *In vitro* DBF-2 activity assays revealed that addition of individually purified MST-1 stimulated DBF-2 activity. In contrast, MST-1-dependent stimulation of DBF-2 was decreased by addition of CDC-7 to the reaction. The same decrease was observed by addition of a kinase dead variant of CDC-7, CDC-7(D195A). As control, CDC-7 and the CDC-7(D195A) did not stimulate DBF-2 (n = 4). Western blot analysis of the precipitated proteins was used to determine comparable kinase levels.

5.2.5 MST-1 coordinates SIN and MOR functions during septum formation

The biochemical analysis of MST-1 and its localization strongly suggest a function of MST-1 in fine-tuning the SIN. However, *Δmst-1* also partly phenocopied MOR mutants in that the formation of multiple, closely spaced septa was observed (Figure 9). In order to determine if MST-1 may regulates

both NDR kinase pathways, SIN and MOR, and accordingly whether MST-1 was capable of activating the MOR kinase COT-1 *in vitro*, it was found that precipitated MST-1 stimulated DBF-2 as well as COT-1 (Figure 13 A, B). In contrast SID-1 only stimulated DFB-2, while POD-6 was specific for COT-1. Thus, SID-1 and POD-6 are pathway-specific activators of the SIN and MOR, respectively, consistent with the phenotypic characteristics of the respective mutants and the SIN/MOR-specific localization patterns (Seiler et al., 2006, Maerz et al., 2009, Dettmann et al., 2012). MST-1 on the other hand functions as promiscuous activator of both pathways. Next, it was tested if the three GC kinases use similar mechanisms of NDR kinase activation by phosphorylating the hydrophobic motifs of DBF-2 and COT-1 (Figure 13 A, B). *In vitro* kinase assays showed that MST-1 was unable to stimulate DBF-2 and COT-1 variants (DBF-2 T671A; COT-1 T589A), in which their hydrophobic motif phosphorylation site was modified. Thus, all three GC kinases activate their target NDR kinase(s) by phosphorylating their hydrophobic motif(s). To further dissect the function of MST-1 during MOR signalling, interaction studies and biochemical analysis were performed. Yeast two-hybrid experiments showed the interaction of MST-1 with the MOR components POD-6 and COT-1 and both interactions were confirmed by *in vivo* co-immunoprecipitation experiments (Figure 13 C/D/E). Since it was shown that CDC-7 reduced the MST-1-dependent stimulation of DBF-2 activity (Figure 12 E), a similar approach was performed using precipitated COT-1 instead of DBF-2 in *in vitro* kinase assays. These assays revealed that addition of purified CDC-7 to a MST-1 ─COT-1 mixture resulted in a decrease of MST-1-dependent stimulation of COT-1 activity (Figure 13 F). Next, GC-kinase displacement assays showed that addition of purified MST-1 to a separately precipitated POD-6/COT-1 complex (Seiler et al., 2006, Dettmann et al., 2012) completely displaced POD-6 (Figure 13 G).

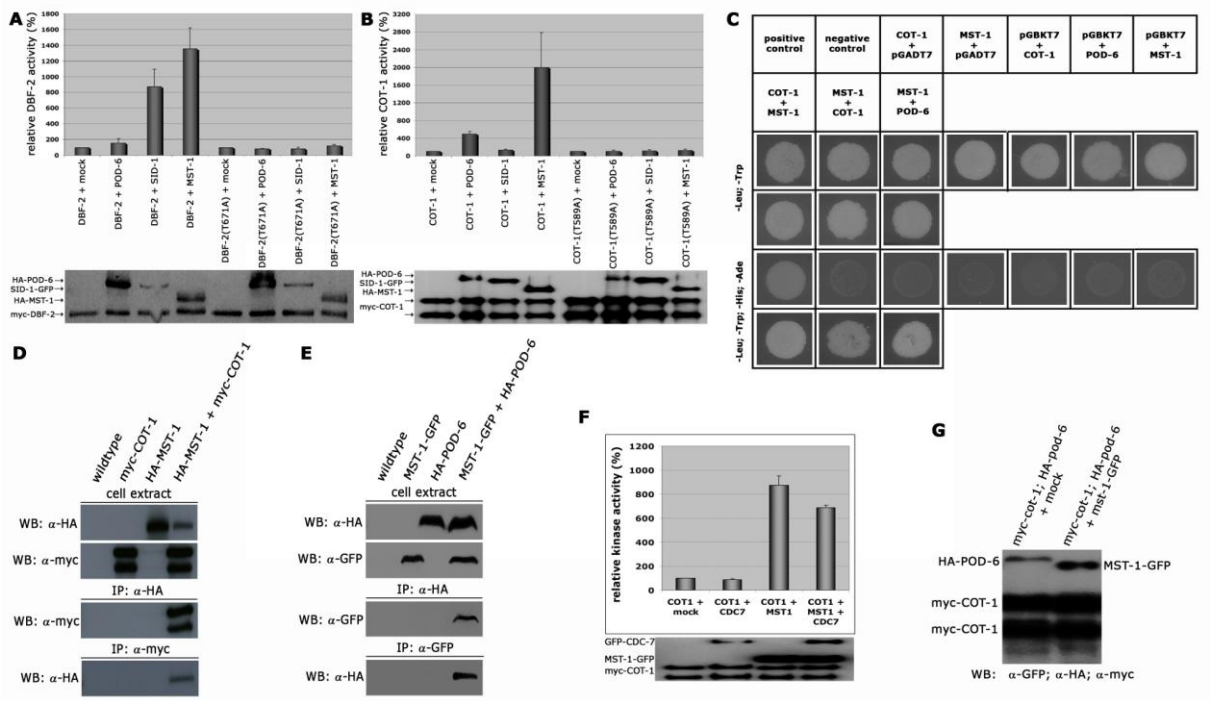

Figure 13: SID-1 and POD-6 are pathway-specific activators of the SIN and MOR, while MST-1 regulates both NDR kinase pathways. (A) MST-1 and SID-1 function in concert to regulate the activity of the SIN effector kinase DBF-2. *In vitro* kinase assays of precipitated MST-1 and SID-1 specifically stimulated DBF-2, but not DBF-2(T671A) (n= 3). (B) COT-1 was specifically phosphorylated by the upstream GC kinases POD-6 and MST-1, but not by SID-1 (n=3). Western blot analysis of the precipitated proteins was used to determine comparable kinase levels. (C) Yeast two-hybrid experiments showed the interaction of COT-1/POD-6 with MST-1. (D) Reciprocal *in vivo* co-immunoprecipitation experiments of myc-COT-1 and HA-MST-1. (E) Reciprocal *in vivo* co-immunoprecipitation experiments of MST-1-GFP and HA-POD-6. (F) Addition of CDC-7 to a COT-1 —MST-1 mixture decreased COT-1 activity in *in vitro* kinase assays. In contrast a CDC-7 —MST-1 mixture, inhibited NDR kinase activity (n = 4). Western blot analysis of the precipitated proteins was used to determine comparable kinase levels. (G) GC-kinase displacement assay showed that precipitation of myc-COT-1 allowed detection of HA-POD-6, whereas addition of seperately purified MST-1-GFP to a myc-COT-1 precipitation resulted in a complete displacement of co-purified HA-POD-6 (n= 3).

5.3 The SIN antagonizes the MOR, which in turn inhibits BUD-3 localization

5.3.1 Genetic relationship between SIN, MOR and BUD mutants

The mechanisms of determining the site of cell division are poorly understood in filamentous fungi. The anillin BUD-4 marks septum placement by organizing the RHO4-BUD3-BUD4 GTPase module in *N. crassa* (Justa-Schuch et al., 2010). In addition to the importance of the SIN for providing the temporal cue for CAR constriction, the activity of the network is also important for CAR assembly (Hachet & Simanis, 2008, Huang et al., 2008, Roberts-Galbraith & Gould, 2008). In *A. nidulans* SidB and its co-activator MobA are members of the SIN and localize to SPBs, the forming septum and function upstream of the AnBud3-Rho4 complex (Si et al., 2010, Bruno et al., 2001, Kim et al., 2006).

In order to determine the genetic relationship between SIN/MOR and BUD components, several *N. crassa* double mutants were generated (Figure 14). *N. crassa* SIN as well as BUD mutants are aseptate (Maerz et al., 2009, Justa-Schuch et al., 2010), while MOR-defective cells produce multiple, closely spaced septa (Seiler et al., 2006, Maerz et al., 2009). Crosses of the MOR mutant *cot-1(ts)* with the SIN mutants *Δdbf-2* or *Δmob-1* resulted in progeny that regained the ability to form septa at restrictive temperature. On the contrary progeny of crosses of *cot-1(ts)* with *Δbud-3* or *Δbud-4* showed thin and aseptate hyphae, which frequently lysed. This epistasis analysis revealed that septum formation in a MOR deletion background does not require a functional SIN cascade and furthermore indicates a function of DBF-2 upstream of COT-1, which in turn inhibits the BUD complex.

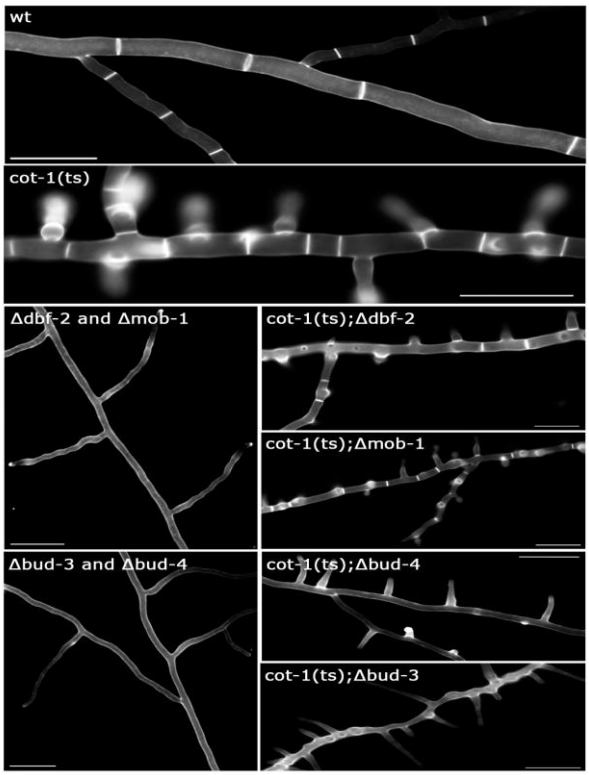

Figure 14: DBF-2 functions upstream of COT-1, which in turn inhibits the BUD complex. Epistasis analysis of the indicated SIN/MOR deletion mutants. *N. crassa* SIN as well as BUD mutants are aseptate, while MOR-defective cells produce multiple, closely spaced septa. Double deletion mutants of *cot-1(ts)* and *Δdbf-2* or *Δmob-1* regained the ability to form septa at restrictive temperature, whereas progeny of crosses of *cot-1(ts)* with *Δbud-3* or *Δbud-4* showed thin and aseptate hyphae. Cell wall and septa were labeled with Calcofluor White.

5.3.2 DBF-2 inhibits COT-1 activity through formation of kinase-kinase heterodimers

Due to the functional relationship between the SIN kinase DBF-2 and the MOR kinase COT-1 both kinases were tested for interaction by *in vivo* co-immunoprecipitation experiments. Purification of GFP-DBF-2 allowed the co-precipitation of myc-COT-1 and vice versa, which confirmed the interaction of DBF-2 with COT-1 *in vivo* (Figure 15 A). NDR kinases contain a conserved basic region, which functions as dimerization domain and binding platform for other regulatory proteins (Maerz et al., 2009, Millward *et al.*, 1998, Hou et al., 2004, He *et al.*, 2005a, Hergovich et al., 2006, Ponchon *et al.*, 2004). In order to determine whether the conserved dimerization domain of COT-1 is sufficient to interact with DBF-2, several yeast two-hybrid experiments were performed (Figure 15 B). Specific interactions were detected between DBF-2 and full length COT-1 and two truncated variants of COT-1 (amino acids 1–212 and 119–212; designated long and short, respectively), indicating that region 119–212 of COT-1 is sufficient to interact with DBF-2. Moreover, DBF-2 (as other NDR kinases) is able to interact with itself.

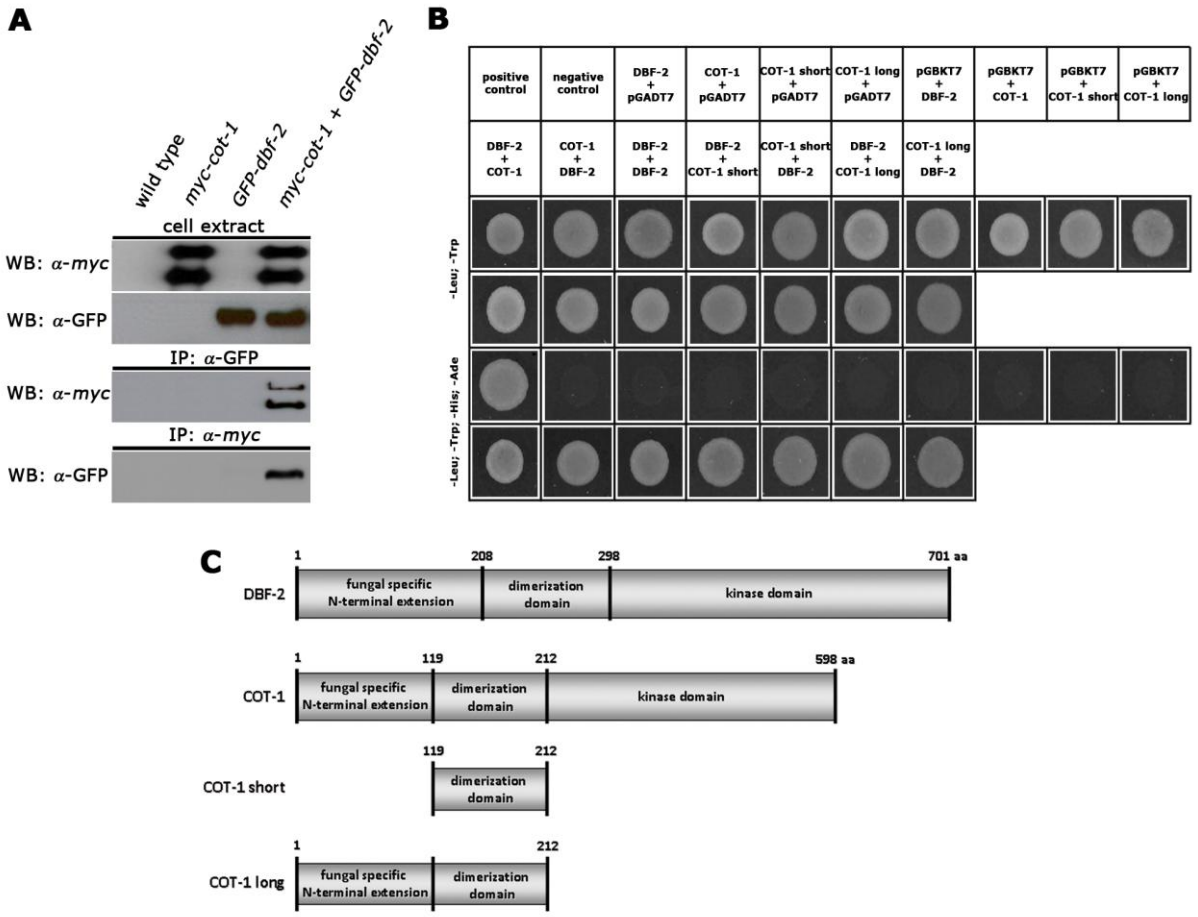

Figure 15: The NDR kinases DBF-2 and COT-1 form kinase-kinase heterodimers. (A) Reciprocal *in vivo* co-immunoprecipitation experiments of GFP-DBF-2 and myc-COT-1. (B) Yeast two-hybrid experiments showed that region 119–212 of COT-1 is sufficient to interact with DBF-2. (C) General domain structure of the NDR kinases DBF-2 and COT-1 and illustration of constructs used for yeast two-hybrid analysis.

Next, it was tested if the interaction of DBF-2 with the COT-1 dimerization domain has an impact on COT-1 kinase activity. Therefore, *in vitro* kinase assays using individually purified COT-1 and DBF-2 were performed and revealed that incubation of COT-1 with DBF-2 resulted in a decrease of COT-1 kinase activity to 70±5% (Figure 16 A). Due to the fact that both kinases displayed activity towards the synthetic peptide encompassing the consensus NDR kinase target motif, the same approach was performed using a catalytically inactive variant DBF-2(D422A). By mixing precipitated COT-1 with separately purified DBF-2(D422A), a further decrease (correlating with the activity of wildtype DBF-2) of COT-1 kinase activity was observed, indicating that DBF-2 inhibits COT-1 activity by formation of hetero-dimers (Figure 16 A). Western blot analysis of the precipitated proteins was used to determine equal kinase levels. To further dissect the mechanism of COT-1 inhibition by DBF-2 analogous *in vitro* kinase assays with increasing DBF-2(D422A) amounts (from 0 ml up to 4 ml) were performed. The results showed a DBF-2(D422A)-dependant, continuing decrease of COT-1 activity (Figure 16 B).

Moreover, it was recently shown that the N-terminal region directly preceding the kinase domain of *N. crassa* COT-1 is also responsible for the interaction with MOB-2 adaptor proteins, which in turn is crucial for COT-1 activity and stability (Maerz et al., 2009). In order to determine if the formation of COT-1 — DBF-2 hetero-dimers results in a MOB-2 displacement, thus decreasing COT-1 activity, a MOB-2 displacement assay was performed. For this purpose a *N. crassa* strain co-expressing functionally tagged myc-COT-1 and HA-MOB-2A proteins was constructed. Precipitation of myc-COT-1 allowed detection of HA-MOB-2A. The addition of seperately purified GFP-DBF-2 to such a myc-COT-1/HA-MOB-2A precipitate resulted in a reduced abundance of co-purified HA-MOB-2A (Figure 16 C). Thus, DBF-2 presumably functions as competitive inhibitor of COT-1 by forming hetero-dimers.

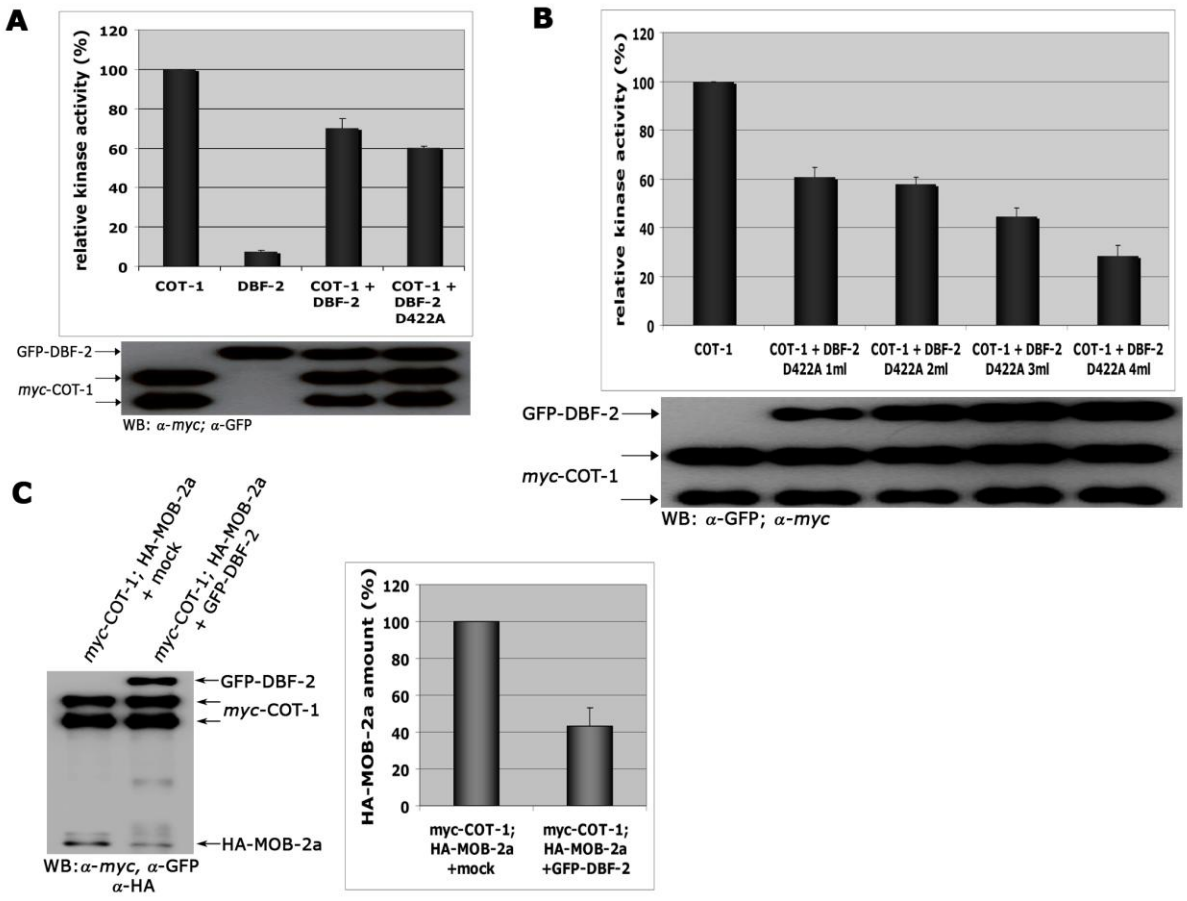

Figure 16: DBF-2 functions as competitive inhibitor of COT-1 by forming kinase-kinase heterodimers. (A) *In vitro* kinase assays using individually purified COT-1 and DBF-2(D422A), incubation of COT-1 with DBF-2(D422A) resulted in a decrease of COT-1 kinase activity to 60±1% (n= 5). (B) *In vitro* kinase assays with increasing DBF-2(D422A) amounts showed a DBF-2(D422A)-dependant, continuing decrease of COT-1 activity to 28±4,5% (n=4). (C) MOB-2 displacement assay showed that precipitation of myc-COT-1 allowed detection of HA-MOB-2A, whereas addition of seperately purified GFP-DBF-2 to a myc-COT-1 precipitation resulted in a reduced abundance of co-purified HA-MOB-2A to 43,2±9,8% (n= 3).

5.3.3 COT-1, but not DBF-2 phosphorylates BUD-3/BUD-4 landmark proteins

As mentioned in section 5.3.1 epistasis analysis revealed that septum formation in a MOR deletion background does not require a functional SIN cascade and furthermore a function of DBF-2 upstream of COT-1, which in turn inhibits the BUD complex. To further determine the functional relationship between both NDR kinases and the BUD-3 — BUD-4 complex, co-immunoprecipitation (co-IP) experiments were performed to test if DBF-2 and/or COT-1 interacted with BUD-3 and/or BUD-4. Purification of BUD-3-GFP as well as BUD-4-GFP allowed co-precipitation of myc-COT-1, which confirmed the interaction of both BUD proteins with COT-1 *in vivo* (Figure 17 A). Analogous experiments were done using strains expressing functionally tagged proteins of either BUD-3-GFP or BUD-4-GFP and myc-DBF-2, but no interaction could be observed (data not shown).

The *in silico* inspection of BUD-3/4 sequence revealed the presence of one and four putative NDR kinase consensus phosphorylation sites (RXXS) located within BUD-3 and BUD-4, respectively (Figure 17 B). Therefore, it was tested whether BUD-3/4 are direct substrates of any of the two NDR kinases. *In vitro* phosphorylation assays using individually purified BUD-3/4 and hyperactive variants of DBF-2(T671E) and COT-1(T589E) showed that BUD-3 as well as BUD-4 were phosphorylated by COT-1(T589E), but not by DBF-2(T761E) (Figure 17 C). In a next step, the predicted NDR kinase consensus sites were mutated to alanine (BUD-3(S798A); BUD-4(4xS2A) to create nonphosphorylatable mutants. *In vitro* kinase assays showed a reduced phosphorylation of precipitated BUD-3(S798A) and BUD-4(4xS2A) by COT-1(T589E) compared to the phosphorylation of wild type BUD-3/4 variants (Figure 17 D). Collectively, these data show that BUD-3 and BUD-4 are *in vitro* substrates of the NDR kinase COT-1, and confirmed the predicted NDR kinase consensus phosphorylation sites located in BUD-3/4.

To obtain better insight into the functional consequences of BUD-3/4 phosphorylation by COT-1, the phenotype of nonphosphorylatable (BUD-3(S798A); BUD-4(4xS2A) and phosphomimetic (BUD-3(S798E); BUD-4(4xS2E) variants was analyzed. While both BUD-4 mutants displayed no significant abnormalities (data not shown), the BUD-3(S798A) and BUD-3(S798E) mutants revealed the formation of multiple, closely spaced septa and moreover, the presence of abnormal cross walls in the form of cortical spirals. However, both BUD-3 variants restored the inability of the *Δbud-3* mutant to form septa.

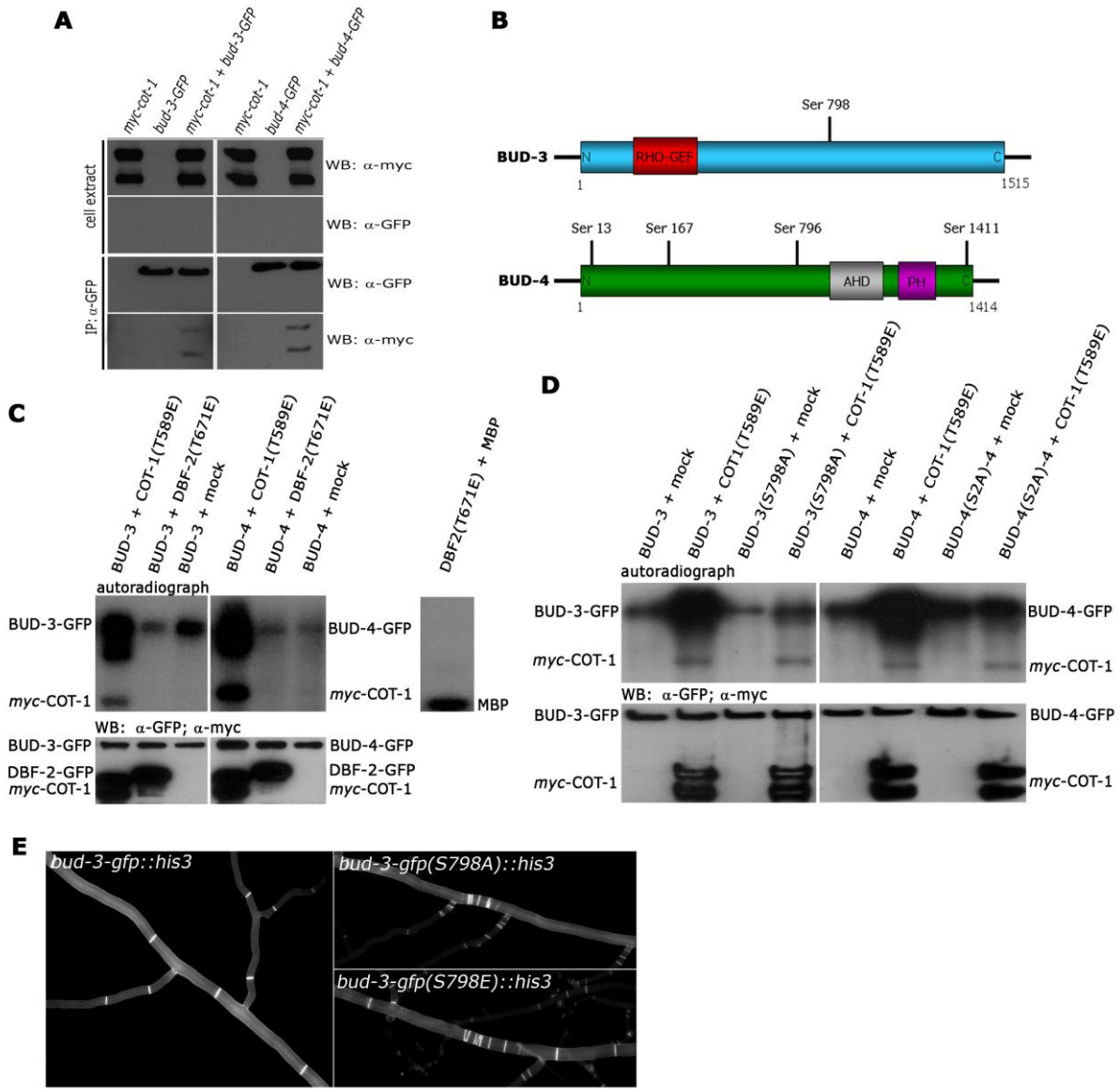

Figure 17: BUD-3 and BUD-4 are *in vitro* substrates of the NDR kinase COT-1. (A) Purification of BUD-3-GFP as well as BUD-4-GFP allowed co-immunoprecipitation of myc-COT-1, which confirmed the interaction of both BUD proteins with COT-1 *in vivo*. (B) General domain structure and predicted NDR kinase phosphorylation sites of BUD-3 and BUD-4 (AHD= anillin homology domain, PH= pleckstrin homology domain). (C) *In vitro* phosphorylation assays showed that BUD-3 as well as BUD-4 were phosphorylated by the hyperactive variant of COT-1(T589E), but not by DBF-2(T761E). The activity of COT-1 was determined by autophosphorylation and of DBF-2 by phosphorylation of maltose binding protein (MBP). (D) *In vitro* kinase assays showed a reduced phosphorylation of BUD-3(S798A) and BUD-4(S2A)-4 by COT-1(T589E) compared to the phosphorylation of wild type BUD-3/4 variants. Western blot analysis of the precipitated proteins was used to verify equal protein levels. (E) Mutation of the COT-1 phosphorylation site S798 of BUD-3 results in misregulated septation. Cell wall and septa were labeled with Calcofluor White.

5.3.4 COT-1 phosphorylation inhibits BUD-3 localization

BUD-3 is a large protein of 1604 amino acids and except for the Rho-GEF domain it lacks recognizable domains that can provide clues for its function (Figure 17 B). Sequence alignment with BUD-3

orthologs present in budding yeast and other filamentous ascomycete fungi also failed to identify highly homologous sequences. However, there are two short sequences, ^{748}LSRRIIQLL^{756} and ^{802}VKLLSNFL^{809}, that resemble amphipathic helices (Figure 18 A) (Bernstein *et al.*, 2000, Szeto *et al.*, 2002). When projected on a helical wheel, one half of the helix is highly hydrophobic, consisting of leucine, phenylalanine and isoleucine residues, whereas the other half is hydrophilic and contains at least one positively charged lysine or arginine residue (Figure 18 A, lower panel). In addition, multiple positively charged residues are present in the sequences flanking the left side of the second helix (basic-rich region - BR). Interestingly, Ser798, which was identified as COT-1 phosphorylation site in BUD-3 is located between this BR motif and the second amphiphatic helix. It is known that amphipathic helices facilitate plasma membrane targeting to some proteins (Szeto et al., 2002, Antonny *et al.*, 1997, Takahashi & Pryciak, 2007), thus BUD-3's localization to the site of septation could be mediated by these identified amphipathic helices. To determine this possibility, BUD-3-Helix-GFP fusion proteins carrying both helices including their flanking regions (aa 739-816) as well as mutated BUD-3-S798A-Helix-GFP and BUD-3-S798E-Helix-GFP constructs were generated (Figure 18 B). Only the BUD-3-S798A-Helix-GFP construct localized at constricting septa, while the wild type variant and the BUD-3-Helix-S798E construct did not. Thus, mimicing the constitutive nonphosphorylation of the putative NDR kinase consensus phosphorylation sites Ser798 of BUD-3 allowed localization at forming septa.

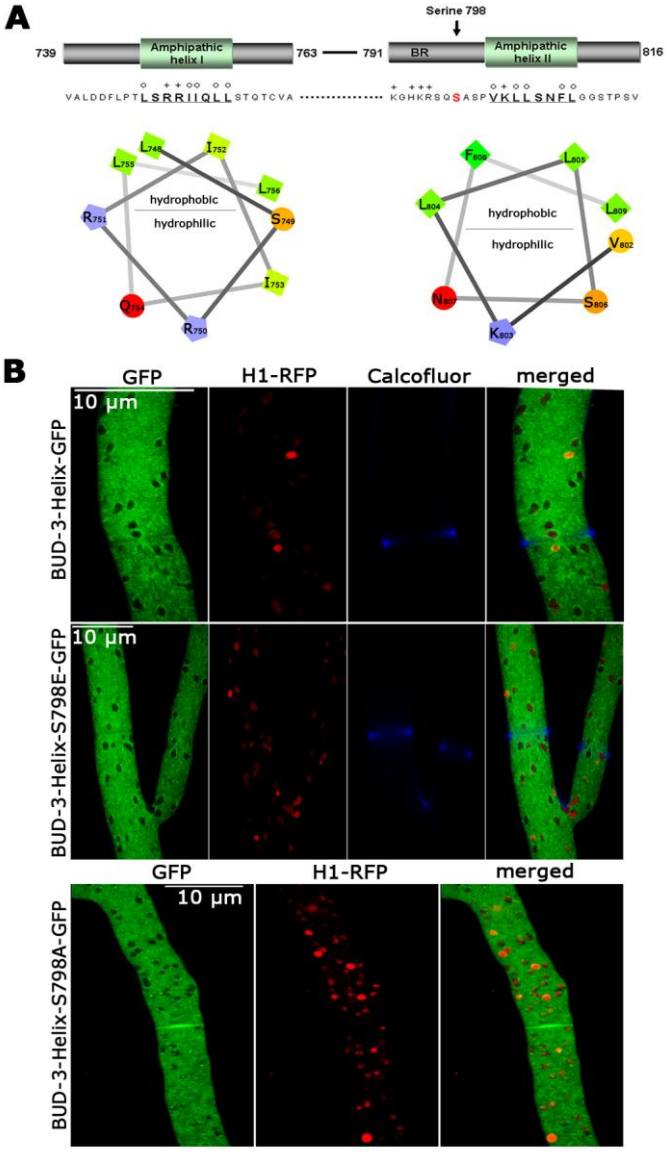

Figure 18: Ser798 of BUD-3 is located between two amphiphatic helices and regulates localization of BUD-3. (A) Upper panel, schematic model and amino acid sequence of the amphipathic helices with flanking regions of BUD-3. Positively charged and hydrophobic residues are indicated with + and o, respectively. Lower panel, a helical wheel projection of the amphipathic helices. (B) Only the constitutive non-phosphorylated BUD-3-Helix-S798A-GFP variant allowed localization at forming septa. Nuclei were labeled with histone H1-RFP, the cell wall was stained with Calcofluor White.

6. Discussion

6.1 The *N. crassa* SIN functions as hierarchical, stepwise kinase cascade

Septum formation is essential for growth and development of uni- and multicellular organisms. The temporal coordination of mitosis and cytokinesis is mediated by a signalling cascade known as the septation initiation network (SIN) in fission yeast and the mitotic exit network (MEN) in budding yeast (Meitinger et al., 2012, Johnson et al., 2012). In contrast to these unicellular yeasts, regulation of septum formation and the composition of the SIN in filamentous fungi is only beginning to be unraveled. An *in silico* analysis using *S. pombe* and *S. cerevisiae* SIN proteins identified homologs for all SIN network components except one scaffold protein in the model mold *N. crassa*. The phenotypic and biochemical analysis of these predicted SIN components allowed (a) the characterization of the SIN kinase cascade consisting of CDC-7, SID-1 and DBF-2 together with their regulatory subunits CDC-14 and MOB-1, respectively, and (b) the establishment of their hierarchical relationship and (c) provided a mechanism of DBF-2 effector kinase activation.

A first aspect of characterization of the *N. crassa* SIN was to determine the activation mechanism of the SIN effector kinase DBF-2 in *in vitro* activity studies. Based on these assays it was determined that DBF-2 is regulated by dual phosphorylation: Ser499 within the activation segment (AS) is auto-phosphorylated, while the hydrophobic motif (HM) site Thr671 is targeted by the upstream kinase SID-1. Current models for NDR kinase activity regulation predict the formation of inactive, competent and active conformations, which correspond to non-phosphorylated, auto-phosphorylated and dual-phosphorylated states, respectively (Maerz & Seiler, 2010, Hergovich et al., 2006). In this study, the full complement of kinase variants harboring individual as well as double mutant substitutions in the two regulatory sites was analysed. While DBF-2(S499A) displayed *in vitro* activity reduced to ca. 1/3rd of the wild type control, DBF-2(T671A) exhibited activities in the range of wild type DBF-2. Thus, auto- but not HM phosphorylation is required for basal kinase activity. However, alanine substitution of both sites resulted in nonfunctional protein, indicating that phosphorylation of both sites is essential for the *in vivo* functionality of DBF-2. This conclusion is supported by the DBF-2(T671E) variant, which showed maximal *in vitro* activity and was the only DBF-2 variant functional *in vivo*. It was further determined that glutamate substitution of the HM site in glutamate- and alanine-substituted Ser499 backgrounds only partially recovered *in vitro* activities and that these kinase variants were nonfunctional *in vivo*. The fact that phosphorylation of Thr671 can only partly overcome a permanent AS modification might suggest that dynamic modification of the AS may be required for full activation and functionality of DBF-2. Another possibility could also be that Ser499 modification might simply impair the functionality of the protein. However, analogous substitutions

of this conserved serine within the AS have successfully been used for the analysis of several fungal (Mah et al., 2001, Jansen et al., 2006, Ziv et al., 2009, Maerz et al., 2012, Liu & Young, 2012) as well as animal (Stegert et al., 2005, He *et al.*, 2005b) NDR kinases. Thus, combined *in vitro* and *in vivo* characterization of these DBF-2 variants suggest that a dynamic phosphorylation/dephosphorylation cycle of the autophosphorylation site rather than the simple sequential phosphorylation of both sites may be critical for *N. crassa* DBF-2 activity and function.

In vitro kinase activity assays provided the first biochemical evidence that SID-1 activates DBF-2 through hydrophobic motif (HM) phosphorylation, analogous to the activation of related fungal and animal NDR kinases by upstream Ste20-related kinases (Stegert et al., 2005, He et al., 2005b, Jansen et al., 2006, Liu & Young, 2012). A direct targeting of DBF-2 by CDC-7 was not observed, but SID-1-dependent stimulation of DBF-2 was further enhanced through CDC-7. Strikingly, this enhanced SID-1-dependent stimulation of DBF-2 was not observed by using a catalytically inactive variant of CDC-7, indicating that CDC-7 transmits signals towards DBF-2 by phosphorylation of SID-1. This hypothesis is further supported by reciprocal *in vivo* co-immunoprecipitation experiments showing that SID-1 co-precipitated with CDC-7 while DBF-2 did not. Although a direct phosphorylation of DBF-2 by CDC-7 might be a prerequisite for HM phosphorylation of DBF-2 by SID-1, this interpretation appears to be unlikely. It was previously shown that the budding yeast kinase Cdc15p phosphorylates Dbf2p on the HM analogous to the phosphorylation of DBF-2 by SID-1, presented in this study (Stegert et al., 2005, He et al., 2005b, Jansen et al., 2006, Liu & Young, 2012). Thus, these data strongly suggest that the *N. crassa* SIN functions as hierarchical, stepwise kinase cascade (Figure 19).

The cellular distribution of the three SIN kinases showed that functional GFP-fusion constructs of CDC-7, SID-1 and DBF-2 localize to spindle pole bodies (SPBs) and septa. In both unicellular yeasts, all components of the SIN/MEN cascade localize to the SPBs, while only the effector kinases Sid2/Dbf2p translocate to the division site, just prior to CAR constriction and septation (Johnson et al., 2012, Meitinger et al., 2012, Chen et al., 2008, Hwa Lim *et al.*, 2003). It was determined that *N. crassa* SID-1, CDC-14 and DBF-2 localize to the cell cortex prior to septum constriction and to the forming septum. CDC-7 was only detected at the septal pore of the mature septum, possibly indicating that this kinase only associates with the septum after constriction. Alternatively, CDC-7 levels below imaging resolution may associate with the other SIN kinases during early stages of septation. The latter is supported by expression analysis of the used GFP fusion constructs that revealed that *ccg-1* driven CDC-7-GFP is significantly lower expressed than the other SIN kinases. Thus, in contrast to the situation in yeast (Meitinger et al., 2012, Johnson et al., 2012), all SIN components associated with SPBs in a constitutive manner in *N. crassa*. Moreover, SPB association of the *N. crassa* SIN cascade is not cell cycle dependent. Together with the finding that SIN activation in *A. nidulans* does not require

SPB association of the NDR kinase SIDB (Kim et al., 2009), these data indicate major differences in the regulation of the SIN in unicellular versus syncytial ascomycetes.

In contrast to a previous report (Dvash et al., 2010), defects of *SIN* mutants in proper completion of the cell cycle was not observed. This is in line with the fact that cell cycle progression was also unaffected in *A. nidulans SIN* mutants (Bruno et al., 2001, Kim et al., 2006, Si et al., 2010). Moreover, meiotic cell divisions are also not affected in *N. crassa SIN* mutants. Re-sequencing of an old laboratory strain identified a mutant called *Banana* as *dbf-2* deletion strain (Baker SE *et al.*, 2012). Its previous characterization had revealed that the eight nuclei derived from the two meiotic and one mitotic divisions are formed in a normal manner in Ban+/Ban asci, but that the resulting nuclei are then enclosed in a single giant ascospore (Raju & Newmeyer, 1977, Freitag et al., 2004). This is consistent with data obtained for budding and fission yeasts, where the SIN is largely dispensable during meiosis, but required for spore wall formation and ascospore morphology (Krapp *et al.*, 2006, Attner & Amon, 2012). Taken together, the results support an essential, but cell cycle-independent function of the SIN during septum formation in vegetative cells in the filamentous ascomycete *N. crassa*.

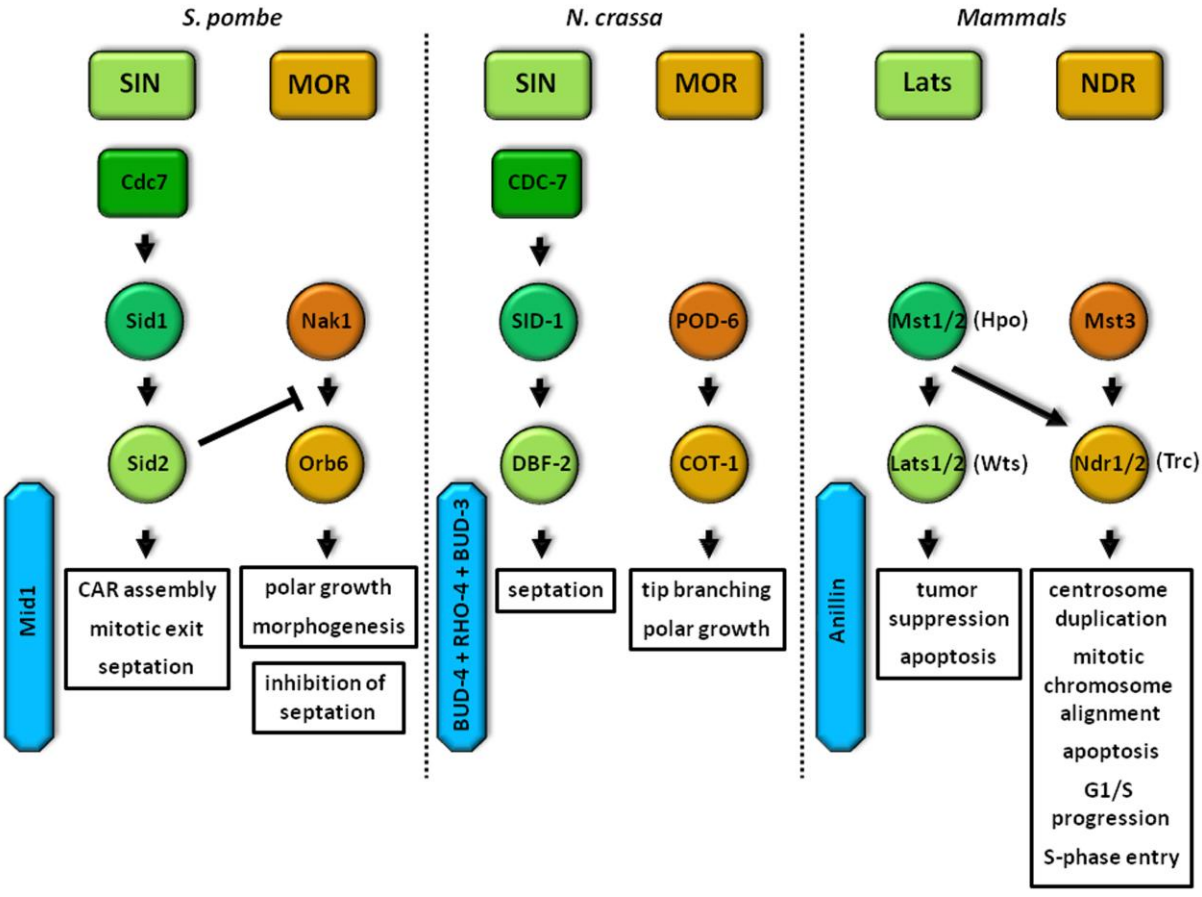

Figure 19: Comparison of highly conserved NDR signalling pathways in *S. pombe*, *N. crassa* and mammals. *D. melanogaster* orthologous Hippo core components are shown in brackets. See text for details.

6.2 Proper actin ring formation and septum constriction requires the SIN-associated Ste20-related GC kinase MST-1

Analysis of SIN deletion phenotypes revealed that Δ*sid-1* and Δ*cdc-14* strains behaved differently than Δ*cdc-7*, Δ*dbf-2* and Δ*mob-1* in that the frequency of appearance of suppressor mutations was much higher in both mutants. The result of suppressor appearance was evident by the increased ability of Δ*sid-1* and Δ*cdc-14* to form septa and to conidiate when compared to other *SIN* mutants (although all *SIN* mutants regain the ability to form septa at some point). In line with this observation, sexual progeny of Δ*sid-1* and Δ*cdc-14* x wt crosses did not form the large, banana-shaped ascospores as described for Δ*cdc-7*, Δ*dbf-2* and Δ*mob-1* containing crosses (Maerz et al., 2009). This indicated that the hypothesis of the SIN as a linear kinase cascade may represent a simplified model. One possibility could be that CDC-7 might also be able to directly target DBF-2 *in vivo,* in parallel to the proven activation of DBF-2 by SID-1, although such a dependency was not determined *in vitro*. Alternatively, additional uncharacterized kinases may function in concert with SID-1 to regulate DBF-2. Intriguingly, the localization at SPBs and constricting septa as well as interaction studies identified MST-1 as SIN-associated kinase. Moreover, crosses of SIN mutants with *Δmst-1* showed a synthetic effect reinforcing a functional relationship of MST-1 and SIN components. Based on *in vitro* kinase assays it was shown that – similar to SID-1 – MST-1 is able to stimulate DBF-2 through phosphorylation of the HM. Analysis of *Δmst-1* revealed the formation of multiple, closely spaced septa and the presence of abnormal cross walls in the form of cortical spirals in older hyphal segments. By monitoring the behavior of the formin BNI-1 (Justa-Schuch et al., 2010) and lifeact-GFP in the *Δmst-1* mutant, it was shown that the failure of correct CAR assembly resulted in acentric constriction and asymmetric position of septal pores and the formation of open actin spirals, which were unable to constrict. These data, strengthen the assumption that MST-1 is part of the SIN and required for fine-tuning SIN signals during septation. GFP-trap affinity purification experiments coupled with mass spectrometry were performed to determine the composition of the *N. crassa* SIN and MST-1 interacting proteins. Precipitates of CDC-7-, SID-1- and DBF-2-GFP fusion proteins recovered the central components of the SIN, while SID-1 and MST-1 were only co-purified together, when CDC-7 was used as bait. Furthermore, the interaction of CDC-7 with MST-1 was confirmed *in vivo* by reciprocal co-immunoprecipitation experiments, and the presence of distinct CDC-7/MST-1 and CDC-7/SID-1 complexes was proven by reciprocal GC-kinase displacement assays. Intriguingly, although both GC kinases MST-1 and SID-1 activate DBF-2 through hydrophobic motif phosphorylation, they are regulated by CDC-7 in the opposite manner. While SID-1-dependent activation of DBF-2 is further enhanced by CDC-7, addition of purified CDC-7 to a MST-1 + DBF-2 mixture resulted in a decreased stimulation of DBF-2. This decreased activation was also observed using a kinase-dead variant of CDC-7, suggesting an inhibition mechanism that depends on protein-

protein interaction rather than phospho-regulation of MST-1 by CDC-7. In summary, these data indicate that MST-1 is a SIN-associated kinase that functions in concert with SID-1 to regulate the SIN effector kinase DBF-2. Given that both GC kinases stimulate DBF-2 by HM-phosphorylation, but are regulated by CDC-7 in an opposite manner, it might be conceivable that distinct input signals guide the specific action of each GC kinase.

The Ste20-related kinase family includes the p21 activated kinases (PAKs) and the germinal centre kinases (GCKs). Both groups can be distinguished by the localization of their kinase domains, which is located in the C-terminal half of PAKs and in the N-terminal region of GCKs. In addition, PAKs possess a conserved N-terminal domain (Cdc42/Rac interactive binding, CRIB), which is required for binding to the Rho GTPases Cdc42 and Rac. Unlike PAKs, GCKs lack the CRIB domain and can be further subdivided into eight groups (I to VIII) based on their structure (Dan et al., 2001). The *S. cerevisiae* genome encodes two group II GCKs with strong sequence similarity to Ste20p (Sps1p and Kic1p), and one with weaker homology (Cdc15p). In contrast, the *S. pombe* genome encodes three group II GCKs (Nak1, Ppk11 and Sid1) besides a Cdc15p ortholog (Cdc7). Nak1 shows homology to *S. cerevisiae* Kic1p whereas *S. pombe* Ppk11 and Sid1 are in different GCK subgroups (Boyce & Andrianopoulos, 2011). Mammalian GCKs MST1 and MST2 are also members of the GCK II subfamily, while MST3 and MST4 belong to the GCK III subfamily (Ling *et al.*, 2008). The phylogenetic analysis of the three *N. crassa* GCKs allowed the classification of fungal GC kinases into functionally distinct subgroups. *N. crassa* POD-6 and the related budding and fission yeast kinases Kic1p and Nak1 clustered together, in line with their conserved function as upstream components of the MOR pathway (Huang et al., 2003, Nelson et al., 2003, Seiler et al., 2006). The second subgroup is composed of *S. pombe* Sid1, *N. crassa* SID-1 and *A. nidulans* SEPM, supporting a conserved function during septation (Guertin et al., 2000, Kim et al., 2009). Fission yeast Ppk11 and the *N. crassa* protein MST-1 are members of the third subgroup, which is most closely related to animal group III GC kinases. Ppk11 was recently characterized as auxiliary factor of the MOR pathway that supports cell separation (Goshima et al., 2010), while the *N. crassa* protein MST-1 had been implicated as part of the SIN in a preliminary analysis (Dvash et al., 2010). Several studies have shown that Ste20-like kinases genetically interact with and phosphorylate members of the NDR family. The yeast Ste20-like kinases Kic1p, Nak1, Sid1 and Cdc15p function genetically upstream of the Cbk1p, Orb6, Sid2 and Dbf2p NDR kinases (Boyce & Andrianopoulos, 2011), but only Cdc15p has been shown to activate its corresponding NDR kinase by direct phosphorylation (Mah et al., 2001). In addition to yeasts, in a recent study it was shown, that the *N. crassa* NDR kinase COT-1 (homologous to yeast Cbk1p and Orb6) is phosphorylated and stimulated by the upstream GCK POD-6 (Maerz et al., 2012). Furthermore, in *D. melanogaster*, one Ste20-like kinase, Hippo (Hpo), can regulate both NDR/LATS kinase family members (Emoto *et al.*, 2006). Similar findings have been reported for the mammalian Ste20-like (MST) kinases. Whereas the

Hpo homologs MST1 and MST2 can regulate all NDR/LATS kinases, (Chan *et al.*, 2005, Vichalkovski *et al.*, 2008), another MST kinase family member, MST3, has been shown to specifically regulate NDR1/2 (Cornils *et al.*, 2011, Stegert et al., 2005). Collectively, the close interplay between NDR kinases and Ste20-related GCKs points to conserved pathways that regulate several cellular processes like cytokinesis, mitotic exit and morphological changes (Figure 19).

6.3 MST-1 connects the SIN and MOR pathway during septum formation

The fungal SIN and MEN networks orchestrate mitotic exit and cytokinesis. One fundamental mechanism by which the SIN/MEN promote cytokinesis is by inhibiting a competing polarity pathway called the MOR/RAM, which is required for initiation of polarized growth following completion of cytokinesis (Ray et al., 2010, Gupta & McCollum, 2011, Weiss, 2012). *N. crassa* MOR mutants display hyperseptation defects (Seiler & Plamann, 2003, Seiler et al., 2006, Maerz et al., 2009), indicating that the MOR inhibits septum formation at predetermined sites. Intriguingly, the phenotypic characteristics of the *mst-1* deletion strain mirror the defects of MOR mutants in that the formation of multiple, closely spaced septa was observed, suggesting a possible function of MST-1 during MOR signaling. Based on this hypothesis it was determined in *in vitro* kinase assays that MST-1 can regulate both NDR kinase pathways by stimulating the SIN kinase DBF-2 as well as the MOR kinase COT-1 through phosphorylation of their hydrophobic motifs. In contrast SID-1 only stimulated DFB-2, while the MOR-associated GCK POD-6 was specific for COT-1. Thus, SID-1 and POD-6 are pathway-specific activators of the SIN and MOR, respectively, consistent with the phenotypic characteristics of the respective mutants and the SIN/MOR-specific localization patterns (Seiler et al., 2006, Maerz et al., 2009, Dettmann et al., 2012). MST-1 on the other hand functions as promiscuous activator of both pathways. Interestingly, the two *Drosophila* NDR kinases Trc and Wts (*N. crassa* COT-1 and DBF-2 homologs, respectively) share the same upstream regulator Hippo (Hpo), which may help coordinate their roles in the establishment and maintenance of dendritic tiling in neuronal cells (Emoto et al., 2006, Emoto, 2011). In mammals the MST1/2 —LATS1/2 pathway (homologous to SIN) plays a role in tumor suppression and growth inhibition but several recent reports now implicate MST1/2 in the additional regulation of NDR1/2 kinases (homologous to MOR) to control various cellular processes like centrosome duplication, mitotic chromosome alignment, and apoptotic signalling (Vichalkovski et al., 2008, Hergovich & Hemmings, 2009, Chiba *et al.*, 2009). Therefore, the regulation of NDR kinases that function in separate pathways by a common upstream kinase of the STE20-like kinase family appears to be a conserved in fungal and animal NDR pathways.

The accessory function of the SIN-associated GC kinase MST-1 during MOR signaling was further supported by yeast two-hybrid and *in vivo* co-immunoprecipitation experiments that revealed the interaction of MST-1 with the MOR components POD-6 and COT-1. However, GC-kinase displacement

assays showed that addition of purified MST-1 to a separately precipitated POD-6/COT-1 complex completely displaced POD-6, suggesting a competitive regulation of COT-1 by both GC kinases. Intriguingly, *in vitro* kinase assays showed that addition of purified CDC-7 to a MST-1 + COT-1 mixture resulted in a decrease of MST-1-dependent stimulation of COT-1 activity. Thus, besides stimulation of COT-1 by MST-1 another mechanism of COT-1 regulation by MST-1 may exist: CDC-7-dependent inactivation of MST-1 may be followed by displacement of active POD-6 through inactive MST-1 resulting in down-regulation of COT-1. Down-regulation of the MOR effector kinase COT-1 through inhibition of MST-1 by CDC-7 may be one mechanism to overcome MOR-dependent negative septation signals and to allow SIN-dependent septum initiation. Possible mechanisms for COT-1 inhibition might include displacement of active POD-6 through inactive MST-1 and/or hetero-dimerization of MST-1 and POD-6. However, additional experiments are required to confirm this hypothesis. For instance, addition of a kinase-dead variant of MST-1 to a POD-6 + COT-1 mixture should decrease the POD-6-dependent stimulation of COT-1. Moreover, this potential decrease in COT-1 activity should be titratable in order to confirm POD-6 displacement by inactive MST-1. Collectively, in addition to its function in SIN signalling, MST-1 regulates the MOR pathway and the predicted antagonistic relationship between the SIN and MOR during septum formation might be, at least in part, coordinated through MST-1. The observed defects in actin ring formation in Δ*mst-1* may be the result of disturbed crosstalk and/or miss-regulation of the two networks.

6.4 Cosstalk between SIN and MOR effector kinases DBF-2 and COT-1 is mediated by heterodimerization of the NDR kinases

In the last years it became evident that the SIN and MOR NDR kinase pathways have contrasting functions in various cellular processes. For instance, a recent study in *S. pombe* indicates that phosphorylation of Nak1 (MOR component and homolog of *N. crassa* POD-6) by Sid2 (SIN-associated NDR kinase and homolog of *N. crassa* DBF-2) promotes SIN activation and inhibits MOR-mediated polarized growth by blocking interaction of Nak1 with the scaffold protein Mor2 (Gupta et al., 2013). Furthermore, in *D. melanogaster* the NDR kinases, Trc (*N. crassa* COT-1 homolog) and Wts (*N. crassa* DBF-2 homolog) have opposing roles in regulation of cell shape and timing of hair morphogenesis in wing cells [Fang, Adler 2010 Dev Biol]. Also, various studies in mammalian systems have shown that their SIN and MOR counterparts, namely, the MST1/2-LATS1/2 and MST3-NDR1/2 signalling pathways have contradictory effects on cell proliferation (Cornils et al., 2011, Visser & Yang, 2010, Hergovich *et al.*, 2008). These observations suggest the possibility that an antagonistic crosstalk similar to the one observed in *N. crassa* may exist between homologous NDR kinase pathways in higher organisms. Alternatively, the two NDR pathways work in concert to promote common cellular

functions. In the budding yeast *S. cerevisiae,* the MEN and RAM signaling networks function together to regulate the Ace2p transcription factor in daughter cell separation (Weiss et al., 2002).

In order to determine the genetic relationship between SIN and MOR components in *N. crassa*, several double mutants were generated. *N. crassa* SIN mutants are aseptate (Maerz et al., 2009), while MOR-defective cells produce multiple, closely spaced septa (Seiler et al., 2006, Maerz et al., 2009). Double mutants between the MOR mutant *cot-1(ts)* and SIN mutants *Δdbf-2* or *Δmob-1* showed that the *cot-1(ts)* mutation was able to rescue the septum formation defect in both SIN mutants at restrictive temperature. Thus, septum formation in a MOR deletion background does not require a functional SIN cascade and reduction in MOR pathway activity likely enhances the ability of weak SIN signalling to septum formation. This data support the idea of the MOR component COT-1 as negative regulator of septation and thus the predicted mutual antagonism between the two NDR kinase pathways.

NDR kinases contain a conserved N-terminal regulatory motif (NTR), known as the MOB association domain, which is crucial for interaction with co-activator Mps-one binder (MOB) proteins and functions as dimerization domain (Bichsel et al., 2004, Maerz et al., 2009, Millward et al., 1998, Hou et al., 2004, He et al., 2005b, Hergovich et al., 2006, Ponchon et al., 2004). *In vivo* co-immunoprecipitation experiments revealed an interaction between the SIN kinase DBF-2 and the MOR kinase COT-1. Moreover, yeast two-hybrid experiments showed that region 119–212 of COT-1 is sufficient to interact with DBF-2, indicating a NTR-mediated formation of kinase-kinase heterodimers. In recent studies it was demonstrated that the *N. crassa* NDR kinase COT-1 forms inactive homodimers and the NTR of COT-1 is responsible for the interaction with MOB-2 adaptor proteins, which in turn is crucial for COT-1 activity and stability (Maerz et al., 2009, Maerz et al., 2012). In *S. pombe*, it was also shown that Sid2 homodimers (DBF-2 homolog) are inactive (Hou et al., 2004). Based on these facts, it was tested if the DBF-2 ―COT-1 heterodimerization has an impact on COT-1 kinase activity and COT-1 ―MOB-2A complex formation. Strikingly, displacement assays and *in vitro* kinase assays revealed a titratable DBF-2-dependent decrease of COT-1 activity and a reduced abundance of HA-MOB-2A in the COT-1 ― DBF-2 heterodimer complex. Collectively, DBF-2 presumably functions as competitive inhibitor of COT-1 by forming heterodimers and displacing MOB adaptor proteins. Thus, the interaction of DBF-2 and COT-1 may provide an additional mechanism for MOR inhibition by the SIN pathway (and vice versa). This predicted interdependent mechanism of NDR kinase pathway regulation is presumably triggered through protein abundance at sites of septum formation. The antagonism between the two pathways may both enhances the efficiency of each pathway by removing a competitor, and may ensure that cytoskeletal rearrangements occur at the correct site and time point. Given the multiple levels of cross-communication identified in this study (SIN and MOR coordination by MST-1 and interaction of DBF-2 and COT-1) and other model

systems (*S. pombe, D. melanogaster*) in recent years, suggest the possibility that the antagonistic crosstalk between homologous NDR kinase pathways might be a general mechanism by which these pathways are coordinated in higher organisms. Thus, a detailed comprehension of crosstalk between the NDR pathways will likely have important implications for the understanding of how cells regulate both growth and proliferation.

6.5 COT-1 regulates the BUD-3 —BUD-4 landmark complex during septum formation

Epistasis analysis revealed that the MOR functions as negative regulator upstream of the BUD complex. In order to determine the genetic relationship between MOR and BUD components, several *N. crassa* double mutants were generated. *N. crassa* BUD mutants are aseptate (Justa-Schuch et al., 2010), while MOR-defective cells produce multiple, closely spaced septa (Seiler et al., 2006, Maerz et al., 2009). Progeny of crosses of *cot-1(ts)* with *Δbud-3* or *Δbud-4* showed thin and aseptate hyphae, which frequently lysed, indicating that the MOR functions upstream of the BUD complex. Moreover, the biochemical analysis revealed that COT-1, but not DBF-2 phosphorylates BUD-3/BUD-4 and that COT-1-dependent phosphorylation inhibits BUD-3 localization. Finally, it was determined that BUD-3 as well as BUD-4 co-precipitated with COT-1, which confirmed the interaction of both BUD proteins with COT-1 *in vivo*. In contrast, no interaction of the BUD complex was observed with DBF-2 (data not shown). The *in silico* inspection of BUD-3/4 sequences revealed the presence of putative NDR kinase consensus phosphorylation sites (R-X-X-S) located within BUD-3 and BUD-4, respectively. Therefore, it was tested whether BUD-3/4 are direct substrates of any of two NDR kinases. *In vitro* phosphorylation assays showed that BUD-3 as well as BUD-4 were phosphorylated by COT-1, but not by DBF-2. Next, the predicted NDR kinase consensus sites within BUD-3 and BUD-4 were mutated to alanine to create nonphosphorylatable mutants. Strikingly, both mutants showed reduced phosphorylation by COT-1. Moreover, BUD-3 and BUD-4 are likely also phosphorylated by other co-purifying kinase(s), since both BUD proteins showed significant incorporation of phosphate without addition of a kinase. Preliminary *in vitro* phosphorylation experiments coupled with mass-spectrometric analysis of BUD-3/4 identified predicted CDK1 (cyclin dependent kinase 1) phosphorylation sites (data not shown). This result may provide a possible connection between cell cycle progression and regulation of septum formation, but further experiments are required to confirm these predicted CDK1 sites located within BUD-3 and BUD-4.

To obtain better insight into the functional consequences of BUD-3/4 phosphorylation by COT-1, the phenotype of nonphosphorylatable (BUD-3(S798A); BUD-4(4xS2A) and phosphomimetic (BUD-3(S798E); BUD-4(4xS2E) variants was analyzed. While both BUD-4 mutants displayed no significant abnormalities (data not shown), the BUD-3(S798A) and BUD-3(S798E) mutants revealed the formation of multiple, closely spaced septa and moreover, the presence of abnormal cross walls in

the form of cortical spirals. However, both BUD-3 variants restored the inability of the *Δbud-3* mutant to form septa, indicating that neither mutation resulted in non-functionality of the protein. BUD-3 is a large protein of 1604 amino acids and except for the Rho-GEF domain it lacks recognizable domains that can provide clues for its function. Sequence alignment with BUD-3 homologs present in budding yeast and other filamentous ascomycete fungi also failed to identify highly homologous sequences. However, there are two short sequences, ^{748}LSRRIIQLL^{756} and ^{802}VKLLSNFL^{809}, that resemble amphipathic helices (Bernstein et al., 2000, Szeto et al., 2002). Interestingly, Ser798, which was identified as COT1 phosphorylation site in BUD-3 precedes the second amphiphatic helix. It is known that amphipathic helices facilitate plasma membrane targeting to several proteins (Szeto et al., 2002, Antonny et al., 1997, Takahashi & Pryciak, 2007), thus BUD-3's localization to the site of septation might be mediated by these identified amphipathic helices. Supporting this hypothesis, the helix and the positively charged residues in the flanking sequences appear to be evolutionarily conserved in Bud3p homologs found in other fungi including *C. albicans*, *A. nidulans* and *S. pombe*. Moreover, it was recently shown that *S. cerevisiae* Bud3p mutants that carry alanine substitutions for the hydrophobic residues in the amphipathic helix, failed to localize to the bud neck (Guo *et al.*, 2011). Analysis of the cellular distribution of three helix constructs (BUD-3-Helix-GFP; BUD-3-S798A-Helix-GFP; BUD-3-S798E-Helix-GFP) revealed that only the BUD-3-S798A-Helix-GFP construct localized at constricting septa. Thus, mimicking the constitutive nonphosphorylation of the putative NDR kinase consensus phosphorylation sites Ser798 of BUD3 allowed localization at forming septa. These data suggest that COT-1-dependent phosphorylation of BUD-3 might prevent its correct localization to sites of septation, thereby presumably inhibiting septation. Although other BUD-3 regulatory and localization mechanisms must exist, the *N. crassa* MOR pathway seems to be directly involved in CAR assembly by regulating BUD-3 (and possibly also BUD-4).

6.6 Outlook

Overall, this study identified that proper septum formation in *N. crassa* requires a stepwise phospho-regulation of a tripartite SIN cascade, as well as an antagonistic interaction between the two NDR pathways SIN and MOR, that is in part coordinated by MST-1 and the formation of heterodimers of the NDR kinases DBF-2 and COT-1. Moreover, a mechanistic link between the MOR and BUD proteins is provided by the regulation of BUD-3 by COT-1.

Despite recent progress in our understanding of septum formation in filamentous fungi, major open questions and tasks remain:

(a) Is septation cell cycle dependent in *N. crassa*?

In *S. pombe* the temporal coordination of mitosis and cytokinesis is mediated by the septation initiation network (SIN) (Gould & Simanis, 1997, Simanis, 2003, Wolfe & Gould, 2005) and cortical actomyosin ring assembly and septum formation is clearly controlled through cell cycle progression in *A. nidulans* (Harris et al., 1994, Harris, 2001, Wolkow *et al.*, 1996). This may potentially also apply to *N. crassa*, although the connection between nuclear cycle and septum positioning is difficult to detect due to its nuclear asynchrony. Moreover, this study revealed that the SIN localization and activity regulation is cell cycle independent and SIN mutants showed no strict block in mitosis in *N. crassa*. Despite the essential role of the SIN in CAR assembly and septum formation, no function in mitosis is described for the SIN in *A. nidulans* (Bruno et al., 2001, Kim et al., 2006, Kim et al., 2009). This is reminiscent of the situation observed in *S. pombe*, where mutations in positive SIN components lead to growth arrest after multiple rounds of mitosis in non-dividing cells, (Krapp & Simanis, 2008). However, preliminary *in vitro* phosphorylation experiments coupled with mass-spectrometric analysis of the essential septation landmark proteins BUD-3/4 identified predicted CDK-1 (cyclin dependent kinase 1) phosphorylation sites. This result may provides a possible connection between cell cycle progression and regulation of septum formation, but further experiments are required to confirm these predicted CDK-1 sites located within BUD-3 and BUD-4. Interestingly, septum formation depends on a threshold level of NimX activity, the sole mitotic cyclin-dependent kinase in *A. nidulans* (Harris & Kraus, 1998, Harris, 2001, Kraus & Harris, 2001). Nevertheless, how NimX regulates nuclear division and septum formation in *A. nidulans* remains unclear, since no septation-relevant targets of cyclin-dependent kinases are known in fungi.

(b) One additional important aspect will be to identify the effectors of the SIN that are currently largely undefined.

One reported SIN target is the Cdc14-like phosphatase Clp1 (Chen et al., 2008). In addition to the essential function of Clp1 in regulating cell cycle progression by inhibition of mitotic CDK activity, Clp1-dependent dephosphorylation of the *S. pombe* PCH-family protein Cdc15 is essential for CAR assembly (Clifford et al., 2008, Roberts-Galbraith et al., 2010, Trautmann et al., 2001). In addition, the budding yeast MEN is involved in targeting the Chitin synthase Chs2p to the bud neck (Meitinger et al., 2010) and also directly regulates the late cytokinetic components Hof1p/Cyk2p and Inn1p (both are PCH proteins and homologs of *S. pombe* Cdc15; (Sanchez-Diaz et al., 2008, Nishihama et al., 2009, Meitinger et al., 2010, Meitinger et al., 2011). Thus, Cdc14p/Clp1 and Hof1p/Cdc15 may also be promising candidates to be targeted by the SIN in *N. crassa*. Moreover, proteomic approaches would allow to identify multiple substrates of the SIN, but so far this method is not established for *N. crassa*.

(c) Further definition of the antagonistic crosstalk between the SIN and MOR pathways

The multiple levels of cross-communication between the SIN and MOR identified in this study and other model systems such as *S. pombe* or *D. melanogaster*, suggest the possibility that the antagonistic crosstalk between homologous NDR kinase networks may be a general mechanism to coordinate these pathways. In this study MST-1 was identified as SIN-associated kinase that also regulates the antagonistic MOR pathway, thereby functioning as promiscuous activator of both pathways. Preliminary data suggest that besides stimulation of COT-1 by MST-1 another mechanism of COT-1 regulation by MST-1 may exist, suggesting that the antagonistic relationship between the SIN and MOR during septum formation might be, at least in part, coordinated through MST-1. However, further investigation will be required to confirm this hypothesis, thus, a project for the near future is to define if MST-1 regulates COT-1 by different mechanisms.
Crosstalk of the SIN and MOR pathways is also achieved by heterodimer formation between DBF-2 and COT-1, thereby displacing MOB adaptor proteins. However, this finding implies that the DBF-2 — COT-1 heterodimerization might also be a conceivable mechanism of the MOR pathway to inhibit the SIN, and that this predicted interdependent NDR kinase mechanisms is presumably triggered through protein abundance. Future work is needed to clarify if a vice versa mechanism of crosstalk between the SIN and MOR pathways exist.

(d) What are the function(s) of the anillin scaffold and GTPase module(s) during CAR positioning and assembly and how are they regulated?

Anillin-related proteins are among the earliest septation markers in all fungal groups, and their potential function as Rho GTPase scaffold is also conserved in animals (Gregory *et al.*, 2008, Field & Alberts, 1995, Straight *et al.*, 2005, Oegema et al., 2000). A detailed analysis of RHO-4 and the interaction with the proposed anillin scaffold BUD-4 will shed light on their function during septum initiation and CAR constriction.

The answers to these questions will not only improve our understanding of septum formation in vegetative hyphae, but also cell differentiation during ascomycete development. Since the SIN and MOR are conserved in mammalian cells (Hippo and Ndr1/2 pathways, respectively), this study and future work on this topic may provide important insights into how the activities of these essential pathways are coordinated.

7. Supplemental material

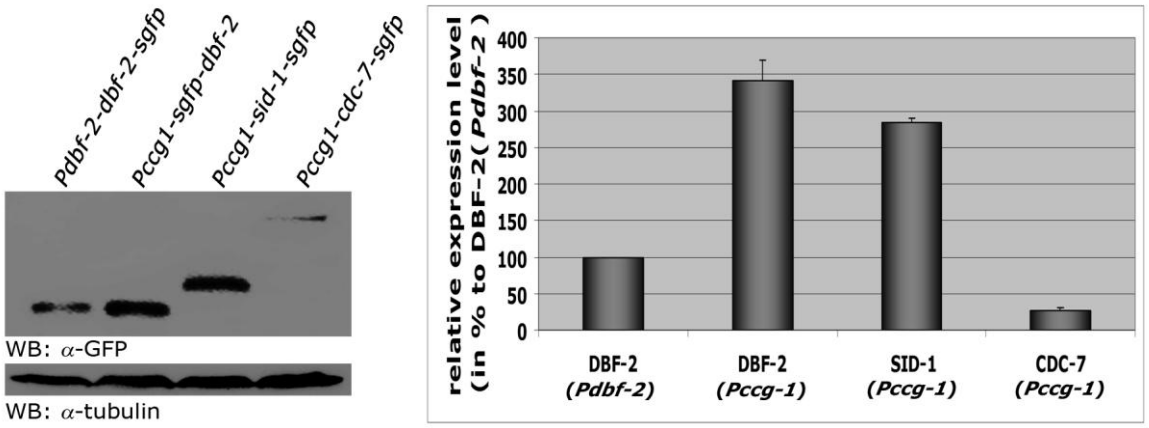

Figure S1: Expression analysis of the used GFP fusion constructs. Anti-GFP Western blot of normalized cell extracts of strains expressing GFP fusion proteins under the control of the indicated promotors (left panal). Quantification of the relative expression levels of the indicated proteins. Protein levels are normalized to DBF-2 (*Pdbf-2*) abundance (n=3) and anti-tubulin Western blot was used to determine equal protein levels.

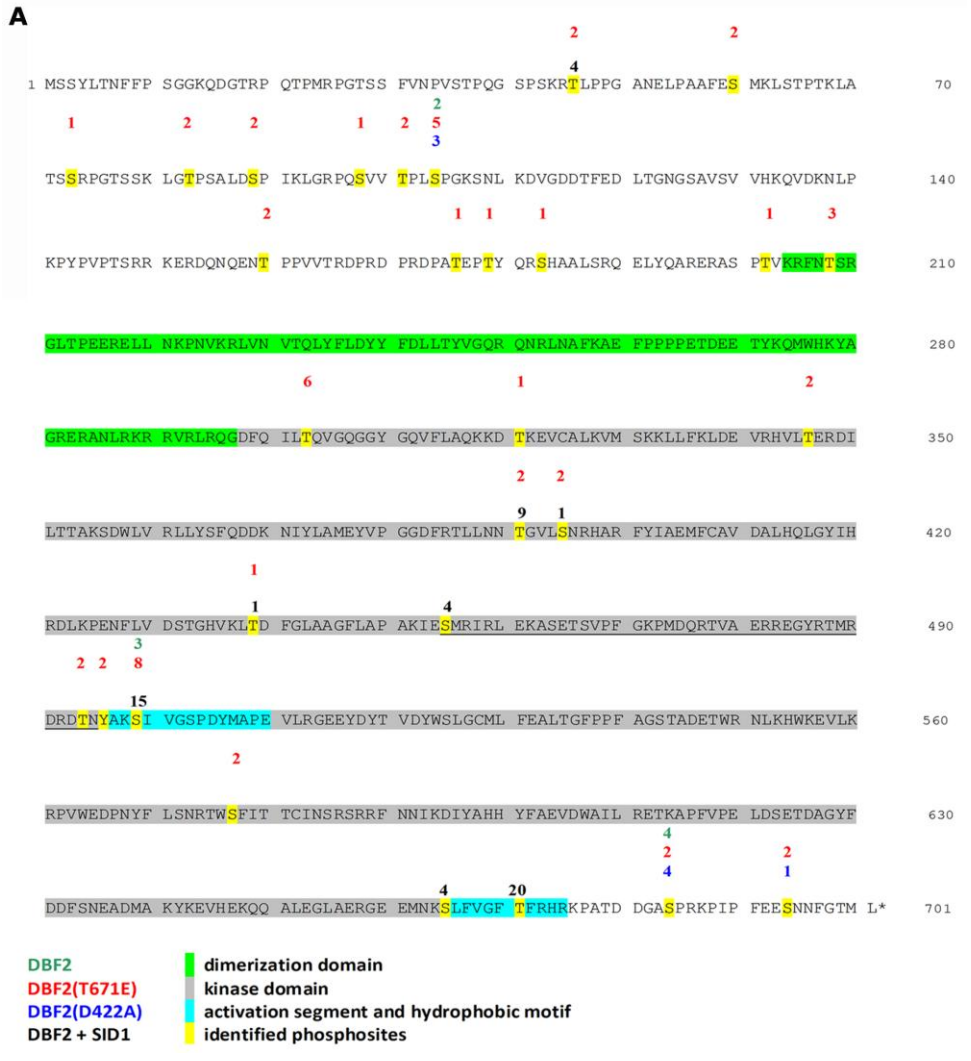

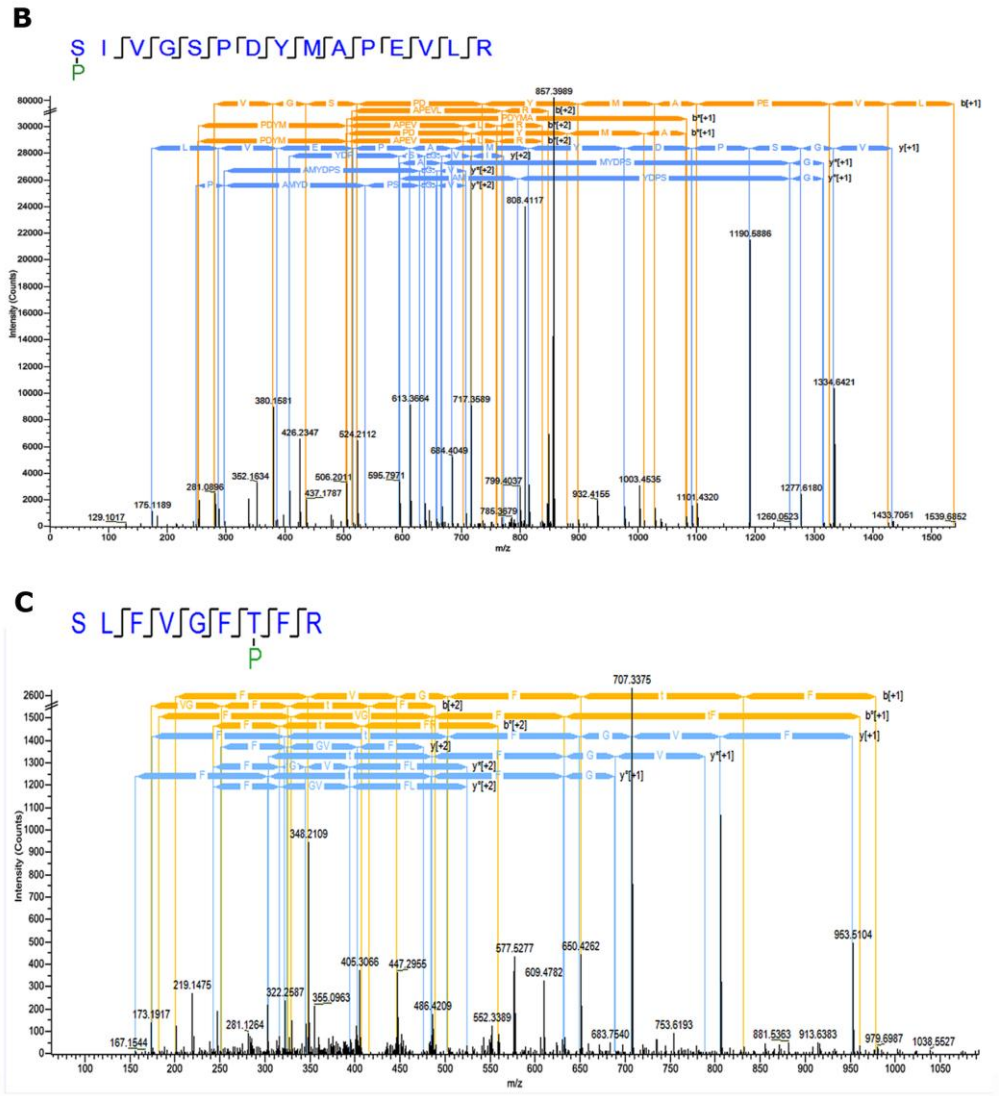

Figure S2: ***In vitro*** **phosphorylation experiments coupled with mass-spectrometric analysis. (A) Ser499 was phosphorylated in wild type DBF-2 and hyperactive DBF-2(T671E), but not DBF-2(D422A), identifying this residue as primary site of auto-phosphorylation. Multiple additional S/T phosphorylation sites were detected in the N-terminal region of DBF-2(T671E). Mass-spectrometric analysis of SID-1-dependant DBF-2 phosphorylation sites identified T671 as primary site of phosphorylation and additional S/T phosphorylation sites are variously distributed. (B) Tryptic peptides generated from wild type DBF-2 displayed HCD-fragmentation spectrum of the peptide SIVGSPDYMAPEVLR with Ser499 phosphorylated. Fragment b-ions (yellow) and y-ions (blue) with an asterisk indicate neutral loss of ammonia (–17 Da), and ions labeled with a circle neutral loss of water (–18 Da), charge states are in brackets. The peptide cross-correlation score for Sequest (XCorr) was 4.9 and the Mascot IonScore was 77. The probability of Ser499-phosphorylation was calculated by the pRS algorithm to be 99.99% [J Proteome Res 10: 5354-5362]. (C) Representative fragmentation spectrum of the peptide SLFVGFtFR with phosphorylation at T671. Fragment ions b* and y* are ions with loss of ammonia (–17 Da), and fragment ions b_o and c_o are ions with loss of water (–18 Da). The number in brackets indicates the charge state of the fragment ion. The peptide was fragmented by CID and fragment ions were detected in the linear ion trap. The peptide was identified with Mascot and Sequest search engines (peptide IonScore of 30 and XCorr of 3.45, respectively). pRS score for phosporylation at tyrosine was 100% [J Proteome Res 10: 5354-5362].**

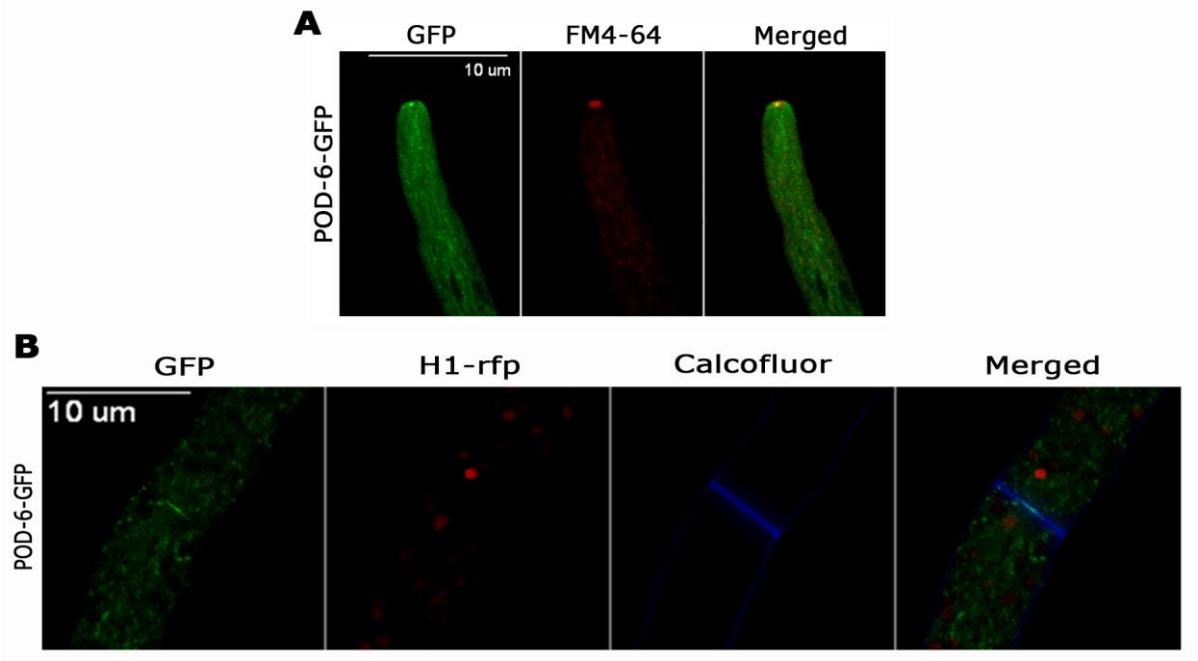

Figure S3: (A) A GFP fusion construct of POD-6 localized at the hyphal tip in a dot-like structure in the distal region of the Spitzenkörper and as membrane-associated apical crescent. (B) POD-6-GFP strongly labeled septa at later stages of septum constriction and accumulated around the mature septal pore. Nuclei were labeled with histone H1-RFP, the cell wall was stained with Calcofluor White and the plasma membrane as well as the Spitzenkörper with FM4-64.

8. References

Almonacid, M., J.B. Moseley, J. Janvore, A. Mayeux, V. Fraisier, P. Nurse & A. Paoletti, (2009) Spatial control of cytokinesis by Cdr2 kinase and Mid1/anillin nuclear export. *Current biology : CB* **19**: 961-966.

An, H., J.L. Morrell, J.L. Jennings, A.J. Link & K.L. Gould, (2004) Requirements of fission yeast septins for complex formation, localization, and function. *Molecular biology of the cell* **15**: 5551-5564.

Antonny, B., S. Beraud-Dufour, P. Chardin & M. Chabre, (1997) N-terminal hydrophobic residues of the G-protein ADP-ribosylation factor-1 insert into membrane phospholipids upon GDP to GTP exchange. *Biochemistry* **36**: 4675-4684.

Aramayo, R. & R.L. and Metzenberg, (1996) Gene replacements at the his-3 locus of *Neurospora crassa*. *Fungal Genetics Newsletter* **43**: 9-13.

Araujo-Palomares, C.L., C. Richthammer, S. Seiler & E. Castro-Longoria, (2011) Functional characterization and cellular dynamics of the CDC-42 - RAC - CDC-24 module in *Neurospora crassa*. *PloS one* **6**: e27148.

Attner, M.A. & A. Amon, (2012) Control of the mitotic exit network during meiosis. *Molecular biology of the cell* **23**: 3122-3132.

Ausubel, F.M., R. Brent, R.E. Kingston, D.D. Moore, J.G. Seidman, J.A. Smith & K.e. and Struhl, (2002) Short protocols in molecular biology: a compendium of methods from current protocols in molecular biology 5th ed. *(New York: Wiley)*.

Bahler, J., A.B. Steever, S. Wheatley, Y. Wang, J.R. Pringle, K.L. Gould & D. McCollum, (1998) Role of polo kinase and Mid1p in determining the site of cell division in fission yeast. *The Journal of cell biology* **143**: 1603-1616.

Baker SE, Wiest A & Plamann M, (2012) Associating genes with phenotypes in Neurospora mutant strains. *Neurospora Conference 2012 Abstract*.

Balasubramanian, M.K., E. Bi & M. Glotzer, (2004) Comparative analysis of cytokinesis in budding yeast, fission yeast and animal cells. *Current biology : CB* **14**: R806-818.

Balasubramanian, M.K., D. McCollum, L. Chang, K.C. Wong, N.I. Naqvi, X. He, S. Sazer & K.L. Gould, (1998) Isolation and characterization of new fission yeast cytokinesis mutants. *Genetics* **149**: 1265-1275.

Balasubramanian, M.K., R. Srinivasan, Y. Huang & K.H. Ng, (2012) Comparing contractile apparatus-driven cytokinesis mechanisms across kingdoms. *Cytoskeleton (Hoboken)* **69**: 942-956.

Barr, F.A. & U. Gruneberg, (2007) Cytokinesis: placing and making the final cut. *Cell* **131**: 847-860.

Berlin, A., A. Paoletti & F. Chang, (2003) Mid2p stabilizes septin rings during cytokinesis in fission yeast. *The Journal of cell biology* **160**: 1083-1092.

Bernstein, L.S., A.A. Grillo, S.S. Loranger & M.E. Linder, (2000) RGS4 binds to membranes through an amphipathic alpha -helix. *The Journal of biological chemistry* **275**: 18520-18526.

Bi, E., P. Maddox, D.J. Lew, E.D. Salmon, J.N. McMillan, E. Yeh & J.R. Pringle, (1998) Involvement of an actomyosin contractile ring in *Saccharomyces cerevisiae* cytokinesis. *The Journal of cell biology* **142**: 1301-1312.

Bichsel, S.J., R. Tamaskovic, M.R. Stegert & B.A. Hemmings, (2004) Mechanism of activation of NDR (nuclear Dbf2-related) protein kinase by the hMOB1 protein. *The Journal of biological chemistry* **279**: 35228-35235.

Bonaccorsi, S., M.G. Giansanti & M. Gatti, (1998) Spindle self-organization and cytokinesis during male meiosis in asterless mutants of Drosophila melanogaster. *The Journal of cell biology* **142**: 751-761.

Boyce, K.J. & A. Andrianopoulos, (2011) Ste20-related kinases: effectors of signaling and morphogenesis in fungi. *Trends in microbiology* **19**: 400-410.

Bruno, K.S., J.L. Morrell, J.E. Hamer & C.J. Staiger, (2001) SEPH, a Cdc7p orthologue from *Aspergillus nidulans*, functions upstream of actin ring formation during cytokinesis. *Molecular microbiology* **42**: 3-12.

Cao, L.G. & Y.L. Wang, (1996) Signals from the spindle midzone are required for the stimulation of cytokinesis in cultured epithelial cells. *Molecular biology of the cell* **7**: 225-232.

Carnahan, R.H. & K.L. Gould, (2003) The PCH family protein, Cdc15p, recruits two F-actin nucleation pathways to coordinate cytokinetic actin ring formation in *Schizosaccharomyces pombe*. *The Journal of cell biology* **162**: 851-862.

Casamayor, A. & M. Snyder, (2003) Molecular dissection of a yeast septin: distinct domains are required for septin interaction, localization, and function. *Molecular and cellular biology* **23**: 2762-2777.

Chan, E.H., M. Nousiainen, R.B. Chalamalasetty, A. Schafer, E.A. Nigg & H.H. Sillje, (2005) The Ste20-like kinase Mst2 activates the human large tumor suppressor kinase Lats1. *Oncogene* **24**: 2076-2086.

Chang, F. & P. Nurse, (1996) How fission yeast fission in the middle. *Cell* **84**: 191-194.

Chen, C.T., A. Feoktistova, J.S. Chen, Y.S. Shim, D.M. Clifford, K.L. Gould & D. McCollum, (2008) The SIN kinase Sid2 regulates cytoplasmic retention of the S. pombe Cdc14-like phosphatase Clp1. *Current biology : CB* **18**: 1594-1599.

Chiba, S., M. Ikeda, K. Katsunuma, K. Ohashi & K. Mizuno, (2009) MST2- and Furry-mediated activation of NDR1 kinase is critical for precise alignment of mitotic chromosomes. *Current biology : CB* **19**: 675-681.

Clifford, D.M., C.T. Chen, R.H. Roberts, A. Feoktistova, B.A. Wolfe, J.S. Chen, D. McCollum & K.L. Gould, (2008) The role of Cdc14 phosphatases in the control of cell division. *Biochemical Society transactions* **36**: 436-438.

Colot, H.V., G. Park, G.E. Turner, C. Ringelberg, C.M. Crew, L. Litvinkova, R.L. Weiss, K.A. Borkovich & J.C. Dunlap, (2006) A high-throughput gene knockout procedure for Neurospora reveals functions for multiple transcription factors. *Proceedings of the National Academy of Sciences of the United States of America* **103**: 10352-10357.

Cornils, H., R.S. Kohler, A. Hergovich & B.A. Hemmings, (2011) Human NDR kinases control G(1)/S cell cycle transition by directly regulating p21 stability. *Molecular and cellular biology* **31**: 1382-1395.

D'Avino, P.P., (2009) How to scaffold the contractile ring for a safe cytokinesis - lessons from Anillin-related proteins. *Journal of cell science* **122**: 1071-1079.

Dan, I., N.M. Watanabe & A. Kusumi, (2001) The Ste20 group kinases as regulators of MAP kinase cascades. *Trends in cell biology* **11**: 220-230.

Davis, B.J., (1964) Disc Electrophoresis. Ii. Method and Application to Human Serum Proteins. *Ann N Y Acad Sci* **121**: 404-427.

Davis, R.H., de Serres, F.J., (1970) Genetic and microbiological research techniques for *Neurospora crassa*. *Methods in enzymology* **17**: 79-143.

Delgado-Alvarez, D.L., O.A. Callejas-Negrete, N. Gomez, M. Freitag, R.W. Roberson, L.G. Smith & R.R. Mourino-Perez, (2010) Visualization of F-actin localization and dynamics with live cell markers in *Neurospora crassa*. *Fungal genetics and biology : FG & B* **47**: 573-586.

Dettmann, A., J. Illgen, S. Marz, T. Schurg, A. Fleissner & S. Seiler, (2012) The NDR kinase scaffold HYM1/MO25 is essential for MAK2 map kinase signaling in *Neurospora crassa*. *PLoS genetics* **8**: e1002950.

Dunlap, J.C., K.A. Borkovich, M.R. Henn, G.E. Turner, M.S. Sachs, N.L. Glass, K. McCluskey, M. Plamann, J.E. Galagan, B.W. Birren, R.L. Weiss, J.P. Townsend, J.J. Loros, M.A. Nelson, R. Lambreghts, H.V. Colot, G. Park, P. Collopy, C. Ringelberg, C. Crew, L. Litvinkova, D. DeCaprio, H.M. Hood, S. Curilla, M. Shi, M. Crawford, M. Koerhsen, P. Montgomery, L. Larson, M. Pearson, T. Kasuga, C. Tian, M. Basturkmen, L. Altamirano & J. Xu, (2007) Enabling a community to dissect an organism: overview of the Neurospora functional genomics project. *Adv Genet* **57**: 49-96.

Dvash, E., G. Kra-Oz, C. Ziv, S. Carmeli & O. Yarden, (2010) The NDR kinase DBF-2 is involved in regulation of mitosis, conidial development, and glycogen metabolism in *Neurospora crassa*. *Eukaryotic cell* **9**: 502-513.

Emoto, K., (2011) The growing role of the Hippo--NDR kinase signalling in neuronal development and disease. *Journal of biochemistry* **150**: 133-141.

Emoto, K., J.Z. Parrish, L.Y. Jan & Y.N. Jan, (2006) The tumour suppressor Hippo acts with the NDR kinases in dendritic tiling and maintenance. *Nature* **443**: 210-213.

Fankhauser, C. & V. Simanis, (1994) The cdc7 protein kinase is a dosage dependent regulator of septum formation in fission yeast. *The EMBO journal* **13**: 3011-3019.

Field, C.M. & B.M. Alberts, (1995) Anillin, a contractile ring protein that cycles from the nucleus to the cell cortex. *The Journal of cell biology* **131**: 165-178.

Fields, S. & O. Song, (1989) A novel genetic system to detect protein-protein interactions. *Nature* **340**: 245-246.

Freitag, M., P.C. Hickey, N.B. Raju, E.U. Selker & N.D. Read, (2004) GFP as a tool to analyze the organization, dynamics and function of nuclei and microtubules in *Neurospora crassa*. *Fungal genetics and biology : FG & B* **41**: 897-910.

Gale, C., M. Gerami-Nejad, M. McClellan, S. Vandoninck, M.S. Longtine & J. Berman, (2001) Candida albicans Int1p interacts with the septin ring in yeast and hyphal cells. *Molecular biology of the cell* **12**: 3538-3549.

Giansanti, M.G., M. Gatti & S. Bonaccorsi, (2001) The role of centrosomes and astral microtubules during asymmetric division of Drosophila neuroblasts. *Development* **128**: 1137-1145.

Gladfelter, A.S., (2006) Control of filamentous fungal cell shape by septins and formins. *Nat Rev Microbiol* **4**: 223-229.

Gladfelter, A.S., J.R. Pringle & D.J. Lew, (2001) The septin cortex at the yeast mother-bud neck. *Current opinion in microbiology* **4**: 681-689.

Goshima, T., K. Kume, T. Koyano, Y. Ohya, T. Toda & D. Hirata, (2010) Fission yeast germinal center (GC) kinase Ppk11 interacts with Pmo25 and plays an auxiliary role in concert with the morphogenesis Orb6 network (MOR) in cell morphogenesis. *The Journal of biological chemistry* **285**: 35196-35205.

Gould, K.L. & V. Simanis, (1997) The control of septum formation in fission yeast. *Genes & development* **11**: 2939-2951.

Gregory, S.L., S. Ebrahimi, J. Milverton, W.M. Jones, A. Bejsovec & R. Saint, (2008) Cell division requires a direct link between microtubule-bound RacGAP and Anillin in the contractile ring. *Current biology : CB* **18**: 25-29.

Guertin, D.A., L. Chang, F. Irshad, K.L. Gould & D. McCollum, (2000) The role of the sid1p kinase and cdc14p in regulating the onset of cytokinesis in fission yeast. *The EMBO journal* **19**: 1803-1815.

Gull, K., (1978) Form and function of septa in filamentous fungi. In: The Filamentous Fungi, Developmental Mycology. J.E.S.a.D.R. Berry (ed). New York: John Wiley & Sons, pp. 78-93.

Guo, J., T. Gong & X.D. Gao, (2011) Identification of an amphipathic helix important for the formation of ectopic septin spirals and axial budding in yeast axial landmark protein Bud3p. *PloS one* **6**: e16744.

Gupta, S., S. Mana-Capelli, J.R. McLean, C.T. Chen, S. Ray, K.L. Gould & D. McCollum, (2013) Identification of SIN pathway targets reveals mechanisms of crosstalk between NDR kinase pathways. *Current biology : CB* **23**: 333-338.

Gupta, S. & D. McCollum, (2011) Crosstalk between NDR kinase pathways coordinates cell cycle dependent actin rearrangements. *Cell division* **6**: 19.

Hachet, O. & V. Simanis, (2008) Mid1p/anillin and the septation initiation network orchestrate contractile ring assembly for cytokinesis. *Genes & development* **22**: 3205-3216.

Harris, S.D., (2001) Septum formation in *Aspergillus nidulans*. *Current opinion in microbiology* **4**: 736-739.

Harris, S.D. & P.R. Kraus, (1998) Regulation of septum formation in *Aspergillus nidulans* by a DNA damage checkpoint pathway. *Genetics* **148**: 1055-1067.

Harris, S.D., J.L. Morrell & J.E. Hamer, (1994) Identification and characterization of *Aspergillus nidulans* mutants defective in cytokinesis. *Genetics* **136**: 517-532.

He, Y., K. Emoto, X. Fang, N. Ren, X. Tian, Y.N. Jan & P.N. Adler, (2005a) Drosophila Mob family proteins interact with the related tricornered (Trc) and warts (Wts) kinases. *Molecular biology of the cell* **16**: 4139-4152.

He, Y., X. Fang, K. Emoto, Y.N. Jan & P.N. Adler, (2005b) The tricornered Ser/Thr protein kinase is regulated by phosphorylation and interacts with furry during Drosophila wing hair development. *Molecular biology of the cell* **16**: 689-700.

Hergovich, A., H. Cornils & B.A. Hemmings, (2008) Mammalian NDR protein kinases: from regulation to a role in centrosome duplication. *Biochimica et biophysica acta* **1784**: 3-15.

Hergovich, A. & B.A. Hemmings, (2009) Mammalian NDR/LATS protein kinases in hippo tumor suppressor signaling. *Biofactors* **35**: 338-345.

Hergovich, A., M.R. Stegert, D. Schmitz & B.A. Hemmings, (2006) NDR kinases regulate essential cell processes from yeast to humans. *Nature reviews. Molecular cell biology* **7**: 253-264.

Hickey, P.C., D. Jacobson, N.D. Read & N.L. Louise Glass, (2002) Live-cell imaging of vegetative hyphal fusion in *Neurospora crassa*. *Fungal genetics and biology : FG & B* **37**: 109-119.

Hirata, D., N. Kishimoto, M. Suda, Y. Sogabe, S. Nakagawa, Y. Yoshida, K. Sakai, M. Mizunuma, T. Miyakawa, J. Ishiguro & T. Toda, (2002) Fission yeast Mor2/Cps12, a protein similar to Drosophila Furry, is essential for cell morphogenesis and its mutation induces Wee1-dependent G(2) delay. *The EMBO journal* **21**: 4863-4874.

Honda, S. & E.U. Selker, (2009) Tools for fungal proteomics: multifunctional neurospora vectors for gene replacement, protein expression and protein purification. *Genetics* **182**: 11-23.

Hou, M.C., D.A. Guertin & D. McCollum, (2004) Initiation of cytokinesis is controlled through multiple modes of regulation of the Sid2p-Mob1p kinase complex. *Molecular and cellular biology* **24**: 3262-3276.

Hou, M.C., D.J. Wiley, F. Verde & D. McCollum, (2003) Mob2p interacts with the protein kinase Orb6p to promote coordination of cell polarity with cell cycle progression. *Journal of cell science* **116**: 125-135.

Huang, T.Y., N.A. Markley & D. Young, (2003) Nak1, an essential germinal center (GC) kinase regulates cell morphology and growth in *Schizosaccharomyces pombe*. *The Journal of biological chemistry* **278**: 991-997.

Huang, Y., H. Yan & M.K. Balasubramanian, (2008) Assembly of normal actomyosin rings in the absence of Mid1p and cortical nodes in fission yeast. *The Journal of cell biology* **183**: 979-988.

Hwa Lim, H., F.M. Yeong & U. Surana, (2003) Inactivation of mitotic kinase triggers translocation of MEN components to mother-daughter neck in yeast. *Molecular biology of the cell* **14**: 4734-4743.

Inoue, H., H. Nojima & H. Okayama, (1990) High efficiency transformation of *Escherichia coli* with plasmids. *Gene* **96**: 23-28.

James, P., J. Halladay & E.A. Craig, (1996) Genomic libraries and a host strain designed for highly efficient two-hybrid selection in yeast. *Genetics* **144**: 1425-1436.

Jansen, J.M., M.F. Barry, C.K. Yoo & E.L. Weiss, (2006) Phosphoregulation of Cbk1 is critical for RAM network control of transcription and morphogenesis. *The Journal of cell biology* **175**: 755-766.

Johnson, A.E., D. McCollum & K.L. Gould, (2012) Polar opposites: Fine-tuning cytokinesis through SIN asymmetry. *Cytoskeleton (Hoboken)* **69**: 686-699.

Justa-Schuch, D., Y. Heilig, C. Richthammer & S. Seiler, (2010) Septum formation is regulated by the RHO4-specific exchange factors BUD3 and RGF3 and by the landmark protein BUD4 in *Neurospora crassa*. *Molecular microbiology* **76**: 220-235.

Kanai, M., K. Kume, K. Miyahara, K. Sakai, K. Nakamura, K. Leonhard, D.J. Wiley, F. Verde, T. Toda & D. Hirata, (2005) Fission yeast MO25 protein is localized at SPB and septum and is essential for cell morphogenesis. *The EMBO journal* **24**: 3012-3025.

Kang, P.J., J.K. Hood-DeGrenier & H.O. Park, (2013) Coupling of septins to the axial landmark by Bud4 in budding yeast. *Journal of cell science* **126**: 1218-1226.

Kaufmann, A. & P. Philippsen, (2009) Of bars and rings: Hof1-dependent cytokinesis in multiseptated hyphae of *Ashbya gossypii*. *Molecular and cellular biology* **29**: 771-783.

Kawabata, T. & H. and Inoue, (2007) Detection of physical interactions by immunoprecipitation of FLAG- and HA-tagged proteins expressed at the his-3 locus in *Neurospora crassa*. *Fungal Genetics Newsletter* **54**: 5-8.

Kim, J.M., L. Lu, R. Shao, J. Chin & B. Liu, (2006) Isolation of mutations that bypass the requirement of the septation initiation network for septum formation and conidiation in *Aspergillus nidulans*. *Genetics* **173**: 685-696.

Kim, J.M., C.J. Zeng, T. Nayak, R. Shao, A.C. Huang, B.R. Oakley & B. Liu, (2009) Timely septation requires SNAD-dependent spindle pole body localization of the septation initiation network components in the filamentous fungus *Aspergillus nidulans*. *Molecular biology of the cell* **20**: 2874-2884.

Krapp, A., P. Collin, A. Cokoja, S. Dischinger, E. Cano & V. Simanis, (2006) The *Schizosaccharomyces pombe* septation initiation network (SIN) is required for spore formation in meiosis. *Journal of cell science* **119**: 2882-2891.

Krapp, A. & V. Simanis, (2008) An overview of the fission yeast septation initiation network (SIN). *Biochemical Society transactions* **36**: 411-415.

Kraus, P.R. & S.D. Harris, (2001) The *Aspergillus nidulans* snt genes are required for the regulation of septum formation and cell cycle checkpoints. *Genetics* **159**: 557-569.

Kume, K., T. Goshima, K. Miyahara, T. Toda & D. Hirata, (2007) A method for Pmo25-associated kinase assay in fission yeast: the activity is dependent on two gC kinases Nak1 and Sid1. *Bioscience, biotechnology, and biochemistry* **71**: 615-617.

Kume, K., S. Kubota, T. Koyano, M. Kanai, M. Mizunuma, T. Toda & D. Hirata, (2013) Fission yeast leucine-rich repeat protein Lrp1 is essential for cell morphogenesis as a component of the morphogenesis Orb6 network (MOR). *Bioscience, biotechnology, and biochemistry* **77**: 1086-1091.

Laemmli, U.K., (1970) Cleavage of structural proteins during the assembly of the head of bacteriophage T4. *Nature* **227**: 680-685.

Laporte, D., V.C. Coffman, I.J. Lee & J.Q. Wu, (2011) Assembly and architecture of precursor nodes during fission yeast cytokinesis. *The Journal of cell biology* **192**: 1005-1021.

Laporte, D., R. Zhao & J.Q. Wu, (2010) Mechanisms of contractile-ring assembly in fission yeast and beyond. *Seminars in cell & developmental biology* **21**: 892-898.

Leonhard, K. & P. Nurse, (2005) Ste20/GCK kinase Nak1/Orb3 polarizes the actin cytoskeleton in fission yeast during the cell cycle. *Journal of cell science* **118**: 1033-1044.

Ling, P., T.J. Lu, C.J. Yuan & M.D. Lai, (2008) Biosignaling of mammalian Ste20-related kinases. *Cellular signalling* **20**: 1237-1247.

Lippincott, J. & R. Li, (1998) Sequential assembly of myosin II, an IQGAP-like protein, and filamentous actin to a ring structure involved in budding yeast cytokinesis. *The Journal of cell biology* **140**: 355-366.

Lippincott, J., K.B. Shannon, W. Shou, R.J. Deshaies & R. Li, (2001) The Tem1 small GTPase controls actomyosin and septin dynamics during cytokinesis. *Journal of cell science* **114**: 1379-1386.

Liu, G. & D. Young, (2012) Conserved Orb6 phosphorylation sites are essential for polarized cell growth in *Schizosaccharomyces pombe*. *PloS one* **7**: e37221.

Longtine, M.S., D.J. DeMarini, M.L. Valencik, O.S. Al-Awar, H. Fares, C. De Virgilio & J.R. Pringle, (1996) The septins: roles in cytokinesis and other processes. *Current opinion in cell biology* **8**: 106-119.

Luo, J., E.A. Vallen, C. Dravis, S.E. Tcheperegine, B. Drees & E. Bi, (2004) Identification and functional analysis of the essential and regulatory light chains of the only type II myosin Myo1p in Saccharomyces cerevisiae. *The Journal of cell biology* **165**: 843-855.

Madhani, H.D. & G.R. Fink, (1998) The control of filamentous differentiation and virulence in fungi. *Trends in cell biology* **8**: 348-353.

Maerz, S., A. Dettmann & S. Seiler, (2012) Hydrophobic motif phosphorylation coordinates activity and polar localization of the *Neurospora crassa* nuclear Dbf2-related kinase COT1. *Molecular and cellular biology* **32**: 2083-2098.

Maerz, S., A. Dettmann, C. Ziv, Y. Liu, O. Valerius, O. Yarden & S. Seiler, (2009) Two NDR kinase-MOB complexes function as distinct modules during septum formation and tip extension in *Neurospora crassa*. *Molecular microbiology* **74**: 707-723.

Maerz, S. & S. Seiler, (2010) Tales of RAM and MOR: NDR kinase signaling in fungal morphogenesis. *Current opinion in microbiology* **13**: 663-671.

Mah, A.S., J. Jang & R.J. Deshaies, (2001) Protein kinase Cdc15 activates the Dbf2-Mob1 kinase complex. *Proceedings of the National Academy of Sciences of the United States of America* **98**: 7325-7330.

Margolin, B.S., M. Freitag & E.U. and Selker, (1997) Improved plasmids for gene targeting at the his-3 locus of *Neurospora crassa* by electroporation. *Fungal Genetics Newsletter* **44**.

Marks, J., I.M. Hagan & J.S. Hyams, (1986) Growth polarity and cytokinesis in fission yeast: the role of the cytoskeleton. *Journal of cell science. Supplement* **5**: 229-241.

Martin-Cuadrado, A.B., J.L. Morrell, M. Konomi, H. An, C. Petit, M. Osumi, M. Balasubramanian, K.L. Gould, F. Del Rey & C.R. de Aldana, (2005) Role of septins and the exocyst complex in the function of hydrolytic enzymes responsible for fission yeast cell separation. *Molecular biology of the cell* **16**: 4867-4881.

Martin, S.G., (2009) Microtubule-dependent cell morphogenesis in the fission yeast. *Trends in cell biology* **19**: 447-454.

McCollum, D. & K.L. Gould, (2001) Timing is everything: regulation of mitotic exit and cytokinesis by the MEN and SIN. *Trends in cell biology* **11**: 89-95.

McMurray, M.A. & J. Thorner, (2009) Reuse, replace, recycle. Specificity in subunit inheritance and assembly of higher-order septin structures during mitotic and meiotic division in budding yeast. *Cell Cycle* **8**: 195-203.

Meitinger, F., M.E. Boehm, A. Hofmann, B. Hub, H. Zentgraf, W.D. Lehmann & G. Pereira, (2011) Phosphorylation-dependent regulation of the F-BAR protein Hof1 during cytokinesis. *Genes & development* **25**: 875-888.

Meitinger, F., S. Palani & G. Pereira, (2012) The power of MEN in cytokinesis. *Cell Cycle* **11**: 219-228.

Meitinger, F., B. Petrova, I.M. Lombardi, D.T. Bertazzi, B. Hub, H. Zentgraf & G. Pereira, (2010) Targeted localization of Inn1, Cyk3 and Chs2 by the mitotic-exit network regulates cytokinesis in budding yeast. *Journal of cell science* **123**: 1851-1861.

Merril, C.R., (1990) Gel-staining techniques. *Methods Enzymol* **182**: 477-488.

Millward, T.A., C.W. Heizmann, B.W. Schafer & B.A. Hemmings, (1998) Calcium regulation of Ndr protein kinase mediated by S100 calcium-binding proteins. *The EMBO journal* **17**: 5913-5922.

Millward, T.A., D. Hess & B.A. Hemmings, (1999) Ndr protein kinase is regulated by phosphorylation on two conserved sequence motifs. *The Journal of biological chemistry* **274**: 33847-33850.

Minet, M., P. Nurse, P. Thuriaux & J.M. Mitchison, (1979) Uncontrolled septation in a cell division cycle mutant of the fission yeast Schizosaccharomyces pombe. *Journal of bacteriology* **137**: 440-446.

Moseley, J.B., A. Mayeux, A. Paoletti & P. Nurse, (2009) A spatial gradient coordinates cell size and mitotic entry in fission yeast. *Nature* **459**: 857-860.

Nelson, B., C. Kurischko, J. Horecka, M. Mody, P. Nair, L. Pratt, A. Zougman, L.D. McBroom, T.R. Hughes, C. Boone & F.C. Luca, (2003) RAM: a conserved signaling network that regulates Ace2p transcriptional activity and polarized morphogenesis. *Molecular biology of the cell* **14**: 3782-3803.

Nishihama, R., J.H. Schreiter, M. Onishi, E.A. Vallen, J. Hanna, K. Moravcevic, M.F. Lippincott, H. Han, M.A. Lemmon, J.R. Pringle & E. Bi, (2009) Role of Inn1 and its interactions with Hof1 and Cyk3 in promoting cleavage furrow and septum formation in S. cerevisiae. *The Journal of cell biology* **185**: 995-1012.

Nishimura, Y. & S. Yonemura, (2006) Centralspindlin regulates ECT2 and RhoA accumulation at the equatorial cortex during cytokinesis. *Journal of cell science* **119**: 104-114.

Noguchi, T. & I. Mabuchi, (2001) Reorganization of actin cytoskeleton at the growing end of the cleavage furrow of Xenopus egg during cytokinesis. *Journal of cell science* **114**: 401-412.

Oegema, K., M.S. Savoian, T.J. Mitchison & C.M. Field, (2000) Functional analysis of a human homologue of the Drosophila actin binding protein anillin suggests a role in cytokinesis. *The Journal of cell biology* **150**: 539-552.

Ohkura, H., I.M. Hagan & D.M. Glover, (1995) The conserved *Schizosaccharomyces pombe* kinase plo1, required to form a bipolar spindle, the actin ring, and septum, can drive septum formation in G1 and G2 cells. *Genes & development* **9**: 1059-1073.

Oliferenko, S., T.G. Chew & M.K. Balasubramanian, (2009) Positioning cytokinesis. *Genes & development* **23**: 660-674.

Ornstein, L., (1964) Disc Electrophoresis. I. Background and Theory. *Ann N Y Acad Sci* **121**: 321-349.

Padmanabhan, A., K. Bakka, M. Sevugan, N.I. Naqvi, V. D'Souza, X. Tang, M. Mishra & M.K. Balasubramanian, (2011) IQGAP-related Rng2p organizes cortical nodes and ensures position of cell division in fission yeast. *Current biology : CB* **21**: 467-472.

Paoletti, A. & F. Chang, (2000) Analysis of mid1p, a protein required for placement of the cell division site, reveals a link between the nucleus and the cell surface in fission yeast. *Molecular biology of the cell* **11**: 2757-2773.

Park, H.O. & E. Bi, (2007) Central roles of small GTPases in the development of cell polarity in yeast and beyond. *Microbiology and molecular biology reviews : MMBR* **71**: 48-96.

Piekny, A.J. & M. Glotzer, (2008) Anillin is a scaffold protein that links RhoA, actin, and myosin during cytokinesis. *Current biology : CB* **18**: 30-36.

Pollard, T.D. & J.Q. Wu, (2010) Understanding cytokinesis: lessons from fission yeast. *Nature reviews. Molecular cell biology* **11**: 149-155.

Ponchon, L., C. Dumas, A.V. Kajava, D. Fesquet & A. Padilla, (2004) NMR solution structure of Mob1, a mitotic exit network protein and its interaction with an NDR kinase peptide. *Journal of molecular biology* **337**: 167-182.

Pringle, A. & J. Taylor, (2002) The fitness of filamentous fungi. *Trends in microbiology* **10**: 474-481.

Raju, N.B. & a.D. Newmeyer, (1977) Giant ascospores and abnormal croziers in a mutant of *Neurospora crassa*. *Experimental Mycology* **1**: 152-165.

Rappaport, R., (1961) Experiments concerning the cleavage stimulus in sand dollar eggs. *The Journal of experimental zoology* **148**: 81-89.

Rappaport, R., (1985) Repeated furrow formation from a single mitotic apparatus in cylindrical sand dollar eggs. *The Journal of experimental zoology* **234**: 167-171.

Rasmussen, C.G. & N.L. Glass, (2005) A Rho-type GTPase, rho-4, is required for septation in *Neurospora crassa*. *Eukaryotic cell* **4**: 1913-1925.

Rasmussen, C.G. & N.L. Glass, (2007) Localization of RHO-4 indicates differential regulation of conidial versus vegetative septation in the filamentous fungus *Neurospora crassa*. *Eukaryotic cell* **6**: 1097-1107.

Ray, S., K. Kume, S. Gupta, W. Ge, M. Balasubramanian, D. Hirata & D. McCollum, (2010) The mitosis-to-interphase transition is coordinated by cross talk between the SIN and MOR pathways in *Schizosaccharomyces pombe*. *The Journal of cell biology* **190**: 793-805.

Reynolds, N. & H. Ohkura, (2003) Polo boxes form a single functional domain that mediates interactions with multiple proteins in fission yeast polo kinase. *Journal of cell science* **116**: 1377-1387.

Richthammer, C., M. Enseleit, E. Sanchez-Leon, S. Marz, Y. Heilig, M. Riquelme & S. Seiler, (2012) RHO1 and RHO2 share partially overlapping functions in the regulation of cell wall integrity and hyphal polarity in *Neurospora crassa*. *Molecular microbiology* **85**: 716-733.

Roberts-Galbraith, R.H., J.S. Chen, J. Wang & K.L. Gould, (2009) The SH3 domains of two PCH family members cooperate in assembly of the *Schizosaccharomyces pombe* contractile ring. *The Journal of cell biology* **184**: 113-127.

Roberts-Galbraith, R.H. & K.L. Gould, (2008) Stepping into the ring: the SIN takes on contractile ring assembly. *Genes & development* **22**: 3082-3088.

Roberts-Galbraith, R.H., M.D. Ohi, B.A. Ballif, J.S. Chen, I. McLeod, W.H. McDonald, S.P. Gygi, J.R. Yates, 3rd & K.L. Gould, (2010) Dephosphorylation of F-BAR protein Cdc15 modulates its conformation and stimulates its scaffolding activity at the cell division site. *Molecular cell* **39**: 86-99.

Salinovich, O. & R.C. Montelaro, (1986) Reversible staining and peptide mapping of proteins transferred to nitrocellulose after separation by sodium dodecylsulfate-polyacrylamide gel electrophoresis. *Anal Biochem* **156**: 341-347.

Sambrook, J. & D. and Russell, (2001) Molecular Cloning: A Laboratory Manual 3rd ed. (New York: Cold Spring Harbor Laboratory Press).

Sanchez-Diaz, A., V. Marchesi, S. Murray, R. Jones, G. Pereira, R. Edmondson, T. Allen & K. Labib, (2008) Inn1 couples contraction of the actomyosin ring to membrane ingression during cytokinesis in budding yeast. *Nature cell biology* **10**: 395-406.

Schiestl, R.H. & R.D. Gietz, (1989) High efficiency transformation of intact yeast cells using single stranded nucleic acids as a carrier. *Curr Genet* **16**: 339-346.

Schmidt, S., K. Hofmann & V. Simanis, (1997) Sce3, a suppressor of the *Schizosaccharomyces pombe* septation mutant cdc11, encodes a putative RNA-binding protein. *Nucleic acids research* **25**: 3433-3439.

Seiler, S. & D. Justa-Schuch, (2010) Conserved components, but distinct mechanisms for the placement and assembly of the cell division machinery in unicellular and filamentous ascomycetes. *Molecular microbiology* **78**: 1058-1076.

Seiler, S. & M. Plamann, (2003) The genetic basis of cellular morphogenesis in the filamentous fungus *Neurospora crassa*. *Molecular biology of the cell* **14**: 4352-4364.

Seiler, S., N. Vogt, C. Ziv, R. Gorovits & O. Yarden, (2006) The STE20/germinal center kinase POD6 interacts with the NDR kinase COT1 and is involved in polar tip extension in *Neurospora crassa*. *Molecular biology of the cell* **17**: 4080-4092.

Shannon, K.B. & R. Li, (2000) A myosin light chain mediates the localization of the budding yeast IQGAP-like protein during contractile ring formation. *Current biology : CB* **10**: 727-730.

Si, H., D. Justa-Schuch, S. Seiler & S.D. Harris, (2010) Regulation of septum formation by the Bud3-Rho4 GTPase module in *Aspergillus nidulans*. *Genetics* **185**: 165-176.

Simanis, V., (2003) The mitotic exit and septation initiation networks. *Journal of cell science* **116**: 4261-4262.

Sohrmann, M., C. Fankhauser, C. Brodbeck & V. Simanis, (1996) The dmf1/mid1 gene is essential for correct positioning of the division septum in fission yeast. *Genes & development* **10**: 2707-2719.

Somers, W.G. & R. Saint, (2003) A RhoGEF and Rho family GTPase-activating protein complex links the contractile ring to cortical microtubules at the onset of cytokinesis. *Developmental cell* **4**: 29-39.

Stegert, M.R., A. Hergovich, R. Tamaskovic, S.J. Bichsel & B.A. Hemmings, (2005) Regulation of NDR protein kinase by hydrophobic motif phosphorylation mediated by the mammalian Ste20-like kinase MST3. *Molecular and cellular biology* **25**: 11019-11029.

Straight, A.F., C.M. Field & T.J. Mitchison, (2005) Anillin binds nonmuscle myosin II and regulates the contractile ring. *Molecular biology of the cell* **16**: 193-201.

Szeto, T.H., S.L. Rowland, L.I. Rothfield & G.F. King, (2002) Membrane localization of MinD is mediated by a C-terminal motif that is conserved across eubacteria, archaea, and chloroplasts. *Proceedings of the National Academy of Sciences of the United States of America* **99**: 15693-15698.

Takahashi, S. & P.M. Pryciak, (2007) Identification of novel membrane-binding domains in multiple yeast Cdc42 effectors. *Molecular biology of the cell* **18**: 4945-4956.

Tamaskovic, R., S.J. Bichsel & B.A. Hemmings, (2003) NDR family of AGC kinases--essential regulators of the cell cycle and morphogenesis. *FEBS letters* **546**: 73-80.

Tanaka, K., J. Petersen, F. MacIver, D.P. Mulvihill, D.M. Glover & I.M. Hagan, (2001) The role of Plo1 kinase in mitotic commitment and septation in *Schizosaccharomyces pombe*. *The EMBO journal* **20**: 1259-1270.

Tasto, J.J., J.L. Morrell & K.L. Gould, (2003) An anillin homologue, Mid2p, acts during fission yeast cytokinesis to organize the septin ring and promote cell separation. *The Journal of cell biology* **160**: 1093-1103.

Towbin, H., T. Staehelin & J. Gordon, (1979) Electrophoretic transfer of proteins from polyacrylamide gels to nitrocellulose sheets: procedure and some applications. *Proc Natl Acad Sci U S A* **76**: 4350-4354.

Trautmann, S., B.A. Wolfe, P. Jorgensen, M. Tyers, K.L. Gould & D. McCollum, (2001) Fission yeast Clp1p phosphatase regulates G2/M transition and coordination of cytokinesis with cell cycle progression. *Current biology : CB* **11**: 931-940.

Vallen, E.A., J. Caviston & E. Bi, (2000) Roles of Hof1p, Bni1p, Bnr1p, and myo1p in cytokinesis in *Saccharomyces cerevisiae*. *Molecular biology of the cell* **11**: 593-611.

Vavylonis, D., J.Q. Wu, S. Hao, B. O'Shaughnessy & T.D. Pollard, (2008) Assembly mechanism of the contractile ring for cytokinesis by fission yeast. *Science* **319**: 97-100.

Verde, F., D.J. Wiley & P. Nurse, (1998) Fission yeast orb6, a ser/thr protein kinase related to mammalian rho kinase and myotonic dystrophy kinase, is required for maintenance of cell polarity and coordinates cell morphogenesis with the cell cycle. *Proceedings of the National Academy of Sciences of the United States of America* **95**: 7526-7531.

Vichalkovski, A., E. Gresko, H. Cornils, A. Hergovich, D. Schmitz & B.A. Hemmings, (2008) NDR kinase is activated by RASSF1A/MST1 in response to Fas receptor stimulation and promotes apoptosis. *Current biology : CB* **18**: 1889-1895.

Visser, S. & X. Yang, (2010) LATS tumor suppressor: a new governor of cellular homeostasis. *Cell Cycle* **9**: 3892-3903.

Vogel, H.J., (1956) A convenient growth medium for Neurospora (Medium N). *Microbial Genet. Bul.* **13**: 42-43.

Vogel, H.J., (1964) Distribution of Lysine Pathways Among Fungi: Evolutionary Implications. *The American Naturalist* **98**: 435-446.

Vogt, N. & S. Seiler, (2008) The RHO1-specific GTPase-activating protein LRG1 regulates polar tip growth in parallel to Ndr kinase signaling in Neurospora. *Molecular biology of the cell* **19**: 4554-4569.

Walther, A. & J. Wendland, (2003) Septation and cytokinesis in fungi. *Fungal genetics and biology : FG & B* **40**: 187-196.

Weiss, E.L., (2012) Mitotic exit and separation of mother and daughter cells. *Genetics* **192**: 1165-1202.

Weiss, E.L., C. Kurischko, C. Zhang, K. Shokat, D.G. Drubin & F.C. Luca, (2002) The *Saccharomyces cerevisiae* Mob2p-Cbk1p kinase complex promotes polarized growth and acts with the mitotic exit network to facilitate daughter cell-specific localization of Ace2p transcription factor. *The Journal of cell biology* **158**: 885-900.

Werner, M., E. Munro & M. Glotzer, (2007) Astral signals spatially bias cortical myosin recruitment to break symmetry and promote cytokinesis. *Current biology : CB* **17**: 1286-1297.

Wloka, C. & E. Bi, (2012) Mechanisms of cytokinesis in budding yeast. *Cytoskeleton (Hoboken)* **69**: 710-726.

Wolfe, B.A. & K.L. Gould, (2005) Split decisions: coordinating cytokinesis in yeast. *Trends in cell biology* **15**: 10-18.

Wolkow, T.D., S.D. Harris & J.E. Hamer, (1996) Cytokinesis in *Aspergillus nidulans* is controlled by cell size, nuclear positioning and mitosis. *Journal of cell science* **109 (Pt 8)**: 2179-2188.

Woodcock, D.M., P. J. Crowther, J. Doherty, S. Jefferson, E. DeCruz, M. Noyer-Weidner, S. S. Smith, M. Z. Michael & M. W. Graham, , (1989) Quantitative evaluation of *Escherichia coli* host strains for tolerance to cytosine methylation in plasmid and phage recombinants. . *Nucleic Acids Res* **17**.

Wu, J.Q., J.R. Kuhn, D.R. Kovar & T.D. Pollard, (2003) Spatial and temporal pathway for assembly and constriction of the contractile ring in fission yeast cytokinesis. *Developmental cell* **5**: 723-734.

Wu, J.Q., V. Sirotkin, D.R. Kovar, M. Lord, C.C. Beltzner, J.R. Kuhn & T.D. Pollard, (2006) Assembly of the cytokinetic contractile ring from a broad band of nodes in fission yeast. *The Journal of cell biology* **174**: 391-402.

Yarden, O., M. Plamann, D.J. Ebbole & C. Yanofsky, (1992) cot-1, a gene required for hyphal elongation in *Neurospora crassa*, encodes a protein kinase. *The EMBO journal* **11**: 2159-2166.

Zhang, L. & A.S. Maddox, (2010) Anillin. *Current biology : CB* **20**: R135-136.

Zhou, M. & Y.L. Wang, (2008) Distinct pathways for the early recruitment of myosin II and actin to the cytokinetic furrow. *Molecular biology of the cell* **19**: 318-326.

Ziv, C., G. Kra-Oz, R. Gorovits, S. Marz, S. Seiler & O. Yarden, (2009) Cell elongation and branching are regulated by differential phosphorylation states of the nuclear Dbf2-related kinase COT1 in Neurospora crassa. *Molecular microbiology* **74**: 974-989.

Zon, L.I., D.M. Dorfman & S.H. Orkin, (1989) The polymerase chain reaction colony miniprep. *Biotechniques* **7**: 696-698.

9. Acknowledgements

Ich möchte mich zunächst bei den Mitgliedern meines Thesis Committees, PD Dr. Stephan Seiler, Prof. Dr. Andreas Wodarz und Dr. Hans Dieter Schmitt, bedanken. Außerdem freue ich mich, dass Prof. Dr. Heike Krebber, Jun.-Prof. Dr. Kai Heimel und PD Dr. Michael Hoppert die Teilnahme als Mitglieder des Committees zur Disputation übernommen haben.
Darüberhinaus bedanke ich mich insbesondere bei Herrn Prof. Dr. Andreas Wodarz für die Übernahme der zweiten Referenz.

Ein ganz besonderer Dank gilt Stephan für die Möglichkeit, dass ich meine Doktorarbeit in seinem Labor anfertigen konnte und für die sehr gute und kompetente fachliche Betreuung.

Ein sehr großer Dank gilt meinen lieben Laborkollegen Matzi und Sarah für das tolle Arbeitsklima während meiner Doktorarbeit. Wir haben sehr viel erlebt, gelacht aber auch diskutiert.
Besonders möchte ich mich aber bei Anne für die unermüdliche, fachliche, kulinarische und private Unterstützung bedanken! Danke!!!

Der größte Dank geht an meine Eltern für die grenzenlose Unterstützung und Motivation während der letzten Jahre. Ohne euch wäre mein Studium und der Weg bis hier her nicht möglich gewesen. Vielen lieben Dank!

Natürlich geht auch ein riesen Dankeschön an den Rest der Familie, die mir immer den Rücken freigehalten haben!

10. Curriculum vitae

Name:	Yvonne Heilig	
Anschrift:	Gutleutstraße 10 79115 Freiburg	
Geburtsdatum:	25.03.1984	
Geburtsort:	Bückeburg	
Staatsangehörigkeit:	Deutsch	
Schulbildung:	1990 bis 1991	Grundschule Eschede
	1991 bis 1994	Grundschule Hermannsburg
	1994 bis 1996	Orientierungsstufe Hermannsburg
	1996 bis 2000	Realschule Hermannsburg
	2000 bis 2003	Fachgymnasium Wirtschaft Celle
Schulabschluss:	2003	Allgemeine Hochschulreife
Studium:	2003 bis 2009	Biologie Studium (Diplom) an der Georg-August-Universität Göttingen
Hochschulabschluss:	Diplom-Biologin	
	Titel der Diplomarbeit:	"Markerproteine für die Septierung in *Neurospora crassa"*
Promotion:	2010 bis 2013	Promotion an der Georg-August Universität Göttingen im Rahmen des Promotionsprogramms "Molecular Biology of Cells" der Göttinger Graduate School for Neurosciences and Molecular Biosciences (GGNB)
	Titel der Doktorarbeit:	"Characterization of NDR kinase signalling pathways during septum formation in *Neurospora crassa"*

Göttingen, den 30. September 2013